12-2018

Historical Channel Change Caused by a Century of Flow Alteration on Sixth Water Creek and Diamond Fork River, UT

Jabari C. Jones
Utah State University

HISTORICAL CHANNEL CHANGE CAUSED BY A CENTURY OF FLOW

ALTERATION ON SIXTH WATER CREEK AND

DIAMOND FORK RIVER, UT

by

Jabari C. Jones

A thesis submitted in partial fulfillment
of the requirements for the degree

of

MASTER OF SCIENCE

in

Watershed Science

Approved:

_____	_____
Patrick Belmont, Ph.D. Major Professor	Peter Wilcock, Ph.D. Committee Member
_____	_____
Edward Hammill, Ph.D. Committee Member	Laurens H. Smith, Ph.D. Interim Vice President for Research and Dean of the School of Graduate Studies

UTAH STATE UNIVERSITY
Logan, Utah

2018

ABSTRACT

Historical channel change caused by a century of flow alteration on Sixth Water Creek and Diamond Fork River, UT

by

Jabari Coleman Jones, Master of Science

Utah State University, 2018

Major Professor: Dr. Patrick Belmont
Department: Watershed Sciences

Changes in hydrology and sediment supply affect the form of rivers. The rate of change of fluvial form is controlled by a variety of factors, including valley confinement, sediment size, and antecedent condition. The Diamond Fork River in central Utah has been altered by trans-basin flows delivered from the Colorado River system for over a century. Beginning in 1915, water used for irrigation was delivered through a tributary, Sixth Water Creek. Daily summer flows regularly exceeded the 500 year flood in the headwaters of Sixth Water, and the 10-25 year flood on lower Diamond Fork. Elevated flows caused drastic geomorphic change - resulting in incision and widening of the channel, and the destruction of riparian vegetation. Beginning in 1997, the outlet for the trans-basin diversion was moved downstream on Sixth Water, bypassing a large landslide, and flows were drastically reduced in 2004. Beginning in 2004, diversion flows could entirely bypass the channel through a pipeline and tunnel system, but flows are delivered to meet environmental requirements, maintaining an elevated flow regime. We conducted an analysis of historical change and contemporary behavior of Sixth Water and Diamond Fork to describe how changes in hydrology and sediment supply affected the rivers.

We used historical aerial photographs, USGS gage measurements, topographic cross-sections, and a lidar dataset to describe past conditions. We conducted GPS surveys, captured

photographs using an unmanned aerial vehicle, collected sediment transport measurements, mapped and measured sediment sources, characterized channel substrate, and deployed tracer gravels to describe the current conditions of the rivers. We delineated eight distinct process domains for the Sixth Water-Diamond Fork system based on channel confinement, slope, and geomorphic character.

Results of our analyses indicate that present-day valley and channel morphology are a product of both long term augmentation and extreme events and that different process domains experienced distinct changes. Long term trans-basin diversions caused several meters of erosion in the bedrock valley of Sixth Water and considerably widened the channel in alluvial reaches. Floods in 1952 and 1983/84 delivered large pulses of sediment and over-widened the channel to the valley margins in alluvial reaches. Floods were followed by a period of recovery that narrowed the channel and reworked sediment. The change of diversion outlet in 1997 and reduction of flows in 2004 initiated a new period of recovery. Vegetation encroached on formerly active channel deposits and the channel narrowed. Due to bed armoring during the period of augmented flows, the present-day flow regime is not able to mobilize the bed at common flows. As a result, the present-day channel is relatively inactive with large deposits of former active channel material in the valley. The changes in channel form and the well constrained hydrology of Sixth Water and Diamond Fork provide insight into the relative role of short term and long term hydrologic disturbance. These findings and complimentary studies will provide managers of Sixth Water and Diamond Fork with a greater understanding of the physical characteristics of the streams, and the resulting effects on ecological communities.

(137 pages)

PUBLIC ABSTRACT

Historical channel change caused by a century of flow alteration on Sixth Water Creek and Diamond Fork River, UT

Jabari Coleman Jones

Changes in the amount of water and sediment that enter a river can change its shape and size. The way that rivers change is affected by a variety of factors, including the size of the sediment in the river, and past changes to the river. The Diamond Fork River in central Utah has been altered by water delivered from the Colorado River system for over a century. Beginning in 1915, water used for irrigation was delivered through a tributary, Sixth Water Creek, with daily summer flows that were much larger than natural flows. This caused drastic change to the rivers, as they became wider and vegetation along the channel margin and floodplain was destroyed. Management changes in 1997 and 2004 reduced the amount of water and sediment added to the river. In this study, we sought to understand how Sixth Water and Diamond Fork changed in the past and what the implications are for the future.

We used data from a variety of sources to describe how and why the river changed in the past. Our results indicate that parts of the river that are not confined by valley walls became very wide during the period of elevated flows and narrowed after the change in management in 1997. Confined reaches experienced minor changes over the period of record. Areas of the channel that were most dynamic in the past are the most susceptible to future change because they have finer sediment that is more easily erodible. Areas that did not experience past changes are unlikely to change in the future without direct intervention from humans or beaver. The findings of this study improve our understanding of Sixth Water and Diamond Fork, and confirm the importance of past changes and valley confinement.

ACKNOWLEDGMENTS

This work was primarily funded by the Utah Reclamation and Mitigation Conservation Commission, and would not have been possible without the support of the Central Utah Water Conservancy District. I would also like thank the USGS Water Science Center in West Valley City and the Spanish Fork District of the Uintah National Forest for access to historical records and photographs.

I would like to thank my co-advisors Peter Wilcock and Patrick Belmont for their support throughout my time at Utah State. The two of them employed something of a yin and yang advising style that provided me with diverse perspectives on how to approach questions and conduct science. Through their insight I grew as a geomorphologist and learned how to think more critically about data collection and interpretation.

The Diamond Fork project has helped me to see the challenges and opportunities of interdisciplinary work. Many thanks to the other members of the Diamond Fork project – Peter, Patrick, Edd Hammill, Trisha Atwood, Josh Epperly, Jereme Gaeta, Brendan Murphy, Hannah Moore, Scott Dietrich, and Jacob Stout – for constructive meetings and a willingness to do the hard work of interdisciplinary, management driven work. I am grateful to Jake for countless hours of field work and conversations about the Diamond Fork, as well as his scientific and personal perspective that had a strong impact on my approach to the project.

Many thanks to my friends and family. The Belmont Lab provided consistent support and academic feedback that has improved my research and presentation skills. Friends I made here helped Logan feel at least a little bit like home. And nothing I do would be possible without my parents, who instilled in me a sense of hard work, a love of learning, and values that shape the way I see the world.

Jabari Coleman Jones

CONTENTS

LIST OF TABLES

LIST OF FIGURES

Figure Page

1. INTRODUCTION

The form of an alluvial river channel is determined by the quantity and size of sediment supplied to the river, the flow regime, the channel gradient, and a variety of other factors (Lane, 1955; Leopold and Wolman, 1957; Schumm, 1977). When one element of this balance is altered, the river adjusts its geometry and grain size to accommodate the change. If flow and sediment supply conditions are stationary over a sufficiently long timescale, the river will reach a new equilibrium state (Leopold and Maddock, 1953; Langbein and Leopold 1964). However, rivers are subjected to a range of disturbances, including extreme flows or large inputs of sediment, and the return period of disturbances is typically shorter than the time required to reach equilibrium. As a result, the form of a river at any given time reflects a combination of past disturbances and current conditions.

Humans are powerful geomorphic agents acting on a relatively short timescale. Humans have altered the supply of water and sediment to nearly all rivers (Hooke, 2000; Wilkinson and McElroy, 2007) and make direct alterations to river channels, through the construction of dams, levees and bridges, as well as in channel gravel mining (Gregory, 2006). Human actions can also change hydrology and sediment supply through land use and land cover change, flow diversions, and subsurface drainage (Gregory, 2006; Belmont et al., 2011; Hooke et al., 2012; Buffington, 2012; Rhoads et al., 2016; Kelly et al., 2017). Predicting how rivers will change in response to human activities and natural disturbances is an essential question for basic geomorphic research and for river management (Dean et al., 2016).

There are currently many methods to predict river response. Lane (1955) proposed a balance between water supply and sediment supply, which is used conceptually to indicate whether a river will be aggradational or degradational. Lane's balance represents the interaction between sediment supply and transport capacity – the ability of a river to transport the supplied sediment with the available water. Lane's balance is formulated as: $Q_s{*}D \propto Q_w{*}S$, where Q_s is

sediment load, D is grain size, Q_w is discharge, and S is channel gradient. This relatively simple relation is a valuable conceptual tool to understand river response, though it does not quantify how channels will change (Henderson, 1966) and therefore is of limited use when multiple factors change simultaneously. In a simplified system such as unisized sediment transport in a flume, change in Q_s, D, or Q_w will directly produce a change in S, as indicated by Lane's balance (Schumm and Khan, 1972). Natural systems are more complex, however, and channel change can take a wide variety of forms. In addition to slope adjustments, channel change can include changes in channel sinuosity and planform (Schumm, 1985; Van Steeter and Pitlick, 1998; Kondolf et al., 2002; Liébault and Piégay, 2002), bed texture (Dietrich et al., 1989; Lisle et al., 1993; Schmidt and Wilcock, 2008), channel width, and depth (Leopold and Maddock, 1953; James, 1991; Surian et al., 2009; Call et al., 2017; Lauer et al., 2017).

Other methods to estimate channel form attempt to accommodate more complex changes. These include channel stability relations (Leopold and Wolman, 1957), quantifying the relative change in transport capacity and supply (Schmidt and Wilcock, 2008; Call et al., 2017), examining temporal and local variation in stream power (Graf, 1983; Gartner et al., 2015), and the development of conceptual models of channel evolution (Schumm et al., 1984; Cluer and Thorne, 2014). Each of these methods has limitations and thus, applying any one method to predict channel change would necessarily be incomplete because geology, climate, vegetation, land use, and disturbance history all influence channel form in complex and heterogeneous ways (Phillips, 2001; Grant et al., 2003; Brierley and Fryirs, 2005). As a result, similar changes in sediment supply and discharge may lead to very different degrees or types of channel change in different rivers or different reaches (Phillips, 2001; Grant et al., 2003; Brierley and Fryirs, 2005; Gaeuman et al., 2005; Dean et al., 2016). Where information is available, the most robust estimate of future channel form would combine each of these methods, i.e. consider the fundamental controls on channel form, identify important discharge thresholds that will influence

channel geometry, estimate how sediment supply and discharge have changed over time, identify areas that are likely to be in sediment surplus or sediment deficit, and track the historical evolution of the channel.

Many studies of channel change have focused on channel width, because channel width has been thoroughly examined in geomorphic literature (e.g. hydraulic geometry) and because measurements of width often represent the only long term channel geometry dataset, derived from historical imagery. Channel narrowing commonly occurs when water is extracted from a river or upstream reservoirs reduce flood peaks and sediment supply (Graf, 1999). When the discharge decreases, alluvial channels tend to narrow, as predicted by hydraulic geometry (Leopold and Maddock, 1953; Li et al., 2015). The mechanisms of narrowing include lateral accretion of floodplains, encroachment of vegetation onto formerly active bars and channel incision that disconnects channel and floodplain (Pizzuto, 1994; Van Steeter and Pitlick, 1998; Allred and Schmidt, 1999; Gurnell, 2014). Channel narrowing often occurs unevenly, with wide, unconfined areas of the channel narrowing more rapidly than narrow areas, such that channels approach a more uniform width (Kondolf et al., 2002; Rinaldi, 2003; Cadol et al., 2011; Dean and Schmidt, 2011). Increases in discharge are also common, as trans-basin diversions, urbanization, and other land use changes can increase base and peak flows (Wolman, 1967; Kellerhals et al., 1979; Kelly et al., 2017; Belmont and Foufoula-Georgiou, 2017). An increase in discharge can promote channel widening, primarily through bank erosion (Leopold and Maddock, 1953; Kellerhals et al., 1979; Bradley and Smith, 1984; Snyder and Kammer, 2008; Lauer et al., 2017).

Sixth Water Creek and the Diamond Fork River in central Utah have experienced substantially altered sediment and flow regimes over the past century. Throughout most of the 20th Century, the rivers were used to convey trans-basin diversions from the Colorado River Basin to central Utah, across the continental divide. Diversion flows greatly exceeded the natural summer discharge and regularly exceeded the peak natural runoff. Between 1997 and 2004, a

system of pipes and tunnels was installed adjacent to the channel to transmit the trans-basin diversion, such that instream flows were greatly reduced compared to the diversion flows of the 20th Century. A small portion of the diversion flows are still released to the channel, maintaining base flows much larger than natural. Sixth Water and Diamond Fork provide a unique opportunity to study channel response to both flow augmentation and flow reduction. There were exceptionally large augmented flows for 80-90 years (depending on location), followed by a return towards the natural flow regime, but with augmentation of all flows, and exceptionally large base flows for the past 15-20 years.

In this study we examine channel response to this unique flow history and evaluate the potential for future channel change on Sixth Water and Diamond Fork. We examine how channel change depends on factors such as valley confinement, slope, substrate size, and vegetation, all of which vary throughout the watershed. We attempt to answer several primary research questions: How have the channels of Sixth Water and Diamond Fork changed during the last century of flow alteration? How have they responded to reduced flows since most of the diversion flows have been removed from the channel? How have changes in flow altered the primary sources and sinks for fine and coarse sediment in Sixth Water and Diamond Fork? How have the magnitudes of sediment supply and sediment storage changed over time?

2. STUDY AREA

The Diamond Fork watershed drains 400 km^2 of mountainous terrain in the Wasatch Mountains of central Utah. The catchment is primarily underlain by Mesozoic sedimentary rocks, with narrow valleys, inactive and active landslides, and alluvial fans controlling valley-bottom geometry (Fig. 2.1). Elevations range from 1500 m at the mouth of Diamond Fork to 3100 m in the uppermost parts of the watershed. Mean precipitation in the basin is 660 mm/year, with the majority falling as snow in the winter months (PRISM Climate Group, 2004). The natural

hydrograph of the river is dominated by a spring snowmelt peak, but the hydrology of the river has been highly altered by flow augmentation.

The Diamond Fork and its largest tributary, Sixth Water Creek, have been used to convey trans-basin diversions from the Colorado River basin for over a century. The first water delivery system to the Diamond Fork watershed, Strawberry Tunnel, was completed in 1913, and releases began in 1915 (Bureau of Reclamation, 1916). The tunnel delivers water from the Strawberry Reservoir directly into the headwaters of Sixth Water Creek, which joins the Diamond Fork 16 km downstream of Strawberry Tunnel (Fig. 2.2). The diverted water is used for irrigation and is delivered based on demand. Before 1997, all trans-basin diversion flows were delivered from Strawberry Tunnel and carried in the stream channel. During this period, flow diversions between 400 and 500 cfs were common during the peak of the growing season, from May to September, as represented by the green dashed line in Fig. 2.3. These flows greatly exceeded the natural summer flows, as shown by the solid red line in Fig. 2.3, and often exceeded the peak runoff each year (Fig. 2.3). Typically, no flows were released between October and April, so that winter flows from 1915 – 1997 were similar to those of the natural flow regime (Fig. 2.3).

As a component of the Central Utah Project Completion Act, a series of pipelines and tunnels were constructed to carry the trans-basin diversion flows and bypass Sixth Water Creek and Diamond Fork River (U.S. Congress, 1992). Syar Tunnel, completed in 1996, transports water from the Strawberry Reservoir to the Syar Tunnel Outlet, located ~10 km downstream from Strawberry Tunnel (Fig. 2.2). Syar Tunnel operation began in 1997, after which time diversion flows bypassed Upper Sixth Water Creek. The Diamond Fork Tunnel and Pipeline system became operational in 2004 and with the construction of this system, diversion flows can entirely bypass the river channel. The pipe and tunnel system includes two flow control structures, one on Sixth Water Creek at Syar Tunnel and one at Monks Hollow Outlet, located 12 km upstream from the mouth of Diamond Fork River (Fig. 2.2).

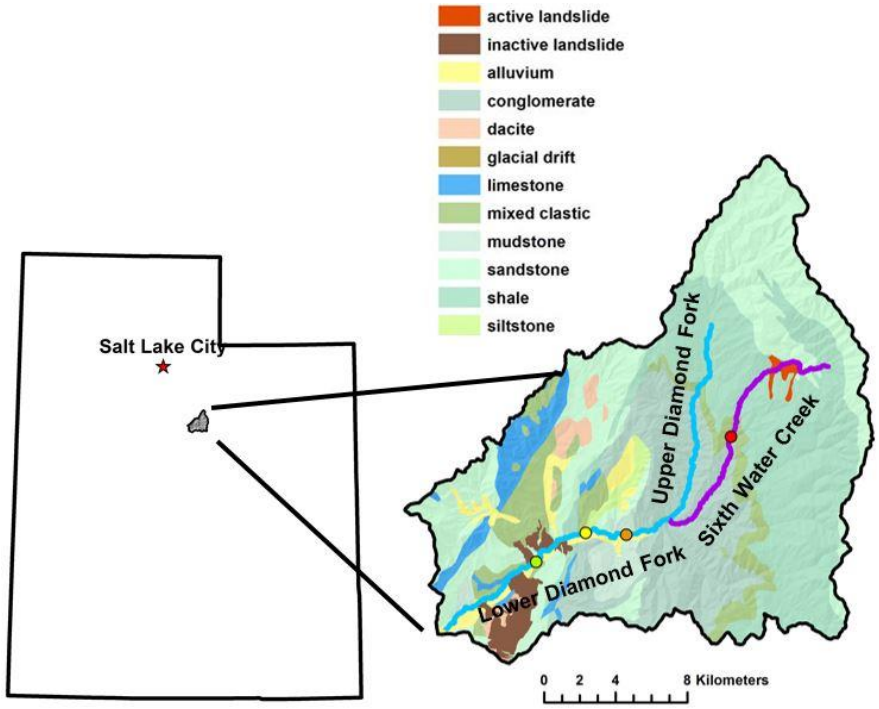

Fig. 2.1. Location map and geologic map of the Diamond Fork watershed in Utah, USA including location of USGS gages. Gages include Sixth Water Creek above Syar Tunnel (red), Diamond Fork above Red Hollow (orange), Diamond Fork below Red Hollow (yellow), and Diamond Fork near Thistle (green).

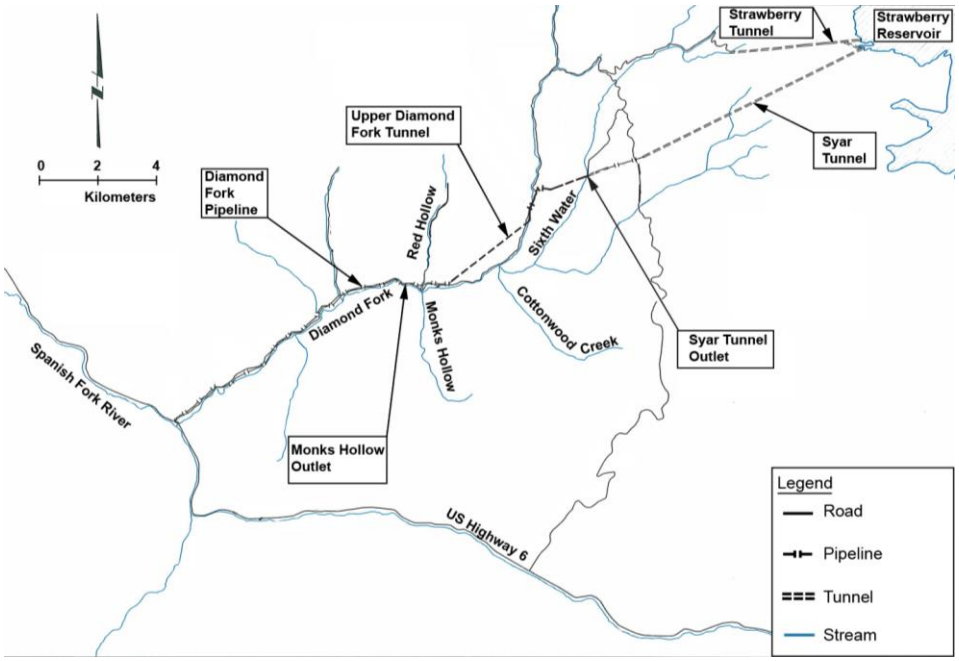

Fig. 2.2. Map showing components of the Diamond Fork water delivery system. Modified from U.S Bureau of Reclamation.

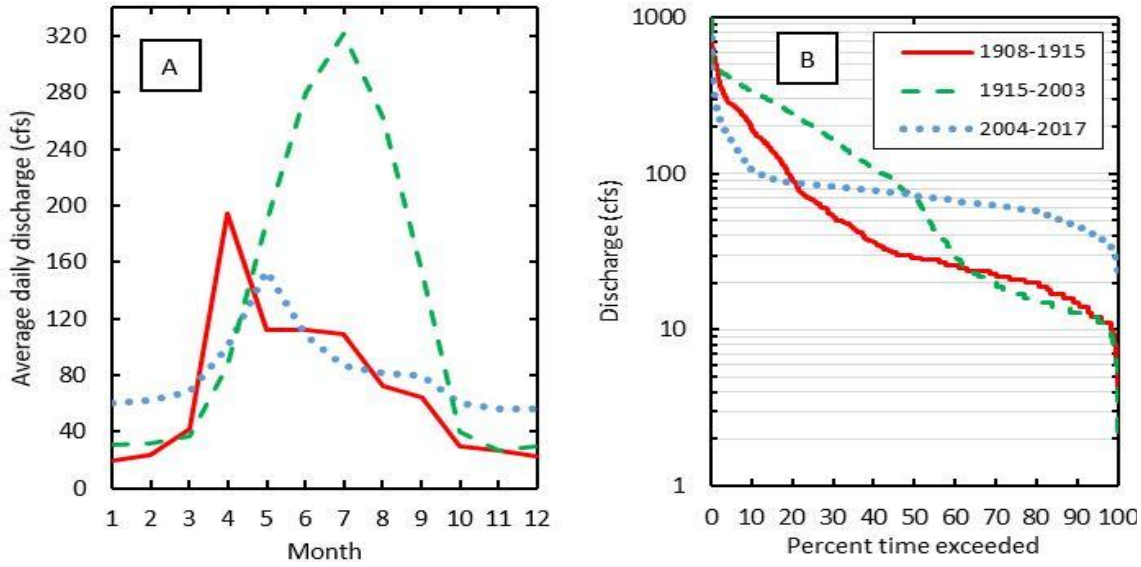

Fig. 2.3. Discharge statistics for three periods of gage data on the lower Diamond Fork. A) Mean monthly discharge and B) flow exceedance curve. The three time periods represent pre-diversion flows (1908-1915), the irrigation flows (1915-2003), and current flow regime (2004-2017).

Although trans-basin diversions can be entirely conveyed by the pipe and tunnel system, diversion water is still discharged into the Sixth Water/Diamond Fork stream channel to meet mandated minimum flow requirements. Minimum flows were implemented in 2004 as part of the environmental commitments of the Central Utah Project Completion Act (U.S. Congress, 1992). The minimum flow requirements are 32 cfs in the summer (May 1 – October 31) and 25 cfs in the winter (November 1 – April 30) as measured at the USGS gage on Sixth Water Creek (Table 2.1, USGS gage 10149000 Sixth Water Creek above Syar Tunnel near Springville, UT), and 80 cfs in the summer (May 1 – September 30) and 60 cfs in the winter (October 1 – April 30) at the USGS gage on lower Diamond Fork (USGS gage 10149400 Diamond Fork above Red Hollow near Thistle, UT). The flows are met by releasing water from each of the tunnel outlets: Strawberry Tunnel Outlet, Syar Tunnel Outlet, and Monks Hollow Outlet. The mandated minimum flows, represented by the dotted blue line in Fig. 2.3, substantially exceed the natural base flow of the

system, particularly in late summer, but are greatly reduced in comparison to the irrigation flows of the 20th Century (Fig. 2.3).

Several large floods have impacted Sixth Water and Diamond Fork during the period of record (Fig. 2.4). The largest recorded flood on the lower Diamond Fork occurred in 1952, with a peak of 1610 cfs. The second largest flood occurred in 1954, at 1020 cfs. The river was ungaged in the early 1980s, but 1983 and 1984 were very large flows years across the state of Utah, and the peak flow in 1984 likely exceeded that of 1952. Since the implementation of mandated minimum flows in 2004, the largest floods occurred in 2006 (peak flow of 531 cfs at the Diamond Fork above Red Hollow gage) and 2011 (peak flow of 887 cfs).

Table 2.1. Period of record of USGS gages on Sixth Water and Diamond Fork.

Gage number	River	Location	Period of record
10149000	Sixth Water	Above Syar Tunnel	Oct 1998 – Present
10149400	Diamond Fork	Above Red Hollow	Oct 2001 – Present
10149500	Diamond Fork	Below Red Hollow	Dec 1953 – Jun 1969, Feb 1989 – Nov 2001
10150000	Diamond Fork	Near Thistle	Mar 1909 – Apr 1911, Mar 1940 – Dec 1956

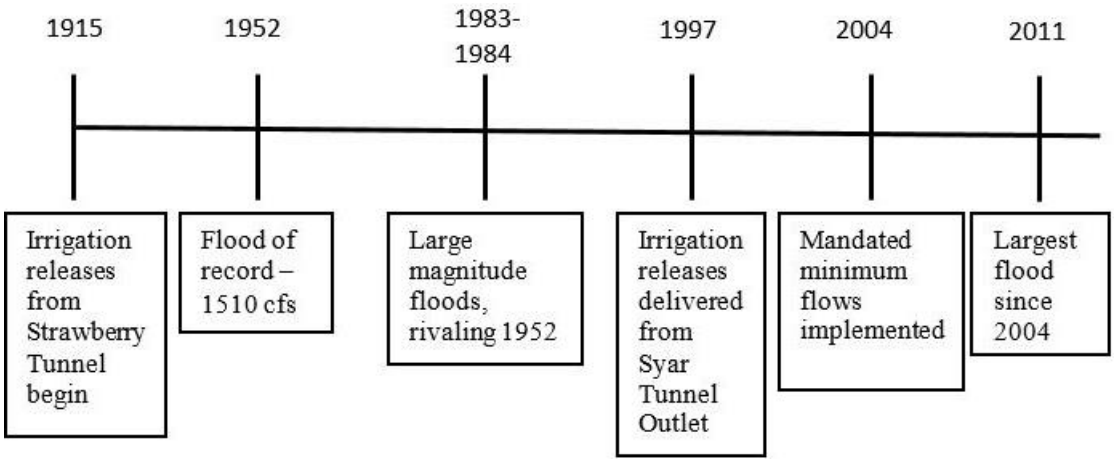

Fig. 2.4. Timeline of significant hydrologic events on Sixth Water and Diamond Fork.

3. METHODS

3.1. Process domain delineation

Channel response to changes in water and sediment supply will be mediated by a range of factors, including the degree to which the channel is confined within its valley, valley slope, and local rock type. We used the River Styles Framework (Brierley and Fryirs, 2005) to delineate different process domains, with the expectation that channel response within each process domain will show less variation than between process domains. We used valley setting, floodplain composition, hillslope and channel gradient, bedrock type, tributary junctions, and channel substrate to define breakpoints between process domains.

3.2. Historic channel change

3.2.1. Planform measurements

We mapped the active channel, wetted channel, number of channel threads, bar surfaces, and islands at 1:1000 scale using ArcMap 10.4 for each year of available imagery (Table 3.1). We defined the active channel as the wetted channel plus the area of the floodplain where vegetation is unable to colonize due to fluvial scour or frequent inundation (Gendaszek et al., 2012; Lauer et al., 2017). We defined bars as subaerial surfaces with no vegetation and differentiated bars as bank attached or mid-channel. Islands were defined as mid-channel features with vegetation. We computed the area of wetted channel, bars, and islands directly in ArcMap.

We measured active channel width for each set of aerial imagery using the Planform Statistics Toolbox in ArcGIS (Lauer, 2006). The tool allows a user to input a shapefile with a left bankline and right bankline, from which it interpolates a centerline, and calculates channel width at a user-specified interval. We used a 10 m interval for each year of available imagery. We then calculated summary statistics (minimum, maximum, median, mean, and 1st and 3rd quartiles) of channel width for each process domain in each year to support an evaluation of changes in

channel width over time.

To quantify the response of channel width to the change of flow regime in 2004, we conducted a quantile regression on the channel width data from 1993 to 2016. This period encompasses the end of the irrigation flow regime, the 1997-2004 transitional period – when large flows were released from the Syar Tunnel Outlet, and the current mandated flow regime (Fig. 2.4). Quantile regression is similar to a standard linear regression, but linear trends are fitted through quantiles of data rather than the mean (Cade and Noon, 2003). The slope of each regression line can then be plotted to visualize the changes in quantiles over time (Fig. 3.1). This provides a more robust assessment of changes across the full spectrum of data compared to conventional regression techniques, and can reveal trends that may be obscured by analyzing only the mean of a dataset (Cade and Noon, 2003).

Table 3.1. Aerial photographs used for planform measurements.

Year	Source	Scale/Resolution	Color	Flight Date	Discharge at Diamond Fork gage (cfs)
1939	Soil Conservation Series	1:30000	B&W	July 21	N/A
1953	Army Map Series	1:63000	B&W	Aug 4	42
1956		1:20000		July 16	293
				July 23	245
1981	USGS NHAP	1:40000	False color	Sep 11	N/A
1982	NHAP	1:40000	False color	Sep 23	N/A
1983	NHAP	1:40000	False color	Sep 5	N/A
1985	NHAP	1:40000	False color	July 31	N/A
1993	USGS DOQQ	1:40000	B&W	Aug 17	205
				Aug 23	423
				Aug 24	440
				Aug 28	397
				Sep 09	197
1995	Trihey & Associates	2 meter	Color	Nov	18

Table 3.1 (cont.)

1997	DOQQ	1:40000	B&W	Jul 7	377
				Sep 30	238
				Oct 4	27
				Oct 5	26
2003	USDA NAIP	2 meter	Color	Aug 31	219
				Sep 03	203
2004	NAIP	1 meter	Color	Aug 28	88
2006	NAIP	1 meter	Color	Aug 26	92
				Aug 28	90
				Aug 31	90
				Sep 02	93
				Sep 03	89
2009	NAIP	1 meter	Color	Jul 10	85
				Aug 10	79
2011	NAIP	1 meter	Color	Aug 06	86
2014	NAIP	1 meter	Color	Aug 11	82
				Sep 03	82
2016	NAIP	1 meter	Color	Aug 2	48
				Aug 19	45

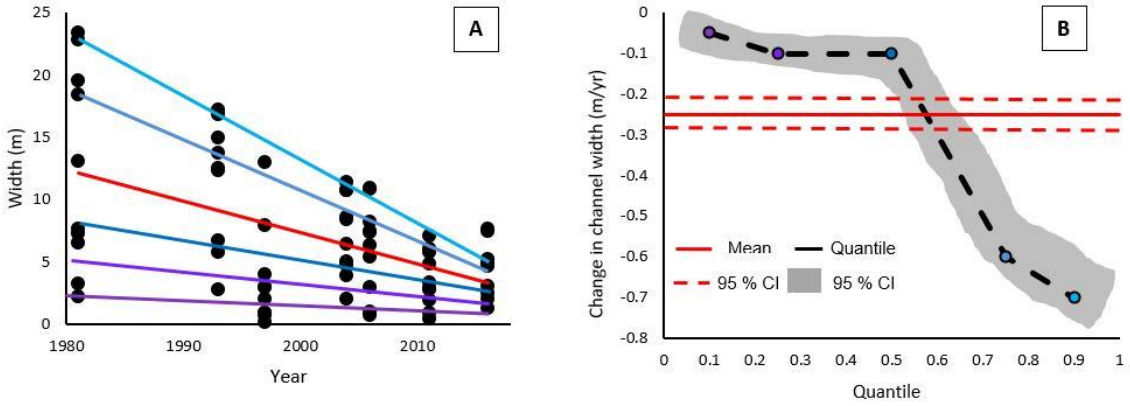

Fig. 3.1. Conceptual illustration of quantile regression. A) Trendlines fitted through different quantiles of data (5th, 25th, 50th, 75th, 90th) as well as the mean, which is shown in red. B) Slope, and 95% confidence interval for each quantile (colored dots) and the mean (red line).

We calculated sinuosity for each process domain using channel centerlines for each year of available imagery by using the Stream Gradient and Sinuosity Toolbox (Dilts, 2015). Sinuosity is known to vary with measurement scale, with longer reaches typically having greater sinuosity (Andrle, 1996). To address this issue, we calculated sinuosity using reach lengths of 100 m, 500

m, and 1000 m, as well as the total length of the process domains (ranging from 2170 m to 6500 m). The 100 and 500 m reach lengths consistently underpredicted sinuosity, and the total length of process domains was chosen as the most robust and repeatable measurement of sinuosity.

3.2.2. Error analysis for aerial photograph measurements

Measurements in air photo analysis are subject to digitization error and co-registration error (Mount and Louis, 2005; Swanson et al., 2011; Lea and Legleiter, 2016). To constrain digitization error, we re-digitized selected reaches four times and calculated summary statistics of channel width, as described above (Toone et al., 2014). The reaches encompassed a variety of channel edge types – overhanging vegetation, areas covered by shadow, and clear banks. Standard error was calculated for each edge type. To assign a single error metric for each process domain, we calculated the percentage of each process domain covered by each edge type and calculated a weighted average of the standard error based on the proportion of each edge type.

Co-registration error was constrained using the method of Lea and Legleiter (2016), in which a spatially variable error surface is constructed based on a network of ground control points (GCPs). We used the 2016 imagery as our reference image and calculated the distance between GCPs for every historic image and the 2016 GCPs. X error and Y error were calculated for every GCP, and X and Y error surfaces were created for each year of imagery by natural neighbor interpolation. We extracted the value of X and Y error at the left and right bank of the active channel polygon at 10 m intervals and computed the difference between the two. The extracted value represents the amount of co-registration error at each point along the channel. We calculated the average co-registration error for each process domain by averaging the value extracted at each 10 m interval. Total error was defined as the sum of squares of the digitization and co-registration error measurements (Toone et al., 2014; Lea and Legleiter, 2016).

3.2.3 Analysis of historical changes in mean streambed elevation

Cross-sections surveyed during discharge measurements at USGS stream gages offer a long-term record of channel geometry data. Each field measurement of discharge is accompanied by a gage height measurement and a cross-section measurement that includes channel width, area, and velocity. These measurements can be used to reconstruct streambed elevations, following the method of Jacobson (1995) and Smelser and Schmidt (1998). The mean streambed elevation is calculated from a USGS discharge measurement as:

$$MSBE = gage\ datum\ height + gage\ height - mean\ depth \quad \text{(Eqn. 3.1)}$$

where $Mean\ depth = Area/width$ (Eqn. 3.2)

We applied the mean streambed elevation analysis to three gages on Diamond Fork – Diamond Fork near Thistle, Diamond Fork Above Red Hollow, and Diamond Fork Below Red Hollow – to analyze vertical adjustment of the river. The three Diamond Fork gages have a non-continuous record that extends from 1940 – present. (Table 2.1).

3.2.4. Fluvial surface mapping

We classified and mapped fluvial terraces, floodplains, and relict channels throughout Sixth Water and Diamond Fork in order to understand the evolution of the Sixth Water and lower Diamond Fork valleys and to assess incision in the system. We used historic aerial imagery and a 2017 lidar dataset collected by the National Center for Airborne Laser Mapping to map features, identify their age, and measure their height above the 2017 channel. We delineated these surfaces using a range of information, relying in particular on slope breaks in the lidar DEM. We identified surfaces present in the 2017 DEM and constrained their age based on the oldest photo in which that surface appeared without any substantial change in subsequent years. We then assigned the year of the first photo as a minimum age of formation, as the surface must have

formed before the photo was taken. To calculate the height of features above the 2017 channel, we created a detrended DEM and calculated the average height within each delineated polygon.

3.2.5. Topographic cross-section re-surveys

Cross-sections at four sites were surveyed in 2005, 2006, and 2007 (BioWest, 2007). We re-surveyed the cross-sections in 2017 using RTK GPS. The location of the wetted channel was noted in each survey, and we calculated area, width, and average depth for the wetted channel. We also extracted the minimum and mean bed elevation within the wetted channel to assess aggradation and incision. We compared channel geometry and bed elevation between surveys to identify changes in channel geometry.

3.2.6. Sediment source measurements

To measure the relative contribution of sediment from hillslopes, we measured the length of active hillslopes along Sixth Water in ArcMap for four sets of air photos – 1956, 1981, 2006, and 2016. We defined active hillslopes as those in contact with the active channel with no vegetation growing at the toe of the slope. We validated the measurements from the 2016 air photos with field observations in October 2017. All active hillslopes identified on air photos were also identified in the field. To constrain uncertainty, we measured the length of hillslopes in the 2016 imagery that would not have been identified as active without field observation, due to shadows or image quality. The relative uncertainty was then calculated and applied to the measurement from each year.

A large active landslide exists adjacent to Sixth Water, approximately 2 km downstream from Strawberry Tunnel (Fig. 2.1). The landslide is in the Green River formation – a unit of interbedded shale and calcareous mudstone. This landslide was likely a significant source of sediment during the time period when large diversion flows were released from Strawberry Tunnel. We measured the offset of features in aerial photographs to estimate movement rates of

the landslide over time. The position of approximately 100 trees that could be reliably identified in aerial photographs from 1993 to 2016 was recorded for each set of imagery. We measured the offset of each tree in successive images to constrain the rate of movement. We calculated uncertainty by extracting the co-registration error from spatially variable error surfaces and used this value to constrain uncertainty. Aerial photographs prior to 1993 could not be rectified with high enough precision to estimate movement on the landslide.

3.2.7. Sixth Water valley cross-sections

We extracted cross-sections upstream and downstream of the Strawberry Tunnel Outlet using the lidar dataset to evaluate incision of Sixth Water caused by irrigation flows. We extracted four cross-sections upstream and four cross-sections downstream of the tunnel outlet. We then normalized the cross-sections to the deepest point to aid the comparison.

3.3. Contemporary channel behavior

Nine sites were chosen for co-located macroinvertebrate, fish, and geomorphic sampling as part of a broader project to which this research contributes. The sites are distributed throughout the watershed to examine longitudinal variation in ecological and geomorphic trends (Fig. 3.2). We revisited the sites multiple times in 2016 and 2017 for pebble counts, unmanned aerial vehicle photography, and topographic surveys. Eight additional sites were selected for sediment transport measurements (Fig. 3.2).

The two field seasons (2016 and 2017) had different hydrologic characteristics, with base flows and peak flows differing between the two years (Fig. 3.3). The first year of our field campaign, 2016, had small spring runoff and summer base flow on lower Diamond Fork gradually decreased from 80 cfs to ~50 cfs. The second year, 2017, had a moderate magnitude, long duration spring runoff and summer base flow was maintained using diversion releases at 80 cfs (Fig. 3.3). A flash flood caused by a convective thunderstorm occurred on Cottonwood Creek

– a tributary that joins lower Diamond Fork about 20 m downstream of the confluence between Diamond Fork and Sixth Water – on July 19, 2017 and caused a peak flow of 712 cfs, as measured at the USGS Above Red Hollow gage (Fig. 2.1). The duration of the flood was short (~2 hours) and the flood peak attenuated sharply as it moved down lower Diamond Fork. The flood delivered fine sediment to the lower Diamond Fork, leaving visible deposition along the channel margin and floodplain. Flow releases were conducted in September 2017 in order to evaluate sediment, channel, and ecosystem response to flows of specific magnitude and duration. Two flow steps were used, each of one-week duration, with magnitude 50 and 100 cfs at the Sixth Water gage and magnitude 100 and 150 cfs at the Diamond Fork gage (Fig. 3.3). On Sixth Water, these flows have a natural return interval of ~1 year for the lower flow and ~4 years for the higher flow. On lower Diamond Fork, 150 cfs has been exceeded by the spring runoff for every year in the gage record. Flows were held to a minimum before, between, and after the step flows.

3.3.1. Pebble counts

To assess channel substrate at the ecological monitoring sites, we conducted Wolman pebble counts ($n \geq 100$) every two months from spring to fall in 2016 and 2017, concurrent with macroinvertebrate sampling (Wolman, 1954). We analyzed the pebble counts to determine differences in substrate between sites and to identify any changes in bed sediment composition over time.

3.3.2. Painted rock tracers

To gain insight into sediment entrainment and transport, we placed painted gravels as tracers at eight sites – seven monitoring sites and one site downstream of the landslide adjacent to Sixth Water (Fig. 3.2). Tracer grain size distribution was set to match the bed material at each site (Appendix A). We placed the grains in lines perpendicular to the stream by replacing clasts of similar size (Erwin, et al., 2011). After each high flow in the stepped flow experiment, we noted

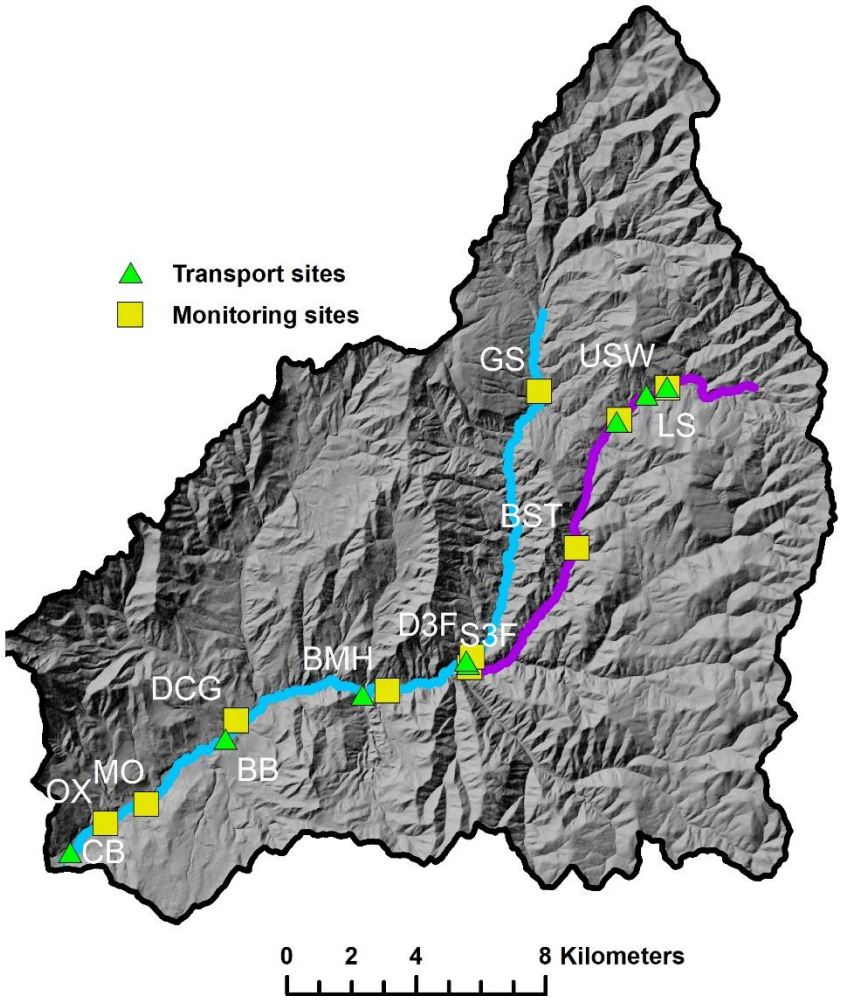

Fig. 3.2. Location of monitoring and sediment transport sites on Sixth Water and Diamond Fork. Monitoring sites: USW – Upper Sixth Water, ARC – Above Rays Crossing, BST – Below Syar Tunnel, S3F – Sixth Water at 3 Forks, GS – Guard Station, D3F – Diamond Fork at 3 Forks, BMH – Below Monks Hollow, DCG – Diamond Campground, MO – Motherlode, and OX – Oxbow. Transport sites: USW – Upper Sixth Water, LS – Landslide, ARC – Above Rays Crossing, S3F – Sixth Water at 3 Forks, D3F – Diamond Fork at 3 Forks, BMH – Below Monks Hollow, BB – Brimhall Bridge, and CB – Childs Bridge.

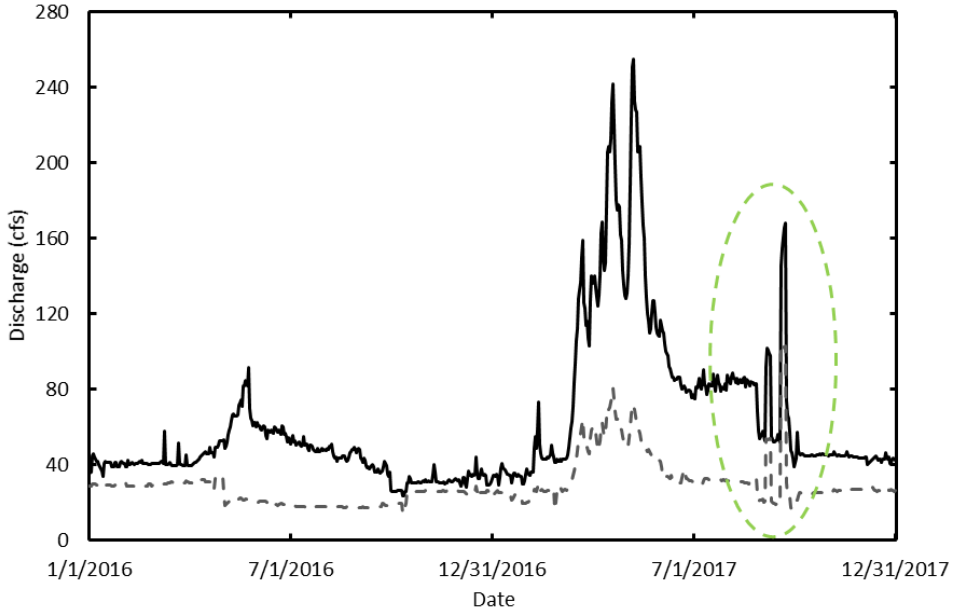

Fig. 3.3. Hydrograph of lower Diamond Fork (solid line) and Sixth Water (dashed line) for the period from January 1, 2016 to December 31, 2017. The stepped flow experiment is highlighted by the green dashed circle.

entrainment and measured the transport distances of mobile grains. Because placing grains on the bed does not fully simulate natural grain geometry, we did not consider grains to be mobile unless they moved more than 1 m. We also assumed that tracers we did not find in the vicinity of placement had been transported downstream, because aggradation and burial at our tracer sites was minimal.

3.3.3. Radio frequency identification tagged tracers

To augment the painted rock tracer study, we deployed gravels and cobbles that were embedded with radio frequency identification (RFID) tagged tracers. These tags allowed us to determine whether or not grains had been buried and allowed us to more easily find grains that were transported downstream. We used 12 mm and 23 mm RFID tags (Fig. 3.4A); the smaller tags were used in 22.6 and 32 mm grains and the larger tags in grains ≥ 32 mm. The RFID tags, were placed in a cut sliced into each rock with a rock saw (Liébault et al., 2012) and sealed with

marine epoxy (Fig. 3.4B). After the sealant dried, we painted the grains white to aid visual identification in the field. We recorded the ID of each rock and gave each a simplified identification number that was written on the rock using a permanent marker for field identification and as a backup in case the RFID tag failed (Fig. 3.4C). We prepared more than 300 rocks in this manner and no rocks were broken during the sawing process. This method provides a promising alternative to the common practice of drilling rocks (Bradley and Tucker, 2012; Olinde and Johnson, 2015).

Prior to the stepped flow experiment, we distributed RFID tagged grains at the Rays Crossing and Motherlode monitoring sites (Fig. 3.5). The grain size of the tracer gravels used at each site spanned the range of bed material measured at the sites where they were placed (Fig.

Fig. 3.4. Pictures of the RFID deployment system. A) 23 and 32 mm PIT tags, B) tracers sealed with marine epoxy, C) tracers painted white and labeled to aid in visual detection, D) tracers deployed in the stream, E) channel spanning RFID antenna powered by a solar panel.

3.5). We selected these sites because they are co-located with ecological monitoring sites and represent relatively dynamic channel segments. We placed 135 gravels at Rays Crossing and 120 at Motherlode. At each site, we placed traces in two locations representative of local geomorphic conditions. To imitate natural bed structure, we removed grains from the bed and replaced them with tracers of a similar size. After placing the grains, we recorded the initial position of each with RTK GPS.

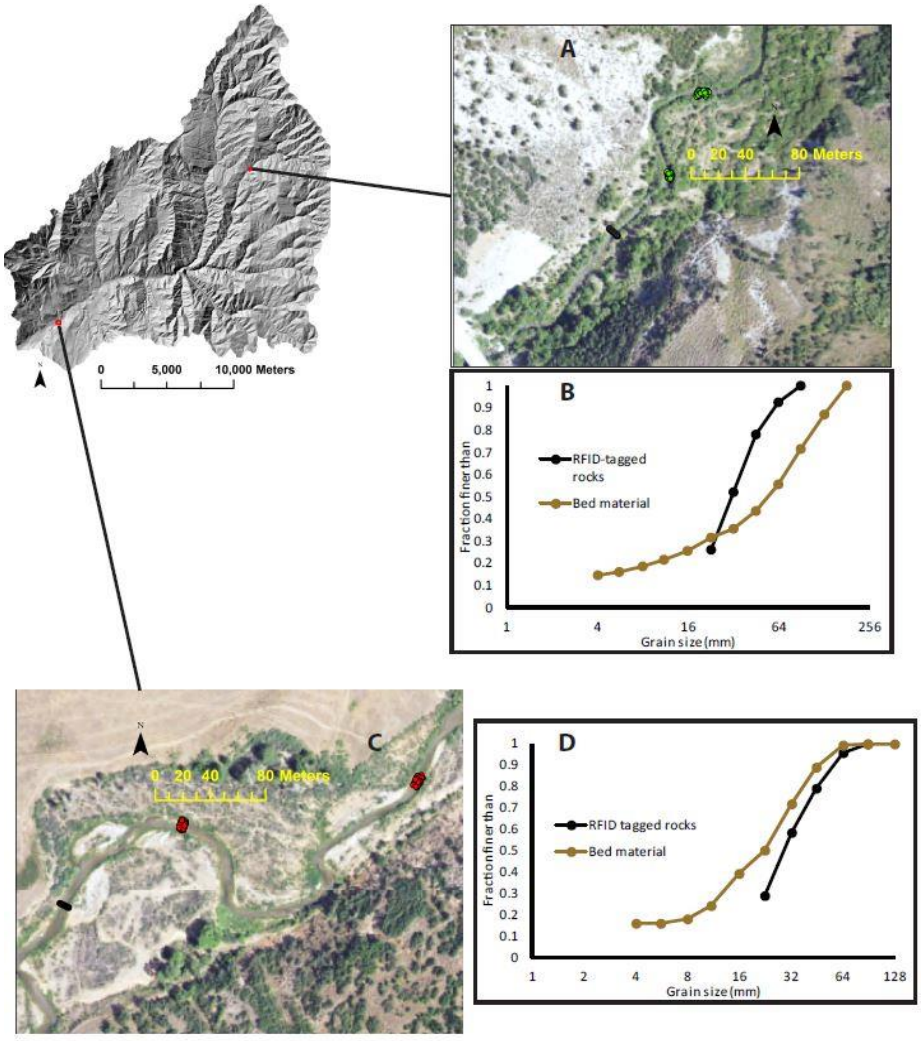

Fig. 3.5. Location and grain size of RFID tracers. A) Location of RFID tracers at Rays Crossing site, B) grain size of tracers at Rays Crossing site, C) location of tracers at Motherlode site, D) grain size of tracers at Motherlode site.

Following the high flow of both stepped flow experiments, we re-located RFID tagged gravels with a portable RFID antenna. The read range of the antenna was ~50 cm and gravels buried 1-2 grains deep were located. We recovered 100% of tracers at the Rays Crossing site, and 98% of tracers at the Motherlode site. Once tracers were identified with the antenna, we recorded their location with RTK GPS. We then computed transport distances for each flow step by measuring the along-stream distance between observations in ArcMap.

3.3.4. Real time kinematic (RTK) GPS channel surveys

We collected high resolution topographic data using Leica RTK GPS rovers in April 2016 and July-September 2017 at each of the ecological monitoring sites (approximately 100 m long). A base station logged data over a fixed point for several hours at each site, and raw data collected by the GPS rovers was corrected using the NOAA online positioning user service. In addition to topography, we surveyed water surface elevations during the stepped flow experiments in September 2017, for future use in sediment transport estimates and hydraulic modeling. Using the topographic survey points, we constructed a triangulated irregular network (TIN) of each site, and derived a digital elevation model (DEM) from the TIN.

We utilized geomorphic change detection (GCD) software to quantify erosion and deposition at two sites where the surveys from 2016 and 2017 were sufficiently detailed (Wheaton et al., 2010, http://riverscapes.xyz). The GCD software calculates the difference in elevation between two DEMs and contains robust methods to constrain uncertainty (Wheaton et al., 2010). The surveys with sufficient detail for GCD analysis were Monks Hollow (comparing surveys before and after the July 19, 2017 flood) and Sixth Water 3 Forks (comparing surveys from April 2016 and July 2017).

3.3.5. Sediment source sampling

During a field campaign in October 2017, we mapped, photographed, and measured the grain size of potential sediment sources on Sixth Water and the lower Diamond Fork. Potential sources were identified in the field as either tributaries, or hillslopes in contact with the channel. Tributary samples were collected from the bed of the tributary and hillslopes were generally sampled no more than 1 m above the channel. We sampled hillslopes that appeared active as well as those with vegetation at the toe. To determine grain size, we extracted and weighed samples from each potential source. Samples were sieved in the field using a gravelometer for grains larger than 64 mm, and sieves for material larger than 22 mm, 8 mm, and 2 mm. The fraction of each size class was weighed to generate a mass-based grain size distribution. Samples weighed at least 5 kg, and the largest grain rarely represented more than five percent of the sample. We located and recorded sample locations in ArcMap to assess the spatial distribution of sediment sources.

3.3.6. Bedload and suspended load sampling

In 2016 and 2017, discharge, bedload, and suspended load transport were measured at eight sites on Sixth Water and Diamond Fork (Fig. 3.2). Sediment transport measurements were conducted over a wide range of discharges to construct a sediment rating curve for each sampling site (Fig. 3.6). We measured discharge using an acoustic Doppler velocimeter concurrent with our sediment sampling. Bedload was measured using different techniques depending on discharge and substrate at each site. For the lowest flows at sites with loose bed material, net frame samplers with a 0.5 mm net were deployed (Bunte et al., 2007). Under other conditions, an Elwha sampler with a 0.5 mm mesh was used. For one high discharge event, the Elwha was deployed from a bridge, otherwise the operator stood in the stream with the sampler. Suspended load was sampled using a depth integrating D-48 sampler (Edwards and Glysson, 1988).

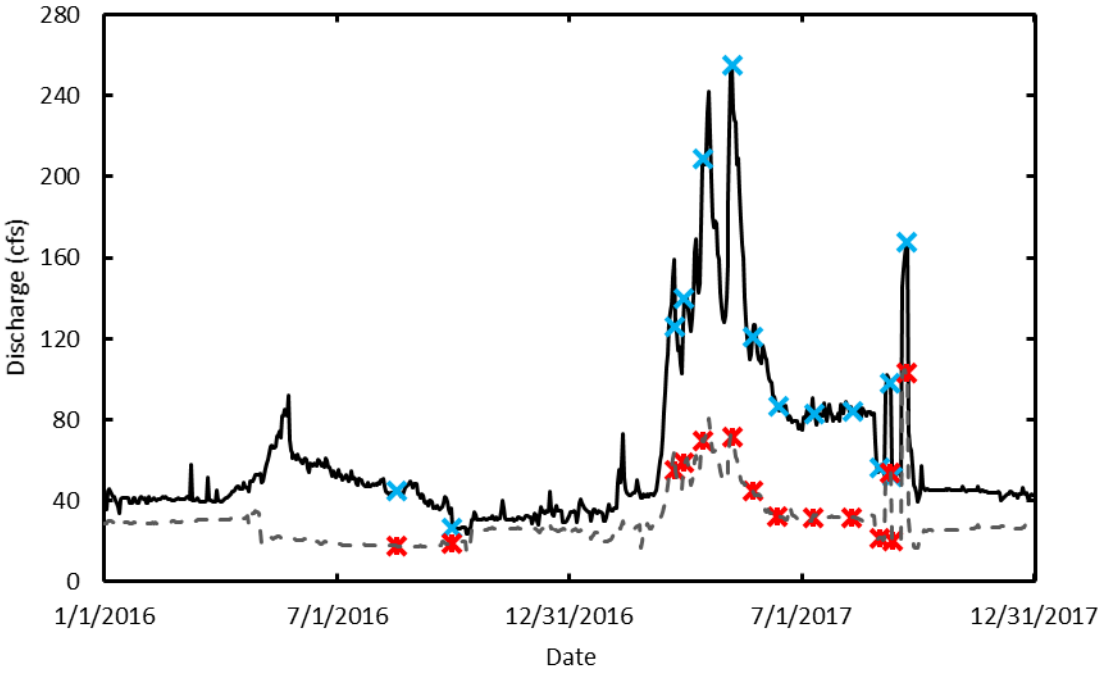

Fig. 3.6. Bedload and suspended load sample dates overlain on hydrograph for Diamond Fork (solid line, blue Xs) and Sixth Water (dashed line, red Xs).

Suspended and bedload sediment were sampled using the equal width increment method (Edwards and Glysson, 1988). For suspended sediment, volumes of water proportional to discharge were collected at equally spaced intervals along a cross-section. The number of intervals varied between sites and discharges. For bedload collected using the Elwha sampler, the sampler was left on the bed for three minutes at 10 equally spaced intervals along a cross-section. We computed overall and size specific transport rates by drying, sieving, and weighing samples.

3.3.7. Unmanned aerial vehicle photography

We collected high resolution aerial imagery at each of the ecological monitoring sites using a DJI Phantom 4 unmanned aerial vehicle (UAV) in spring 2016, summer 2017, and fall 2017. Individual photographs were mosaicked using Adobe Photoshop to create continuous images of the sites. We conducted a qualitative assessment of changes in channel geometry

between successive photos. We identified areas that changed between successive images and drew polygons to highlight geomorphic changes between successive photos.

4. RESULTS

We identified eight process domains between Strawberry Tunnel and the mouth of Diamond Fork (Fig. 4.1), primarily based on degree of valley confinement and valley slope. Channel morphology and channel-floodplain connectivity vary among process domains, so we use process domains to organize a description of channel geometry and channel change.

4.1. Sixth Water Process Domains

The **Upper Sixth Water Canyon** reach extends 2200 m from the Strawberry Tunnel Outlet in a confined valley setting with hillslopes abutting the channel. The bedrock is easily erodible interbedded shale and calcareous mudstone and there are bedrock steps and plunge pools

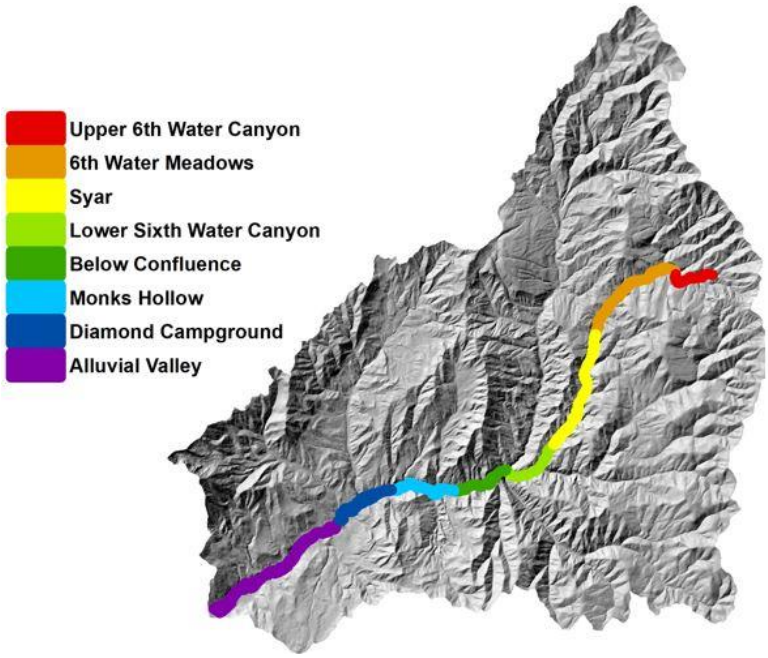

Fig. 4.1. Location of process domains on Sixth Water and Diamond Fork.

where mudstone beds are in contact with the channel. The plunge pool morphology is supported by a steep gradient of 5.3% (Table 4.1). Other bed material includes boulders, and a small proportion of cobbles and gravel (Fig. 4.2). There are very small pockets of floodplain with grass and willow.

The **Sixth Water Meadows** reach is in a partially confined valley setting, with 30% of the channel confined by the valley walls. The confining material is relatively weak, consisting of interbedded shale and calcareous mudstone, along with a large active landslide (Fig. 2.1). Finer sediment (sand and gravel) is present in the channel in areas where the channel abuts the hillslopes. Otherwise the bed material consists of cobbles, with gravel and boulders (Table 4.1). The overall slope of the reach is 4.8%, but there are areas of lower slope, where sediment accumulation can occur. In these areas, floodplain and terrace surfaces line both sides of the channel. Most of the reach lacks topographic complexity. The channel has complex topography only in areas where there are bedrock forced pools or beaver ponds are present (Fig. 4.2). This reach contains two monitoring sites, Upper Sixth Water and Rays Crossing.

Table 4.1. Attributes of process domains on Sixth Water.

Process domain	Percent confinement	Confining material	Slope (%)	Substrate	Geomorphic units	Percent pool	Length (km)
Upper Sixth Water Canyon	73	Shale mudstone	5.3	Bedrock boulder cobble	Bedrock scour pools cascades	21	2.1
Sixth Water Meadows	30	Shale mudstone active landslide	4.8	Cobble boulder gravel	Long runs broken up by beaver dams	19	3.4
Syar Tunnel	64	Limestone sandstone	3.1	Cobble boulder gravel	Runs, few pools and riffles	14	6.0
Lower Sixth Water Canyon	87	Conglomerate	4.0	Boulder bedrock cobble gravel	Bedrock scour pools cascades	35	3.0

Fig. 4.2. Representative photographs of process domains on Sixth Water. A) Upper Sixth Water Canyon, B) 6th Water Meadows, C) Syar, D) Lower Sixth Water Canyon.

The **Syar** reach is mostly confined, with 60% of the channel confined by valley walls. Bedrock in the reach is limestone, sandstone, and mudstones that are more resistant than the bedrock in upstream reaches (Table 4.1). The majority of the reach is made up of long runs with few bedrock forced pools and pool-riffle sequences (Fig. 4.2). Cobbles are the primary bed material, with gravel sourced from local hillslopes and tributaries. The slope of this reach is the lowest on Sixth Water, at 3.1%, but floodplain surfaces are discontinuous and only where the valley is locally unconfined. The Syar Tunnel outlet enters at the upstream end of this reach and the Below Syar Tunnel monitoring site is just downstream of the flow control structure.

The **Lower Sixth Water Canyon** process domain represents the downstream 3 km of Sixth Water and is the most confined reach in the system, with 87% of the channel confined by the valley walls (Table 4.1). The confining material is a conglomerate bedrock that is relatively

resistant to erosion. The valley is narrow and steep, with a slope of 4.0% and there is little floodplain development in the reach. Bed material includes bedrock, cobble, and boulders, with large bedrock pools (Fig. 4.2). There is a monitoring site, Sixth Water at 3 Forks, at the downstream end of the process domain, just upstream of the confluence between Sixth Water and Diamond Fork.

4.2. Sixth Water Channel Change

4.2.1. Upper Sixth Water Canyon

The reach is highly confined by steep bedrock valley walls and has limited capacity for planform adjustment. The channel was slightly wider and had somewhat greater width variability during the period of irrigation flows. Between 1956 and 1993, average active channel width was 11 m, with areas up to 30 m wide. In 1997, average channel width decreased to 8.0 m and has remained stable since (Table 4.2, Fig. 4.3).

Table 4.2. Summary of channel attributes of Upper Sixth Water Canyon.

Year	Average width	Sinuosity	Percent multi-threaded
1956	11.0 ± 0.23	1.35	0
1981	12.1 ± 0.36	1.36	0
1993	10.7 ± 0.34	1.31	0
1997	8.0 ± 0.49	1.30	0
2004	8.9 ± 0.23	1.29	0
2006	7.5 ± 0.22	1.30	0
2009	8.6 ± 0.22	1.30	0
2011	7.9 ± 0.33	1.30	0
2014	10.5 ± 0.33	1.28	0
2016	9.6 ± 0.33	1.30	0

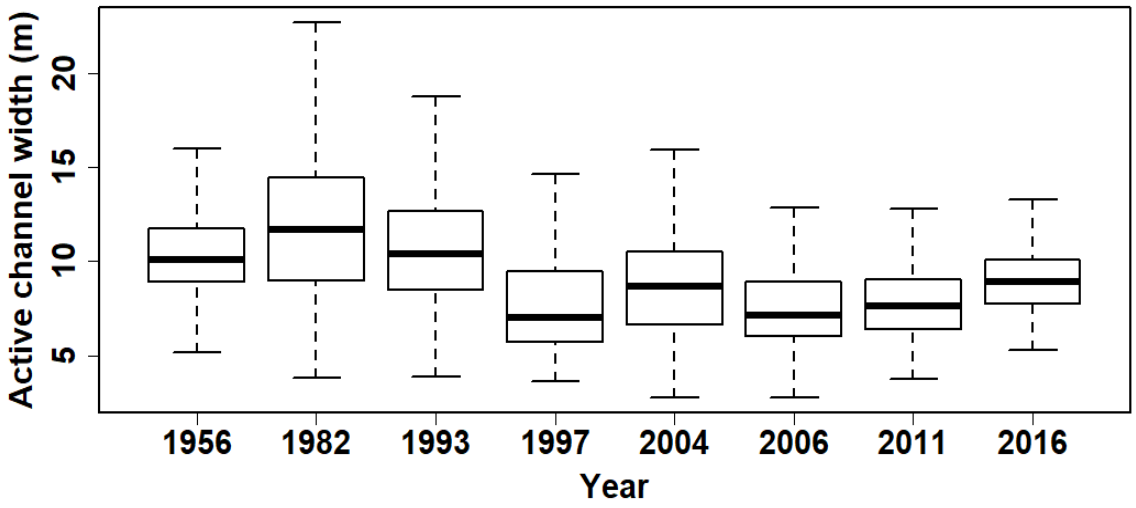

Fig. 4.3. Box plot of channel width in the Upper Sixth Water Canyon process domain. The box represents the 25th percentile, median (bold black line), and 75th percentile of channel width measurements. The upper whiskers represent the 75th percentile + 1.5 * IQR and the lower whiskers represent the 25th percentile – 1.5 * IQR.

Upper Sixth Water Canyon served as a sediment source during the period of irrigation flows. The bedrock is weak shale and interbedded mudstones, and hillslopes were highly active during this period. Directly downstream of the Strawberry Tunnel outlet, incision ranging from several meters to more than 10 m occurred over the course of the 20th Century (Fig. 4.4). The signal of downcutting is less pronounced further downstream, but the deep, incised valley suggests that sediment was sourced from this reach during the 20th Century. As a result of the high sediment load, the channel was more complex and the sinuosity of the reach was higher prior to 1993 (Table 4.2, Fig. 4.5). The activity of the hillslopes has decreased over time and the sinuosity of the reach has been stable since 1993.

4.2.2. Sixth Water Meadows

In 1956, the reach had an average active channel width of 27 m and had multiple threads with large active gravel bars (Fig. 4.6, Fig. 4.7A). The width of the channel was highly variable, ranging from 4 m in the narrowest sections to more than 90 m in the widest areas. The channel

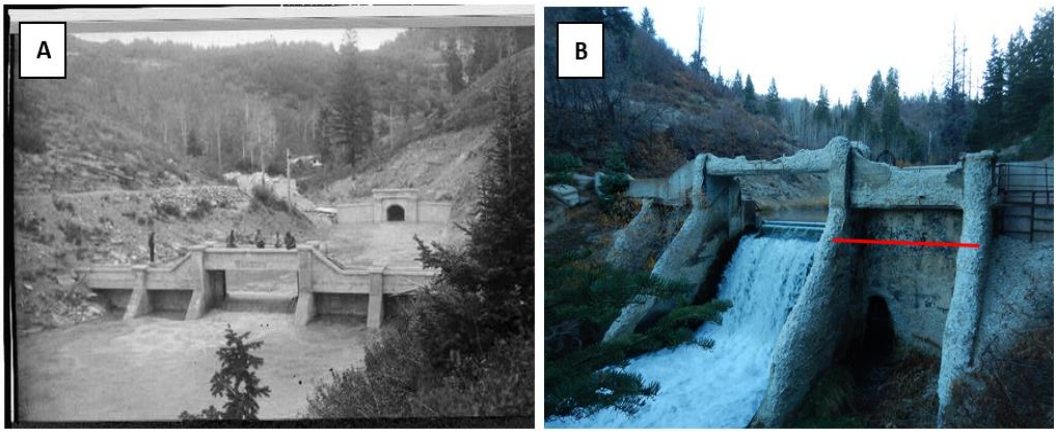

Fig. 4.4. Comparison of Strawberry Tunnel Outlet from A) ca. 1915 and B) October 2017. Red line in B) shows approximate water level in 1915 photo.

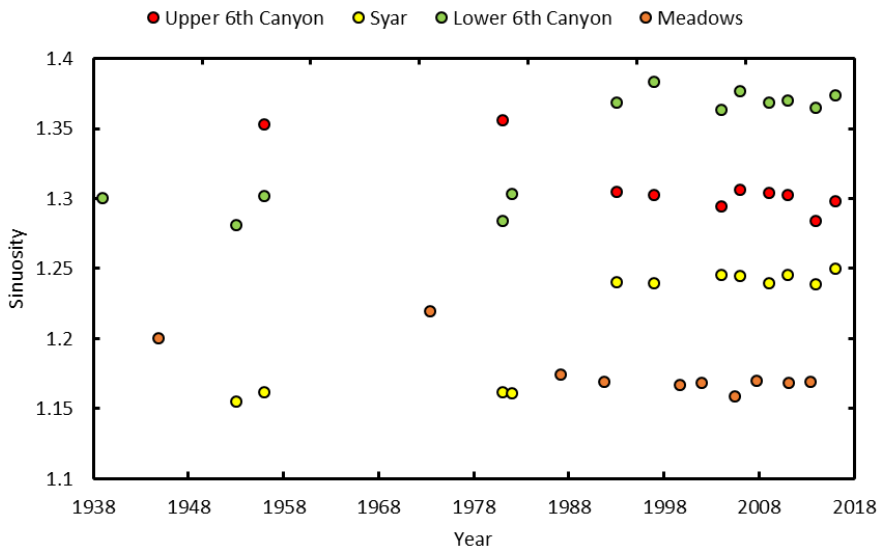

Fig. 4.5. Sinuosity of process domains on Sixth Water Creek calculated from historic air photos. Sinuosity was calculated at the scale of each process domain.

narrowed between 1956 and 1981, with the widest sections of the channel experiencing the greatest narrowing. The upper quartile and maximum channel width values decreased by 22 and 52 m, respectively (Fig. 4.6). The narrowing occurred as vegetation established on surfaces that were bare in the 1950s (Fig. 4.7B). By 1981, the reach had narrowed to an average of 14.9 m

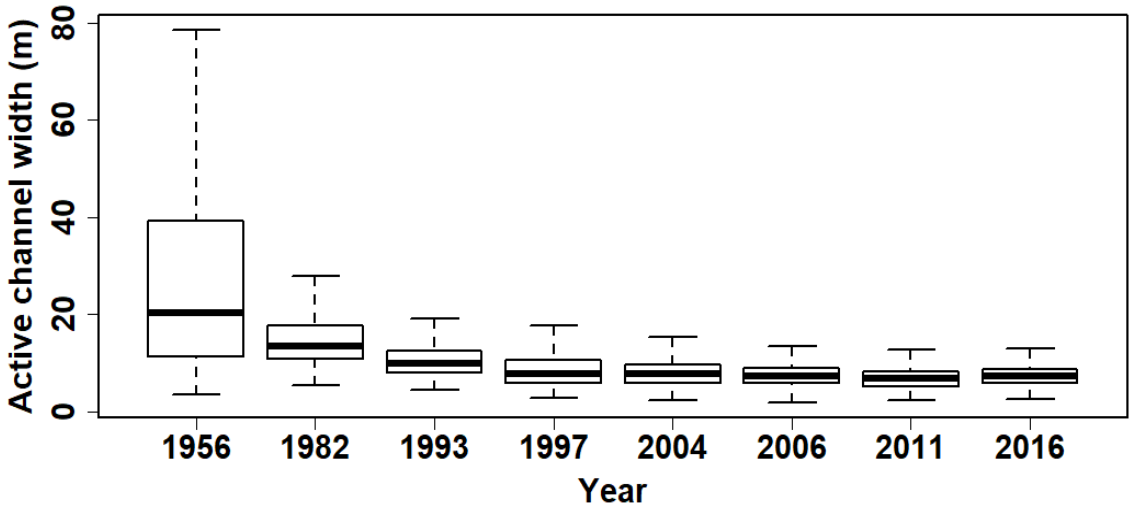

Fig. 4.6. Box plot of active channel width in the Sixth Water Meadows process domain.

wide. The river was single threaded, with small active gravel bars. Many of the bars present in the 1981 and 1982 photos were vegetated by 1993, as the channel narrowed to 10.9 m (Fig. 4.7). The channel continued to narrow between 1993 and 1997 as vegetation encroached at the channel margins. Since 1997, channel width has been relatively stable, with an average width of about 8 m (Table 4.3).

High sediment loads coming from upstream likely drove the deposition and reworking of bars in the 1950s and 1980s in the Sixth Water Meadows reach. In addition to sediment coming from the Upper Sixth Water Canyon, the large landslide at the upstream end of the Sixth Water Meadows reach acted as a sediment source. The landslide was very active during the period of irrigation flows, with toe scarps on river left and river right (Fig. 4.8). Currently there is only one section of the landslide that is actively deforming, with a rate of movement of 0.4 m/yr based on measurements of tree movement from aerial photography.

Since 2004, the channel in Sixth Water Meadows has been limited in its capacity for adjustment due to the lower sediment supply and the presence of coarse fill terraces. The bars that were active in the 1950s are an average of 2 m above the current channel and bars that were

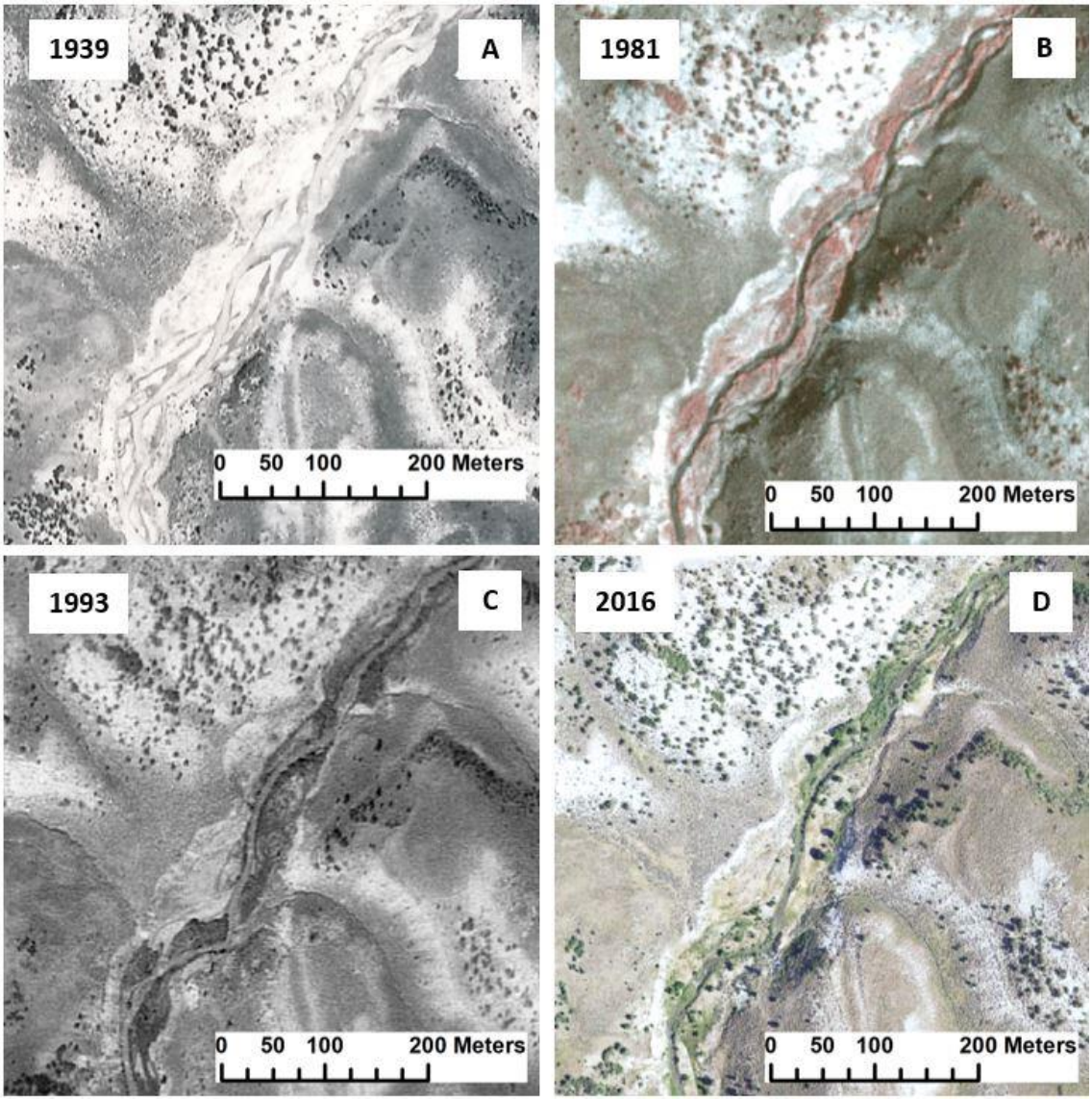

Fig. 4.7. Aerial photographs of the Sixth Water Meadows process domain. The photos show a wide channel with unvegetated bars in 1956 (A), with a subsequently narrowed and vegetated channel (B-D).

active in the 1980s are an average of 1.25 m above the current channel. These deposits are common in Sixth Water Meadows and line both sides of the channel for much of the reach (Fig. 4.9). The volume and caliber of material stored in these deposits cannot be reworked under the current flow regime, so they act as confining features along a substantial length of the channel boundary.

Cross-section re-surveys from the Upper Sixth Water site illustrate the lack of channel change between 2005 and 2017 (Fig. 4.10, Appendix B). Channel area, width, minimum bed elevation, and average bed elevation were all essentially unchanged and channel migration of 1 m occurred at only one of the six cross-sections (XS 6 in Fig. 4.10). The most channel complexity and change in the Sixth Water Meadows process domain occur where beaver have constructed dams. There are 5 or 6 large beaver ponds in the reach that create channel complexity and floodplain access, including at the Upper Sixth Water monitoring site (Fig. 4.11).

Table 4.3. Summary of channel attributes of Sixth Water Meadows.

Year	Average width	Sinuosity	Percent multi-threaded
1956	27.0 ±0.43	1.2	8.0
1981	14.9 ± 0.46	1.2	6.0
1982*	9.1 ± 0.46	1.22	4.6
1993	10.9 ± 0.31	1.18	2.0
1997	9.0 ± 0.37	1.17	3.3
2004	7.9 ± 0.29	1.17	0
2006	7.5 ± 0.21	1.17	0
2009	8.9 ± 0.21	1.16	0
2011	7.0 ± 0.31	1.17	0
2014	8.6 ± 0.31	1.17	0
2016	7.6 ± 0.31	1.17	0

Notes: * Image coverage is incomplete

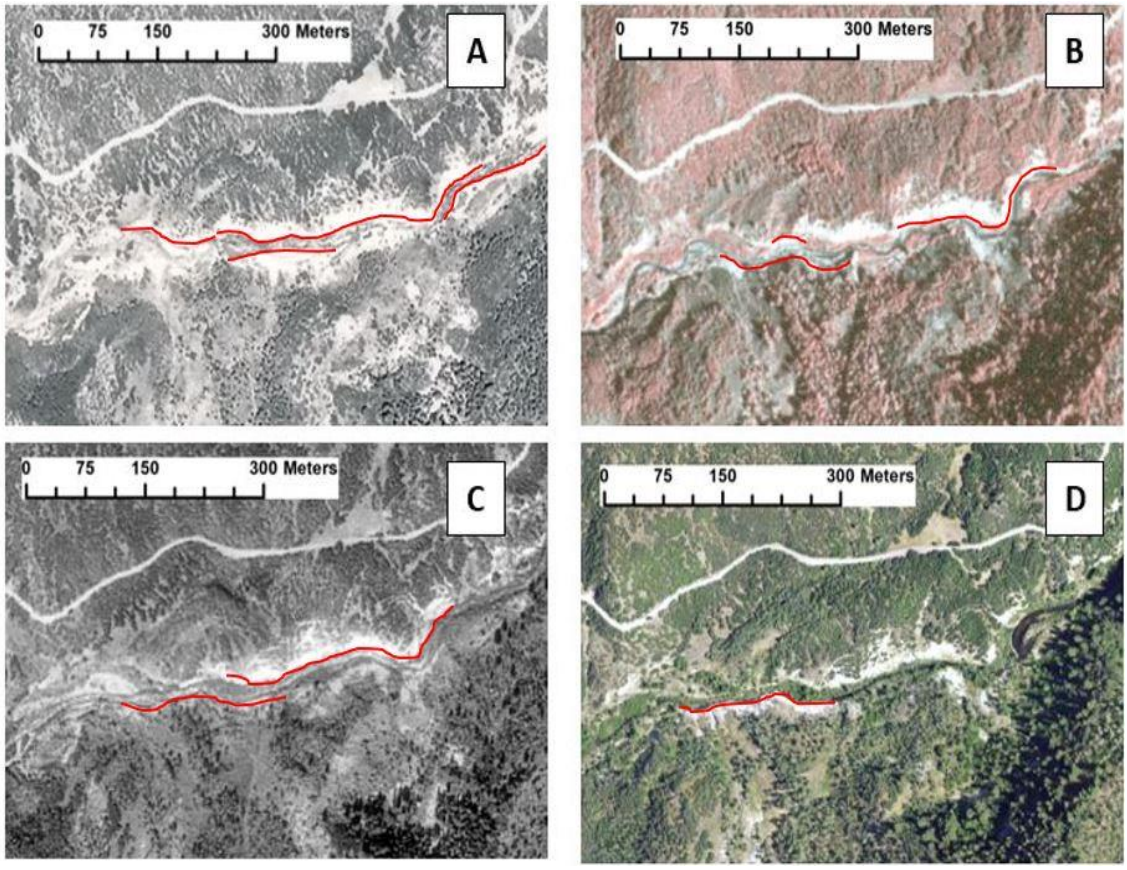

Fig. 4.8. Aerial photographs of the large landslide on adjacent to Sixth Water in A) 1956, B) 1981, C) 1993, and D) 2016. Red lines indicate toe scarps with a direct channel connection and no toe vegetation at the time of the photo.

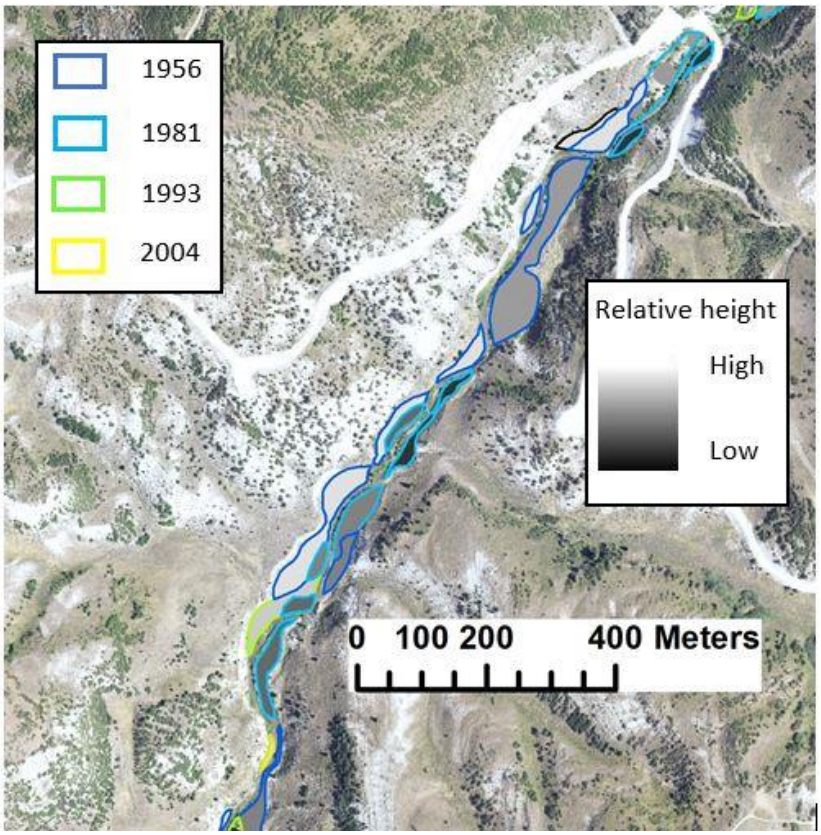

Fig. 4.9. Map of fill terraces in Sixth Water Meadows process domain. Each polygon is a separately mapped terrace, the border color denotes the year the terrace first appears in aerial photographs, and the color of the polygon represents the relative height above the 2017 channel.

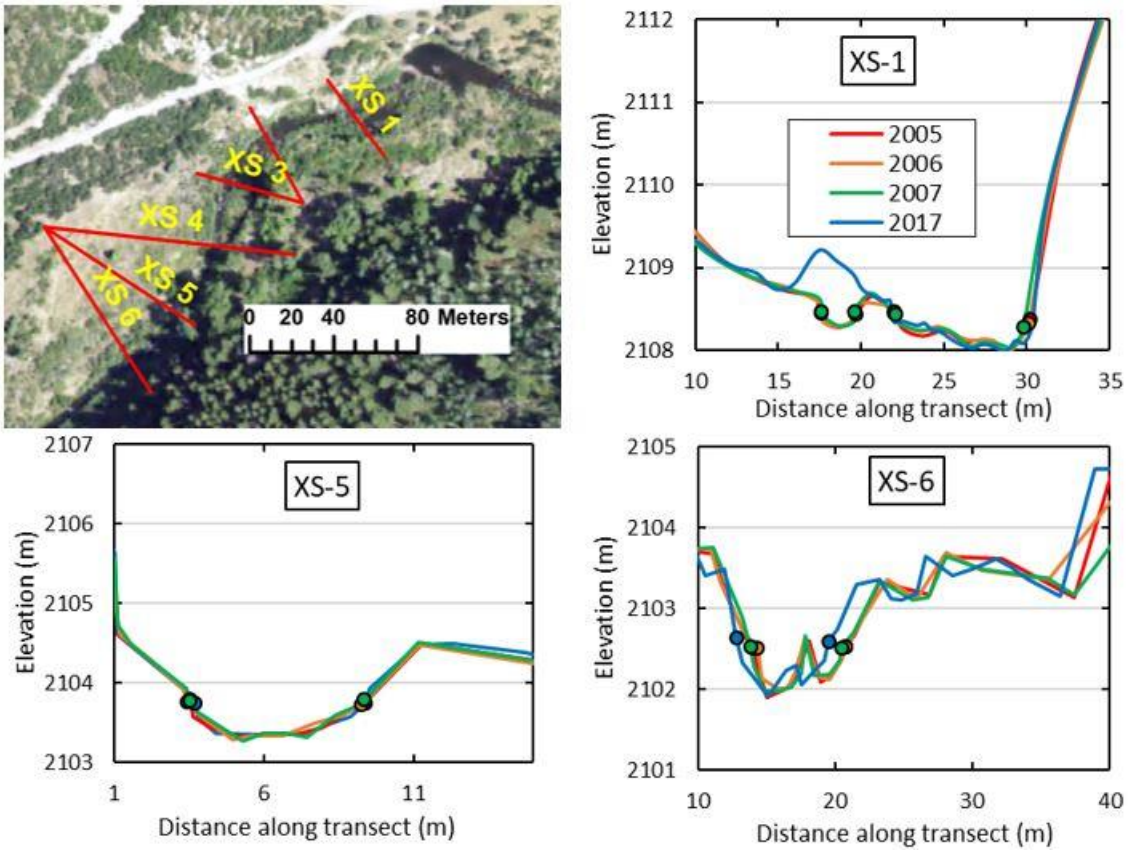

Fig. 4.10. Location of cross-sections at upper Sixth Water sample site and profiles of cross-sections 1, 5, and 6.

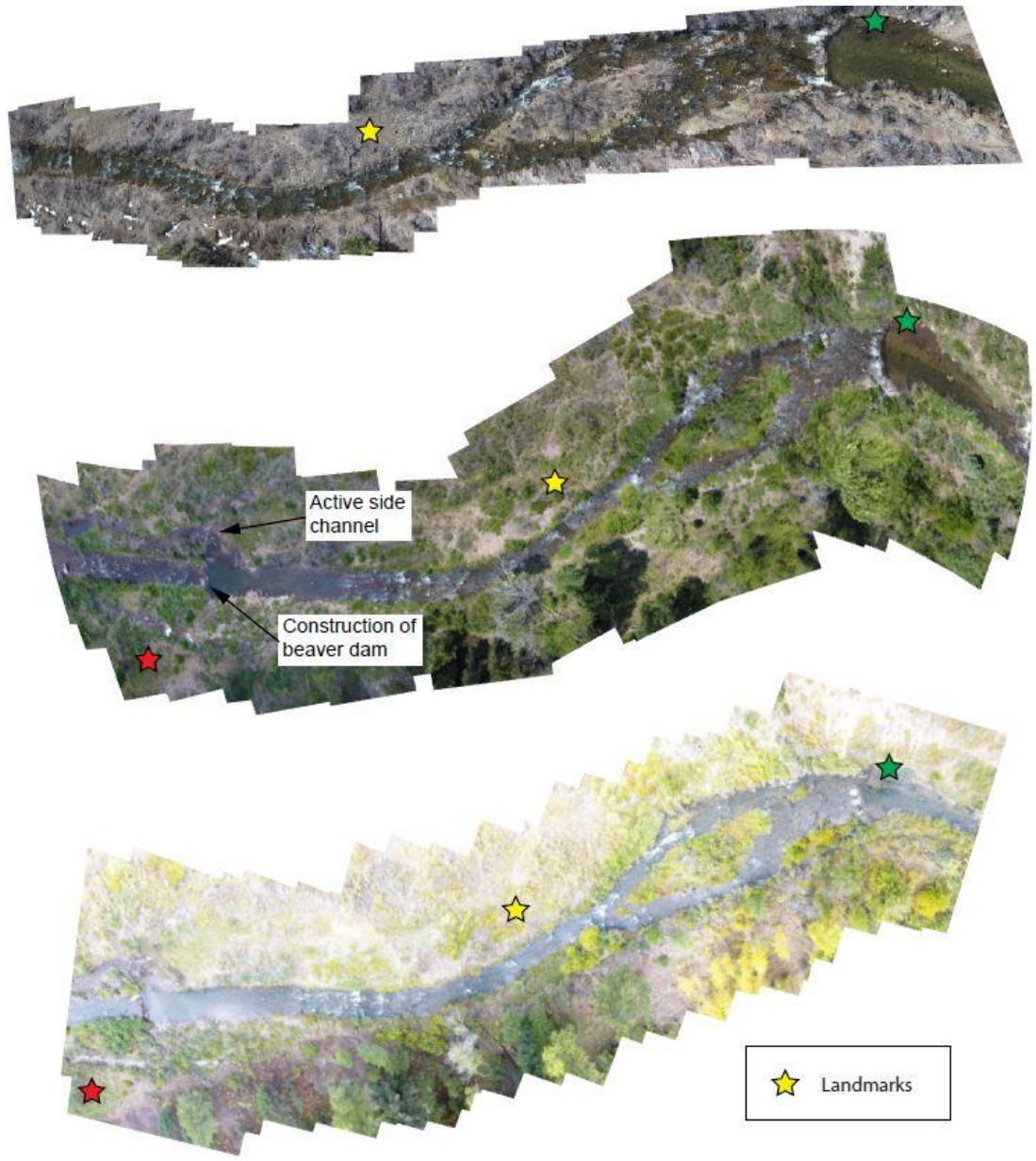

Fig. 4.11. Mosaicked aerial photographs of the Upper Sixth Water sample site collected by UAV on A) April 12, 2016, B) July 17, 2017, and C) September 23, 2017.

The river also has a limited ability to transport bed material in Sixth Water Meadows under current flow conditions. Results of the painted rock and RFID tracers suggest that floods of a common magnitude on Sixth Water cannot transport bed material (Appendix A). No significant movement of painted rocks was recorded at the Upper Sixth Water or Rays Crossing site at 50 or 100 cfs. Similarly, the RFID tracers at the Rays Crossing site were not transported during the stepped flow experiment. Finer gravels (22.6 and 32 mm) placed just downstream of the active section of the landslide were mobile at the 100 cfs stepped flow, but bed material of this size represents a small fraction of material in the reach (Fig. 4.12).

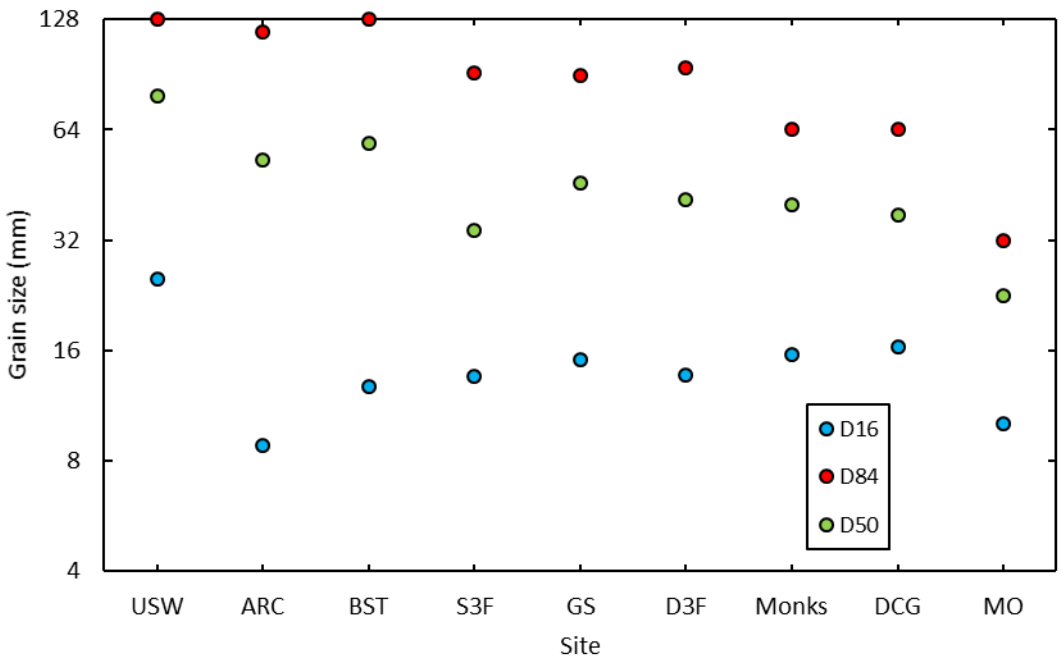

Fig. 4.12. Average grain size statistics from pebble counts at monitoring sites on Sixth Water and Diamond Fork. Site names: USW – Upper Sixth Water, ARC – Above Rays Crossing, BST – Below Syar Tunnel, S3F – Sixth Water at 3 Forks, GS – Guard Station, D3F – Diamond Fork at 3 Forks, BMH – Below Monks Hollow, DCG – Diamond Campground, and MO – Motherlode. Full details of pebble counts presented in Appendix C.

4.2.3. Syar reach

The Syar reach has been predominantly single threaded over the period of record, with large active gravel bars in the 1950s in areas where the valley is wide (Fig. 4.13). The channel narrowed from 1956 to 1982, going from a width of 17 m in 1956 to 10.3 m in 1981, and 13.5 m in 1982. Most of the narrowing occurred in the widest parts of the channel, as the maximum channel width decreased by 19 m between 1956 and 1981 (Fig. 4.14). During the 1980s, some bars remained active and some new bars were formed but the channel narrowed to 10.3 m in 1982 (Fig 4.14). Channel width remained consistent from 1982 to 1997 and then decreased to 8.5 m in 2004 as vegetation encroached on channel margins. Since 2004, channel width has not changed considerably (Table 4.4).

The lack of change since 2004 shows that the channel has limited capacity for adjustment in the current flow regime. Similar to Sixth Water Meadows, there are fill terraces made of coarse material that constrain the channel. Surfaces from the 1950s are about 2 meters above the channel and those from the 1980s are about 1 m above the channel. There was no significant entrainment of painted rocks during the stepped flow experiment, suggesting that bed material cannot be entrained by common floods. There was also no change recorded in UAV photos from 2016 to 2017 at the Below Syar Tunnel sample site (Jones, 2018).

4.2.4. Lower Sixth Water Canyon

The highly confined Lower Sixth Water Canyon reach was slightly wider during the period of irrigation flows than it is under the current flow regime, but has experienced little change over the period of record (Table 4.5). Active channel width was 12 m in 1939, 15 m in the 1950s, 12 m in the 1980s and 1990s and has averaged 10 m since 2004 (Fig. 4.15). The channel was single threaded during this entire time period, with few bars. There are a few fill terraces near the confluence of Sixth Water and Diamond Fork that were active in 1939 and the 1950s, that are

now 1-2 m above the current channel (Fig. 4.16).

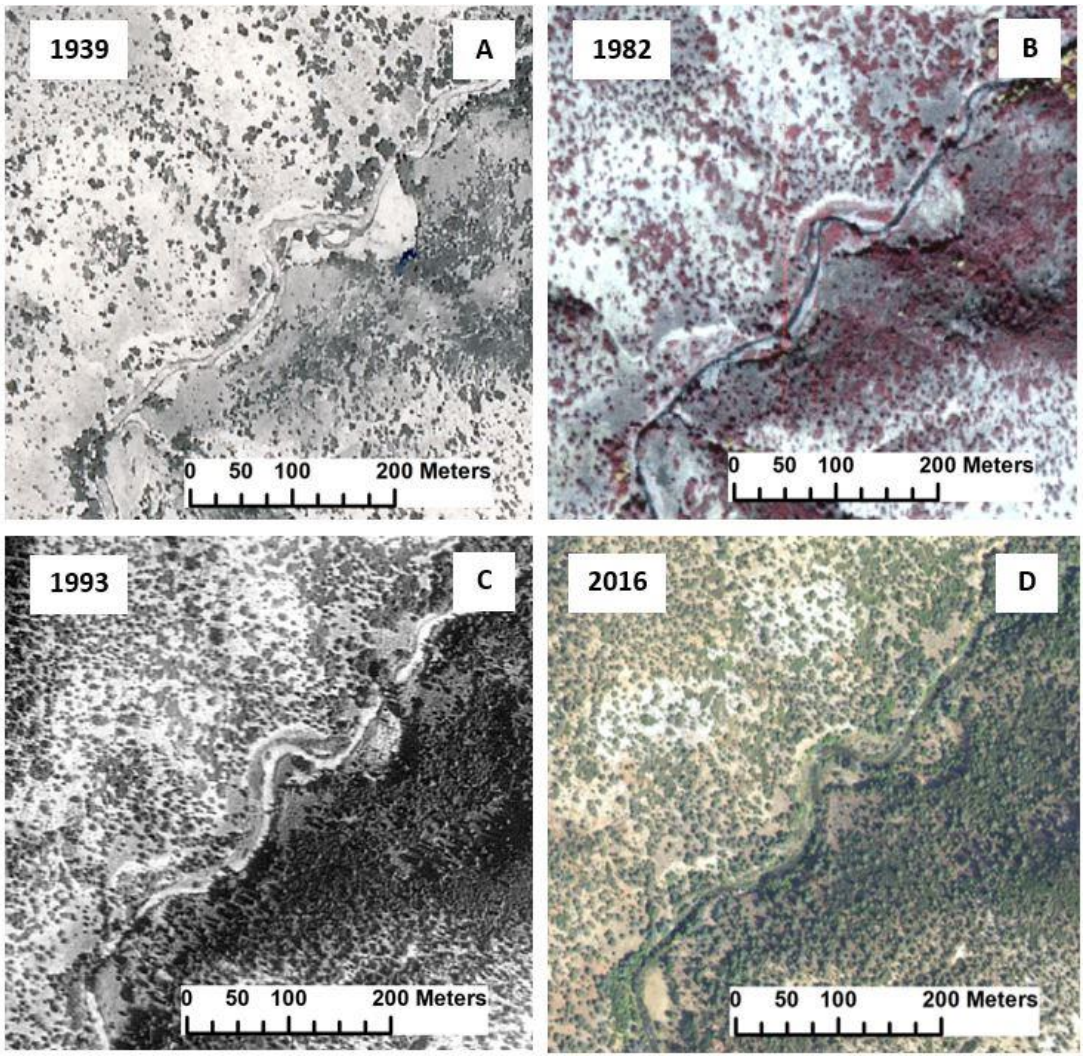

Fig. 4.13. Aerial photographs of a reach within the Syar process domain. The photos show a channel with large, unvegetated bars in 1956 (A), followed by subsequent vegetation encroachment and channel narrowing (B-D).

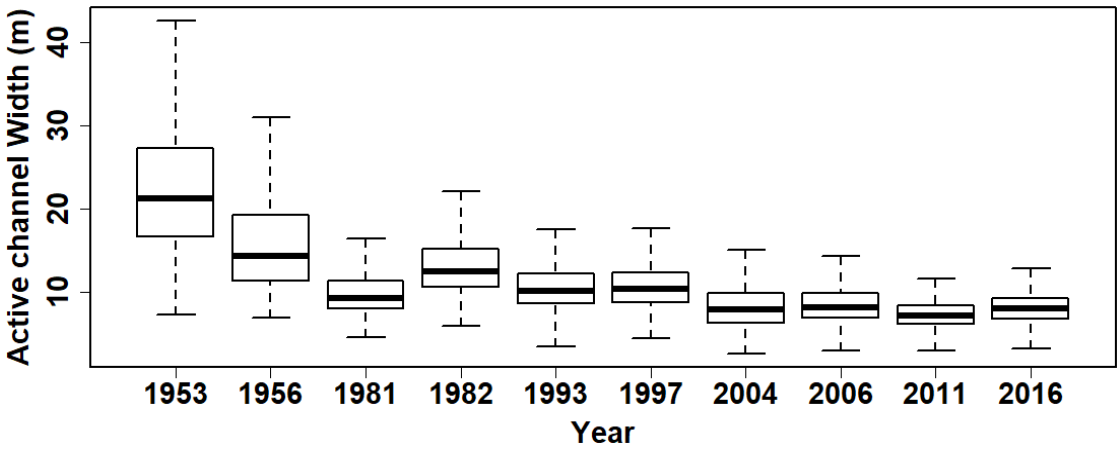

Fig. 4.14. Box plots of active channel width in the Syar process domain.

Table 4.4. Summary of channel attributes of Syar process domain.

Year	Average width	Sinuosity	Percent multi-threaded
1953	23.1 ± 0.32	1.16	N/A
1956	16.9 ± 0.39	1.16	3.2
1981	13.5 ± 0.50	1.16	6.0
1982	10.3 ± 0.46	1.16	4.4
1993	10.8 ± 0.35	1.24	3.6
1997	11.1 ± 0.37	1.24	1.1
2004	8.3 ± 0.23	1.24	0
2006	8.6 ± 0.22	1.25	0
2009	8.9 ± 0.30	1.24	0
2011	7.5 ± 0.34	1.24	0
2014	10.0 ± 0.34	1.24	0
2016	8.2 ± 0.35	1.25	0

Table 4.5. Summary of channel attributes of Lower Sixth Water Canyon.

Year	Average width	Sinuosity	Percent multi-threaded
1939	12.6 ± 1.17	1.30	0
1953	14.9 ± 0.69	1.28	0
1956	14.5 ± 0.28	1.30	0
1981	11.9 ± 0.36	1.28	0
1982	11.6 ± 0.49	1.30	0
1993	9.4 ± 0.48	1.37	0
1997	11.9 ± 0.59	1.38	0
2004	10.3 ± 0.45	1.36	0
2006	9.8 ± 0.40	1.38	0
2009	10.3 ± 0.45	1.37	0
2011	10.5 ± 0.54	1.37	0
2014	13.3 ± 0.66	1.37	0
2016	10.9 ± 0.66	1.37	0

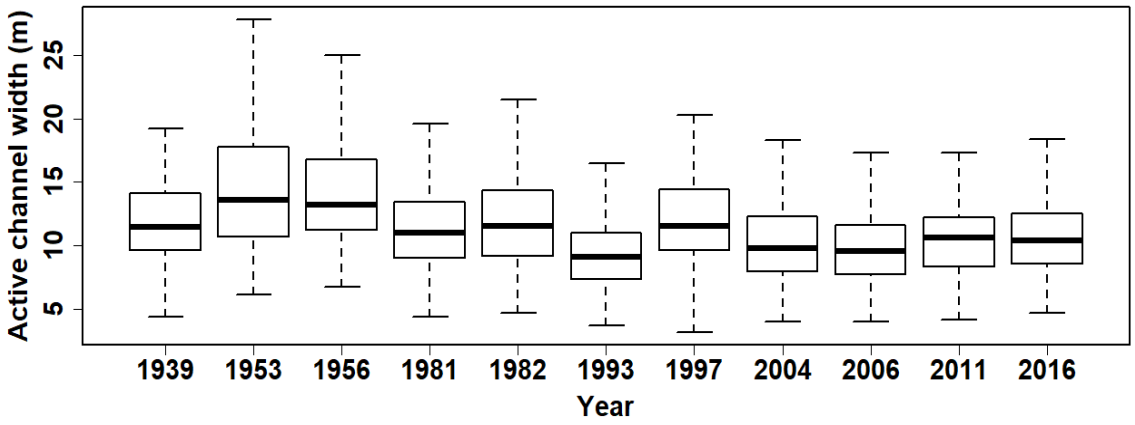

Fig. 4.15. Box plots of active channel width in the Lower Sixth Water Canyon process domain.

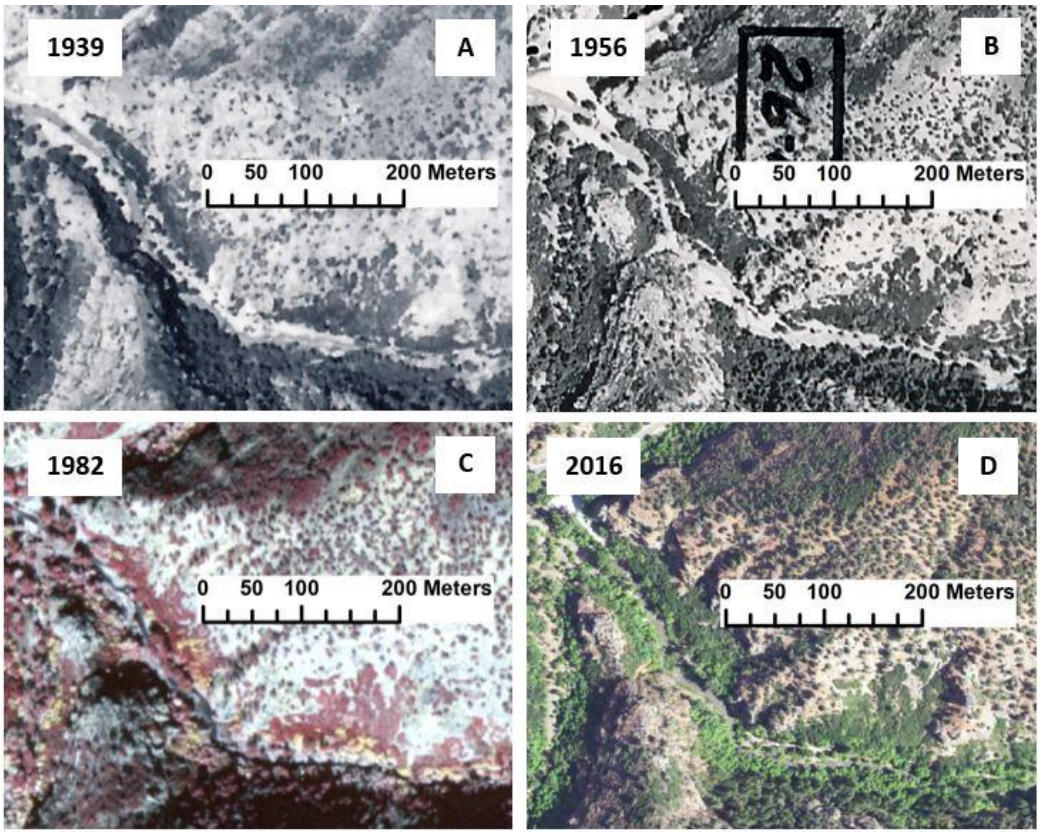

Fig. 4.16. Air photos showing Sixth Water just upstream of its confluence with Diamond Fork. Some unvegetated bars were present in 1939 (A) and 1956 (B), but those bars were vegetated by 1982 (C). The channel experienced minimal change between 1982 and 2016 (D).

The Sixth Water at 3 Forks monitoring site is less confined and more active than most of the process domain. Bed material at the Sixth Water at 3 Forks site is finer grained than upstream reaches (Fig. 4.12), and is mobile at relatively common flows. About 40% of the painted rocks placed at the site were mobile during the 100 cfs flow in the stepped flow experiment (Fig 4.17). Although bed material is mobile at common flows, the geomorphic change detection analysis revealed that erosion and deposition were concentrated in areas where structural elements were present. A beaver dam was constructed at the downstream end of the site during the fall and winter of 2016, and cleared in early spring 2017. Backwater from the beaver dam caused 30 to 50 cm of deposition of fine sediment on the floodplain on river right. Up to 90 cm of erosion was

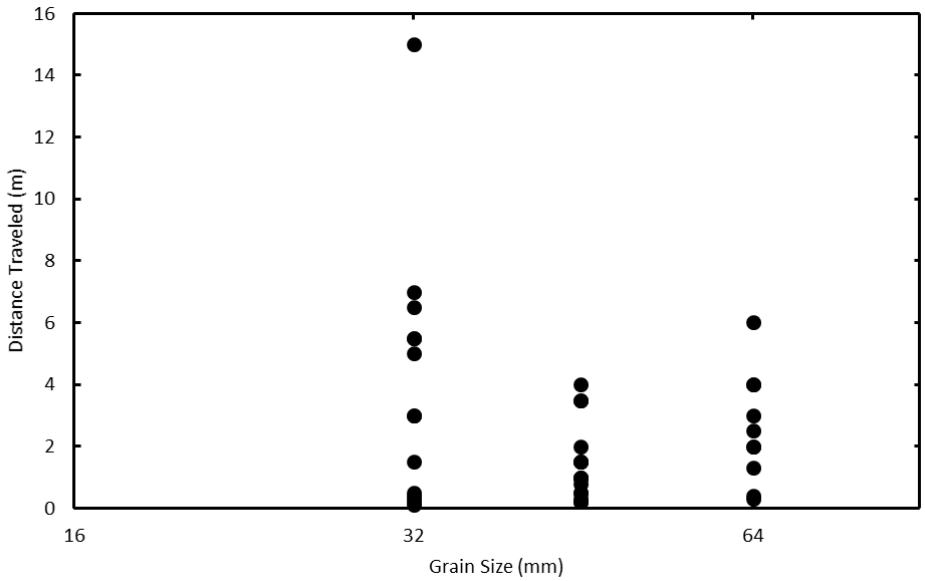

Fig. 4.17. Transport distance of painted gravel tracers at Sixth Water at 3 Forks site following the 100 cfs flow steps.

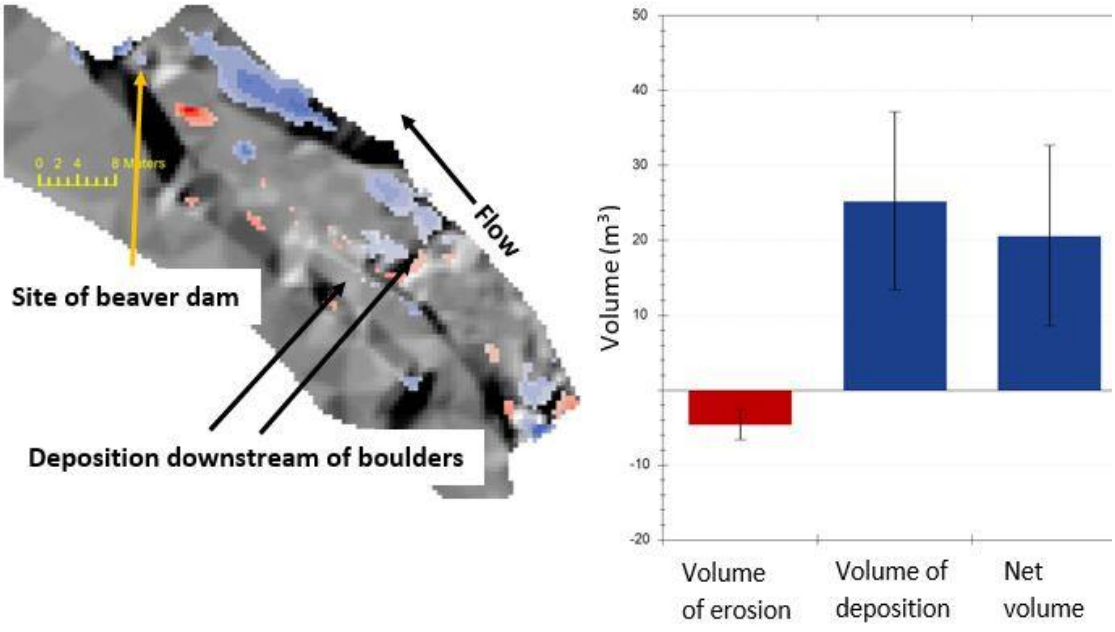

Fig. 4.18. Spatial (A) and numerical (B) results of geomorphic change detection analysis at the Sixth Water at 3 Forks monitoring site. Areas of red in A) represent erosion and areas of blue represent deposition, with darker colors symbolizing larger magnitude.

recorded at the downstream end of a remnant log of the beaver dam (Fig. 4.18). Ten to 30 cm of deposition also occurred on the downstream side of large boulders in the channel. Where there were no structural elements, no significant erosion or deposition was recorded.

4.3. Sixth Water sediment sources

4.3.1. Length of active hillslopes over time

Hillslopes on Sixth Water were more active during the period of irrigation flows than they are currently. Even with uncertainty, there was a significant decrease in the length of active hillslopes along Sixth Water, as measured from aerial photographs between 1956 and 2016 (Fig. 4.19). This suggests that the amount of sediment supplied to the channel from hillslopes has decreased over time. Interestingly, the length of active hillslopes in 1981 is less than 1956 even though the flow regime did not change during that period. This mirrors the narrowing of Sixth Water Meadows and Syar between 1956 and 1981. Hillslopes continued to become vegetated and stabilized in the ten years between 2006 and 2016. The decrease in active hillslope length from 2006 to 2016 suggests that hillslopes either had not fully adjusted to the new flow regime by 2006 or that hillslope mass wasting is not tightly coupled with flow in the stream channel.

4.3.2. Sediment source samples

Thirty-five potential sediment sources were sampled on Sixth Water upstream from the confluence with Fifth Water (Fig. 4.20). The majority of samples were collected from active hillslopes, though this does not reflect the relative distribution of active and inactive hillslopes. All active hillslope samples on Sixth Water were finer grained than the bed material of the channel. The median grain size at all Sixth Water sample sites was 32 mm or greater (Fig. 4.12), while all sediment samples had a median grain size less than 32 mm (Fig. 4.20). Based on grain size, active hillslopes can be divided into two classes – hillslopes that contribute significant gravel (gray in Fig. 4.20B) and those that do not (black in Fig. 4.20B). Sources that contribute

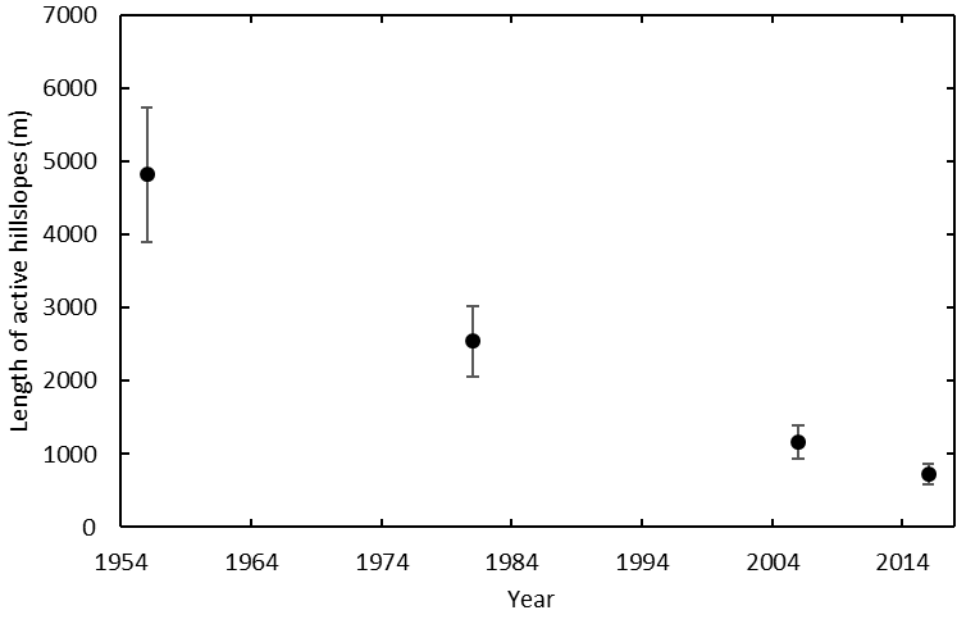

Fig. 4.19. Length of active hillslopes on Sixth Water, as measured from aerial photographs from 1956, 1981, 2006, and 2016.

significant gravel have 40% or more of their grains between 8 and 90 mm while those that do not have 90% or more of their grains finer than 22.6 mm. Tributary samples also contained sediment that is finer than the bed material of Sixth Water (Fig. 4.20C). The majority of sampled tributaries deliver a significant fraction of medium gravel (8 to 22.6 mm) and minimal coarse material.

4.4. Sixth Water fluvial surfaces

Fluvial surfaces are common on Sixth Water in areas where the valley is partially confined. The majority of these areas occur in the Sixth Water Meadows and Syar process domains, where the valley is wider and deposition can occur (Fig. 4.21). The majority of these deposits were unvegetated in the 1950s and early 1980s. Air photos from 1956 are the first that cover the Syar and Sixth Water Meadows process domain, and the deposits were unvegetated in this set of photos, suggesting that they were deposited or reworked during the flood of 1952 (Fig.

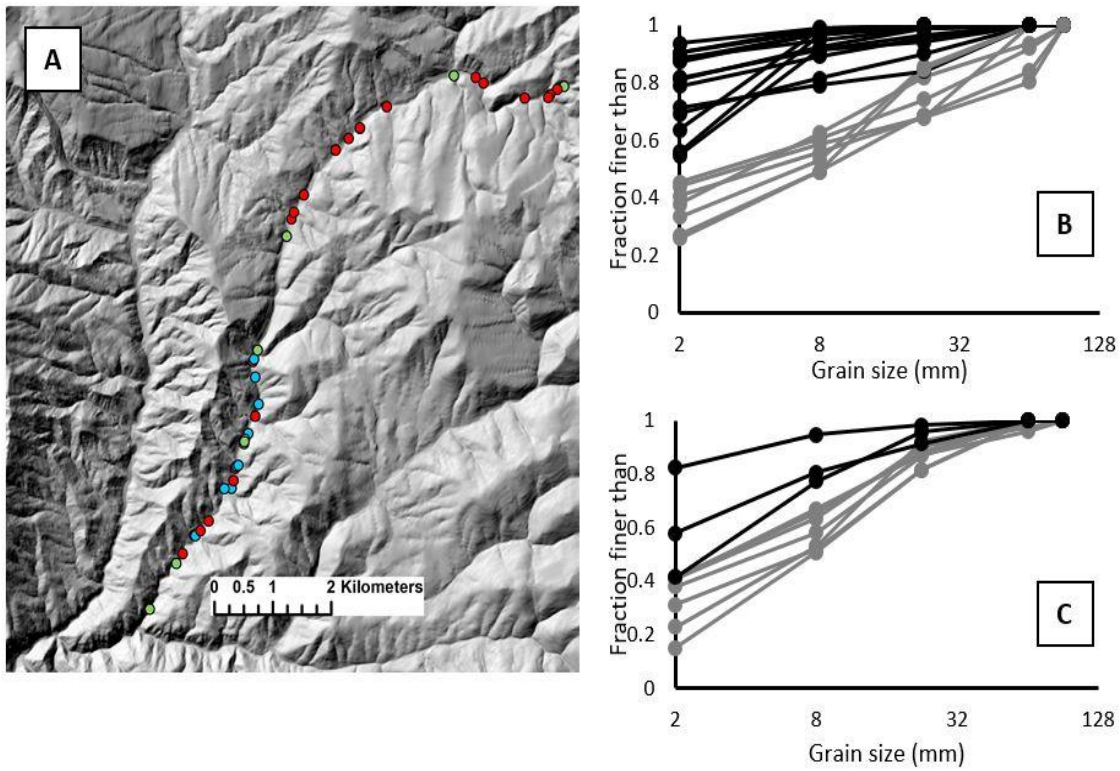

Fig. 4.20. Sediment source samples collected on Sixth Water. A) Location of samples including active hillslopes (red), inactive hillslopes (green), and tributaries (blue), B) grain size distribution of active hillslopes, and C) grain size distribution of tributaries. Gray data series in B) and C) represent sediment sources that contribute significant gravel and black data series represent those that are primarily fine grained.

4.7, Fig. 4.13, Fig. 4.22). The terraces that were formed in the 1950s were vegetated by the 1980s, and the majority were not reworked during the high flows of 1983 and 1984. The deposits formed in the 1980s experienced some reworking, but were largely vegetated by 1997.

4.5. Incision of Sixth Water

Several pieces of evidence suggest that segments of Sixth Water incised after the introduction of high flows in 1915, but it is difficult to fully constrain incision due to a lack of pre-diversion data and observations. Incision primarily occurred in the Upper Sixth Water reach, which is highly confined and has limited capacity for lateral adjustment. Repeat photographs of

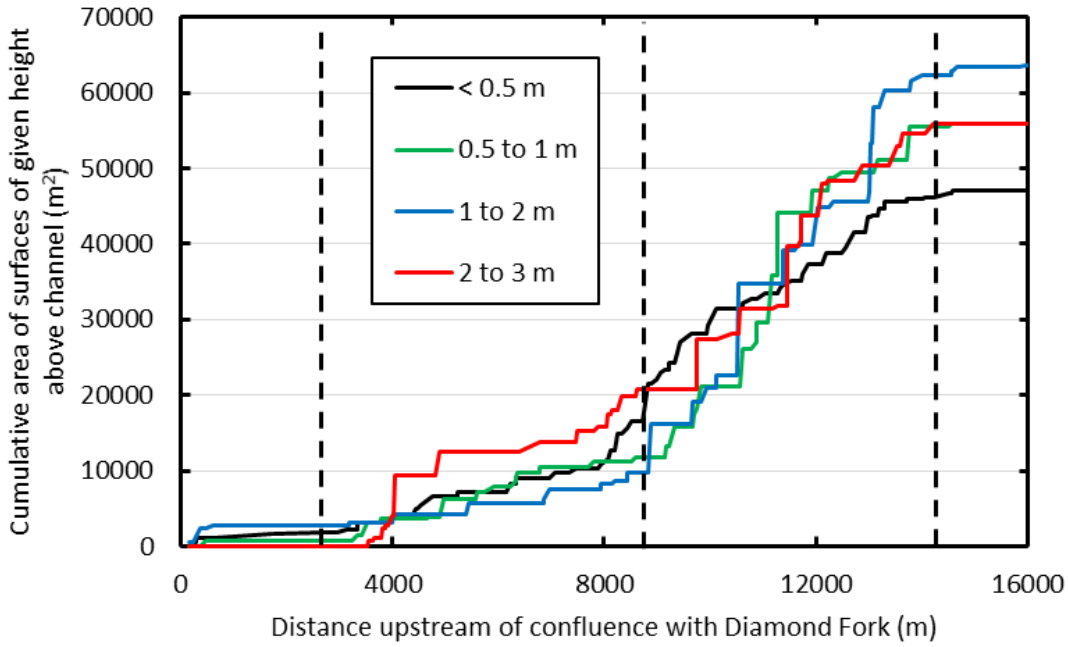

Fig. 4.21. Cumulative area of fluvial surfaces on Sixth Water with distance upstream. Surfaces are separated by their height above the current channel. Vertical dashed lines represent process domain breaks. From left to right the process domains are: Lower Sixth Water Canyon, Syar, Sixth Water Meadows, and Upper Sixth Water Canyon.

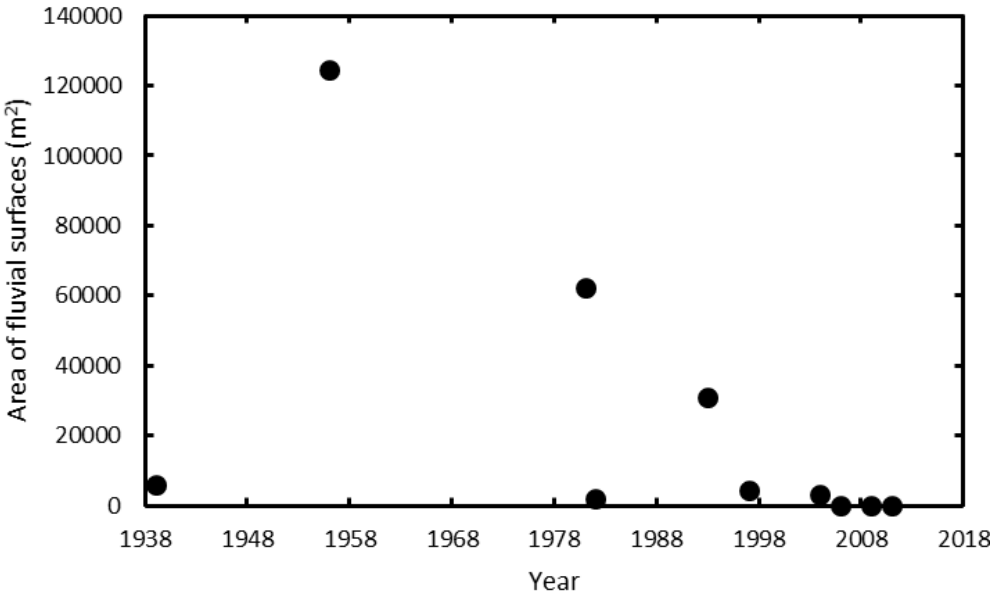

Fig. 4.22. Area of fluvial surfaces on Sixth Water plotted by year of formation.

the Strawberry Tunnel Outlet from 1915 and 2017 show differences in water surface elevation and hydraulics that suggest incision occurred downstream from the outlet, though it is unknown whether or not there were other structures downstream from the tunnel outlet in 1915 that may have influenced the water surface elevation (Fig. 4.4). Topographic cross-sections extracted from upstream and downstream of the Strawberry Tunnel Outlet show a distinct change in valley geometry downstream of the Strawberry Tunnel Outlet (Fig. 4.23). The cross-sections downstream of Strawberry Tunnel have a distinct break in slope and near channel curvature that suggests several meters of incision (Fig. 4.23). In places the amount of incision may be 10 m or more.

It is not possible, from the results presented in this thesis, to estimate the amount of sediment transported by incision of Sixth Water for the purposes of a sediment budget or to provide a quantitative constraint for sediment supply to downstream reaches. One approach for obtaining a quantitative estimate would involve comparing the topography of the Sixth Water valley bottom with a comparable, unincised valley bottom. However, it is difficult reliably trace the amount of incision in Sixth Water because evidence of incision is inconsistent along the valley. Additionally, it is difficult to reproduce the valley cross-section analysis in other areas because there is not a sufficiently comparable valley bottom with lidar coverage for quantitative analysis. Existing lidar coverage is limited to Sixth Water and Diamond Fork, the latter of which has a different lithology and valley setting. The lidar does not extend to Fifth Water and Cottonwood Creek, which have similar lithology and valley settings to Sixth Water and would be a more reliable comparison. We also have very limited knowledge of the timing of incision. Further, we have very limited information regarding the grain size of material through which Sixth Water incised. For these reasons, we have not attempted to provide a quantitative estimate of sediment quantity and type associated with incision of Sixth Water.

Despite the difficulties that prevent a quantitative estimate of sediment eroded during

incision of the Sixth Water during the 20th Century, several other pieces of information provide constraints on the amount of incision. In the Sixth Water Meadows process domain, there is a rating flume that was constructed in 1914 (US Bureau of Reclamation, 1915) that is about 6 meters above the current channel (Fig. 4.24).This flume is several kilometers downstream of the Strawberry Tunnel Outlet, suggesting that incision occurred many places in the Sixth Water valley. In the Upper Sixth Water Canyon process domain, there appears to be a road that leads to Strawberry Tunnel that is several meters above the current channel and has collapsed into the channel in some places (Fig. 4.25A**)**. Though we do not currently have precise information to determine how high above the pre-diversion channel the road was, photos of Sixth Water in the early 20th Century suggest many meters of incision (Fig. 4.25). More information is needed to constrain the amount of incision that occurred on Sixth Water and its spatial variability, but the information presented suggests that areas of Sixth Water incised several meters to as much as 10 m in various locations over the course of the 20th Century.

4.6. Diamond Fork process domains

The reach **downstream of the confluence** is the first 2900 m of Diamond Fork downstream from its confluence with Sixth Water. The reach is partially confined, with valley walls that confine 26% of the channel and a road that provides additional confinement on the north side of the valley. The reach is considerably less steep than process domains on Sixth Water, with a slope of 1.1% (Table 4.6). The channel has low sinuosity with a riparian corridor of large trees, and floodplain pockets where the valley is wide (Fig. 4.26). Bed material is primarily cobble, with boulders and gravel, as well as some bedrock in the channel.

The **Monks Hollow reach** is partially confined by alluvial fans and bedrock. The Monks Hollow outlet is located at the upstream end of this reach, providing flow input during some periods of the year. Bed material is made up of cobble, boulders, and gravel. The reach has a

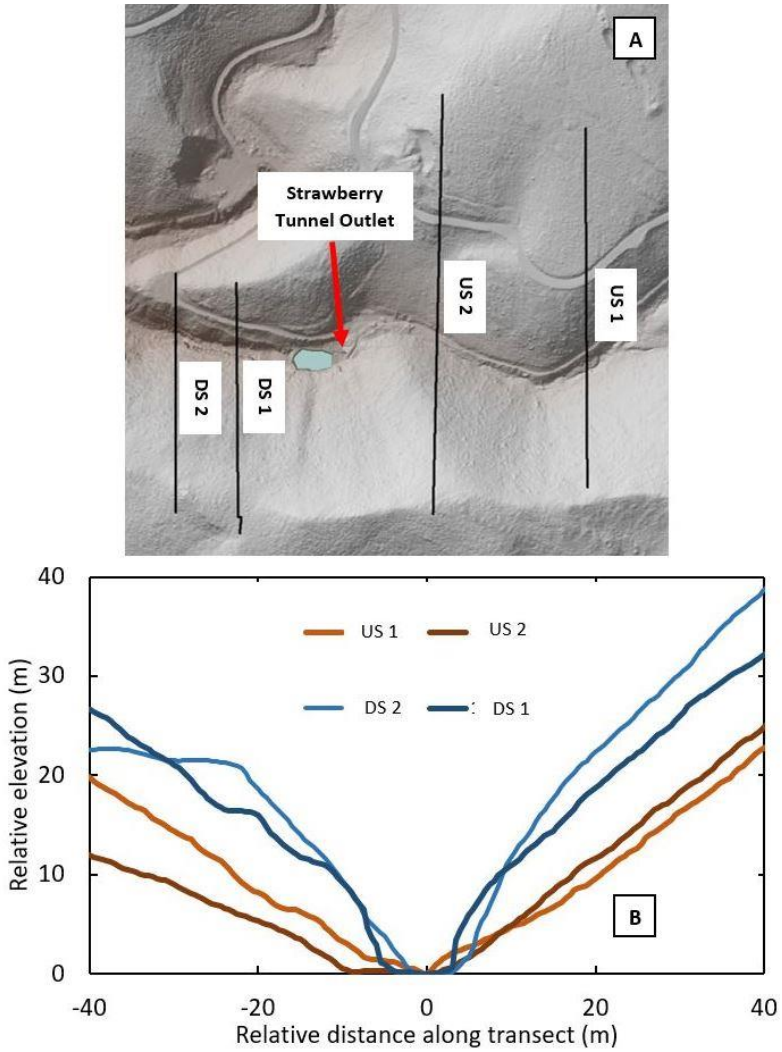

Fig. 4.23. Cross-sections extracted across Upper Sixth Water Canyon from lidar DEM. A) location of cross-sections, B) profile of cross-sections. Cross-sections were normalized so that the lowest point in each cross-section plotted as 0 distance along transect and 0 elevation.

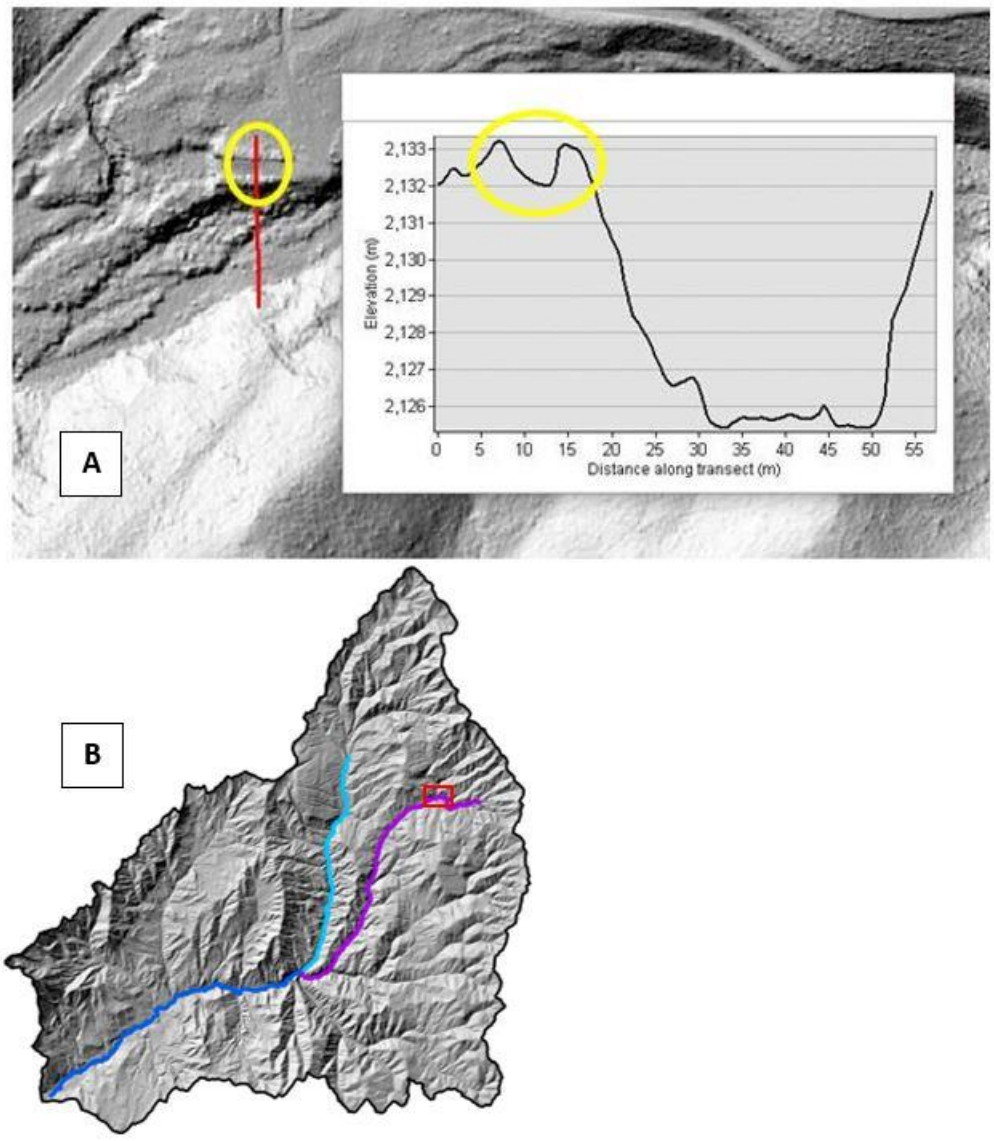

Fig. 4.24. Location and topography of former US Bureau of Reclamation rating flume. A) Profile across Sixth Water Creek showing US Bureau of Reclamation rating flume constructed in 1915 (in yellow circle). B) Location of rating flume in Diamond Fork watershed (red rectangle).

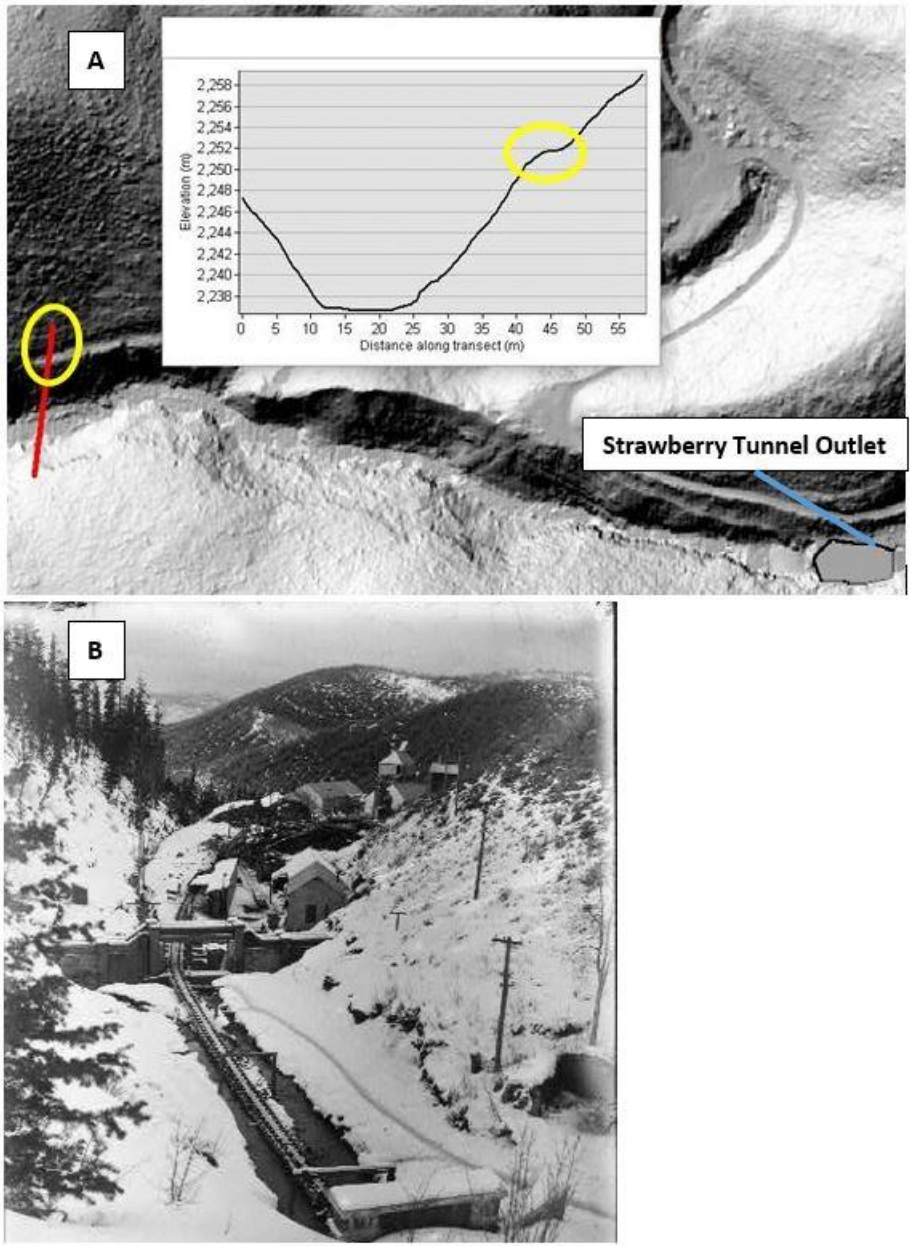

Fig. 4.25. Location and topography of pre-diversion road in Upper Sixth Water Canyon. A) Profile across Sixth Water Creek showing a road used to access Strawberry Tunnel in the early 20th Century (yellow circle). B) View looking downstream at the Strawberry Tunnel Outlet and the camp used by construction workers.

slope of 1.1% and point bars and pool-riffle-run sequences are relatively common. For much of the reach, both sides of the channel are lined by a narrow riparian corridor containing large cottonwood trees (Fig. 4.21). The Monks Hollow monitoring site is located in this process domain.

The **Diamond Campground** reach is unconfined by bedrock, but terraces, alluvial fans, and campground infrastructure create local confinement. The reach is relatively low slope, with a slope of 0.92%, and unconfined areas have floodplain and terrace surfaces on both sides of the channel with multiple elevations and vegetation ages (Fig. 4.21). Bed material in the reach is primarily gravel with cobbles and some fines. The Diamond Campground monitoring site is located just downstream of the Diamond Campground.

The **Diamond Fork alluvial valley** reach encompasses the final 8100 m of Diamond Fork upstream of Highway 6 and the confluence with Spanish Fork. The reach is mostly unconfined, but terraces, alluvial fans and inactive landslides provide local confinement. Most of the reach consists of low slope, unconfined sections with wide, well-developed floodplains with multiple vegetation ages and types (Fig. 4.21). Bed material of the reach is primarily medium to coarse gravel, and bed cementation is observed in some areas (Table 4.2).

4.7. Diamond Fork channel change

4.7.1. Downstream of confluence

The active channel width of the reach has been variable over time, but was greater during the period of irrigation flows than under the current flow regime. In 1939, the average active channel width was 20 m and increased to 25 m by 1956 (Table 4.7). Where the valley is wide, the river was braided with large active gravel bars in 1939 and 1956 (Fig. 4.27, Fig. 4.28). By 1981, many of the active gravel bars had become vegetated and the channel width decreased to 12 m. In 1985, there were many fresh gravel bars and the active channel width increased to 25 m. Those

Table 4.6. Attributes of process domains on lower Diamond Fork.

Process domain	Percent confinement	Confining material	Slope (%)	Substrate	Geomorphic units	Percent pool	Length (km)
Below Confluence	26	Alluvial fans sandstone roads	1.5	Cobble boulder gravel, bedrock	Long runs pool/riffle sequences woody debris	N/A	2.9
Monks Hollow	33	Sandstone alluvial fans, roads	1.1	Cobble gravel boulder	Point bars pool/riffle/run sequences woody debris	N/A	3.5
Diamond Campground	26	Terraces alluvial fans	0.92	Gravel cobble sand	Point bars pool/riffle/run sequences	14	3.4
Above Mouth	22	Alluvial fans, terraces	0.69	Gravel cobble sand	Point bars instream bars	15	8.1

Fig. 4.26. Representative photos of lower Diamond Fork process domains. A) Downstream of confluence, Monks Hollow, Diamond Campground, Alluvial Valley.

Table 4.7. Summary of channel attributes of Below the Confluence process domain.

Year	Average width	Sinuosity	Percent multi-threaded
1939	20.1 ± 0.77	1.14	5.9
1953	24.0 ± 0.45	1.15	N/A
1956	25.4 ± 0.33	1.15	4.0
1981	11.8 ± 0.56	1.18	0
1982	12.3 ± 0.54	1.18	1.8
1983	15.0 ± 0.65	1.17	1.4
1985	24.9 ± 0.60	1.17	N/A
1993	12.9 ± 0.41	1.20	0
1997	13.5 ± 0.52	1.18	0
2004	10.0 ± 0.37	1.19	1.4
2006	11.6 ± 0.31	1.19	0.4
2009	11.0 ± 0.39	1.19	1.4
2011	10.5 ± 0.46	1.20	0
2014	10.3 ± 0.46	1.20	0
2016	10.0 ± 0.46	1.14	0

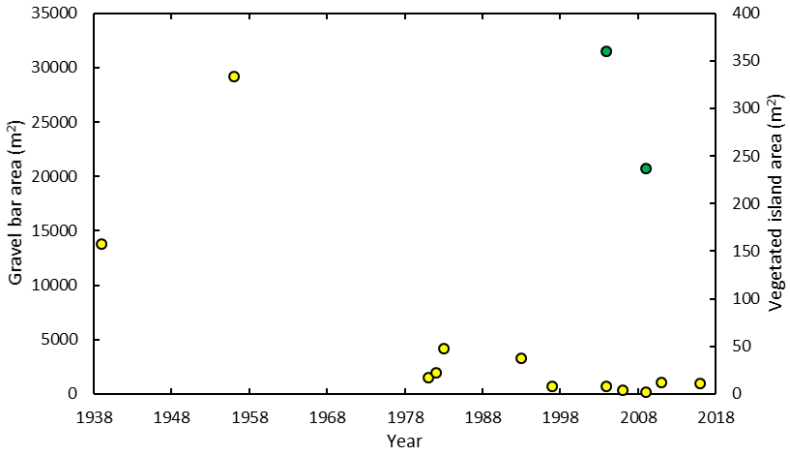

Fig. 4.27. Area of gravel bars (yellow) and vegetated islands (green) in Below the Confluence process domain, as digitized from aerial photographs.

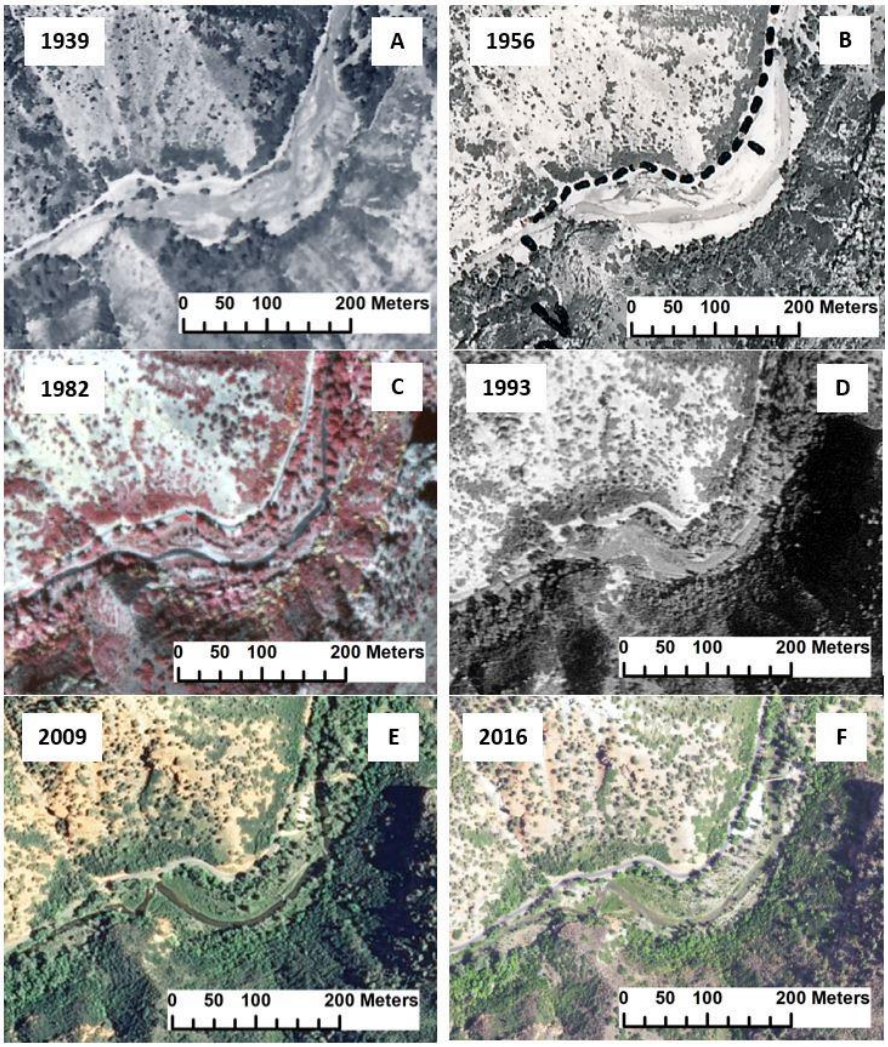

Fig. 4.28. Aerial photographs of a section of the Below the Confluence process domain. Channel had large, unvegetated bars in 1939 and 1956 photos (A and B), and channel margins became vegetated as the channel narrowed in later years (C-F).

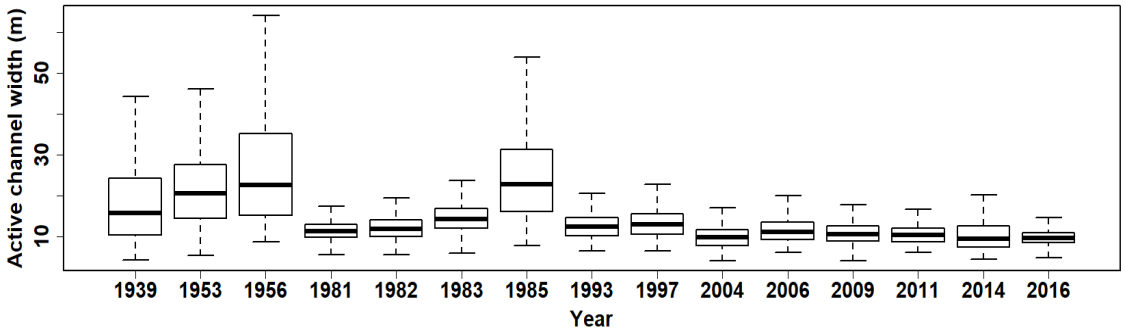

Fig. 4.29. Box plots of active channel width in the Below the Confluence process domain.

deposits were vegetated by 1993 and the channel width decreased to 13 m. The channel narrowed slightly in 1997 and 2004, to 10 m, as vegetation encroached on bars that were active in 1993 (Table 4.7). Channel width has been relatively consistent since 2004, as there has been almost no floodplain growth in that time period (Fig. 4.29).

4.7.2. Monks Hollow

The pattern of channel width change in the Monks Hollow reach is similar to the Downstream of the Confluence reach. The channel was wide and single threaded in 1939, when the average active channel width was 16.2 m. The reach widened to 20.8 m in 1953, but never became multi-threaded, even though fresh gravel bars were deposited and banks retreated (Table 4.8). Many of the bars that were active in the 1950s were vegetated in 1981 as the channel narrowed to 13.6 m. The river widened again in 1983 and 1985 to a maximum of 30.8 m, as large active bars formed at the channel margins (Fig. 4.30). By 1993, many of the bars present in 1985 had become vegetated as the channel narrowed to 16.9 m. The channel gradually narrowed between 1993 and 2004 as vegetation encroached on the margin of the channel. Since 2004, channel width has been relatively stable, with slight increases as new bars were deposited in 2006 and 2011 (Fig. 4.31).

Table 4.8. Summary of channel attributes of Monks Hollow process domain.

Year	Average width	Sinuosity	Percent multi-threaded
1939	16.2 ± 0.85	1.22	2.1
1953	20.8 ± 0.46	1.21	N/A
1956	19.2 ± 0.36	1.23	3.3
1981	13.6 ± 0.52	1.27	1.2
1982	13.8 ± 0.53	1.26	1.8
1983	19.4 ± 0.53	1.26	1.8
1985	30.8 ± 0.78	1.26	N/A
1993	16.9 ± 0.69	1.20	1.8

Table 4.8 (cont.)

1995*	13.7 ± 0.48	1.28	1.5
1997	14.2 ± 0.50	1.26	0.9
2003*	14.9 ± 0.31	1.28	0
2004	12.4 ± 0.27	1.29	0.5
2006	13.7 ± 0.27	1.27	0.2
2009	12.4 ± 0.30	1.28	1.1
2011	13.0 ± 0.42	1.29	2.6
2014	10.5 ± 0.42	1.29	0.5
2016	11.4 ± 0.42	1.22	1.2

*Note: Image coverage is incomplete

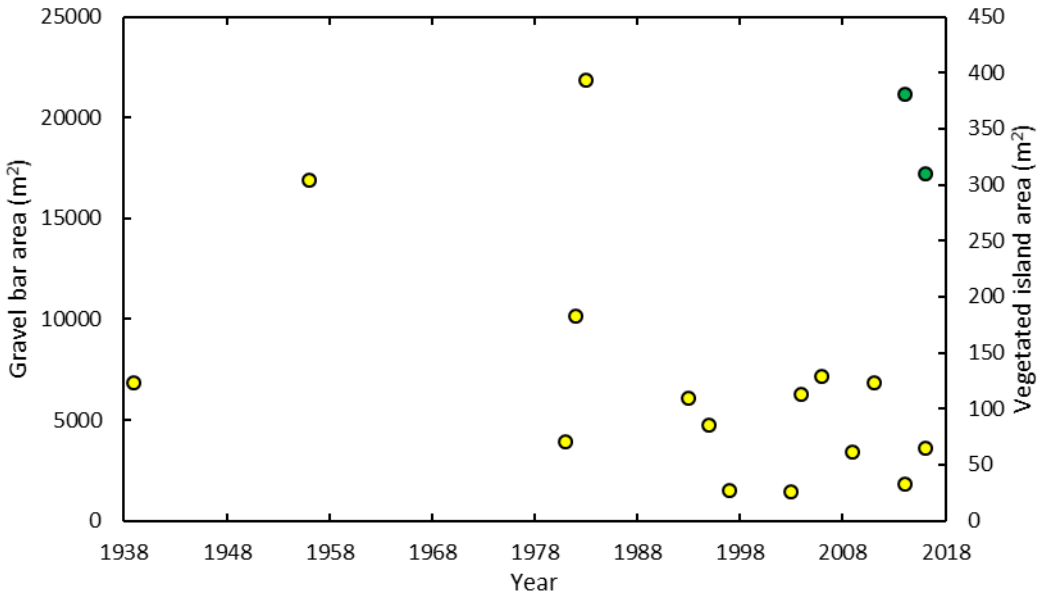

Fig. 4.30. Area of gravel bars (yellow) and vegetated islands (green) in the Monks Hollow process domain.

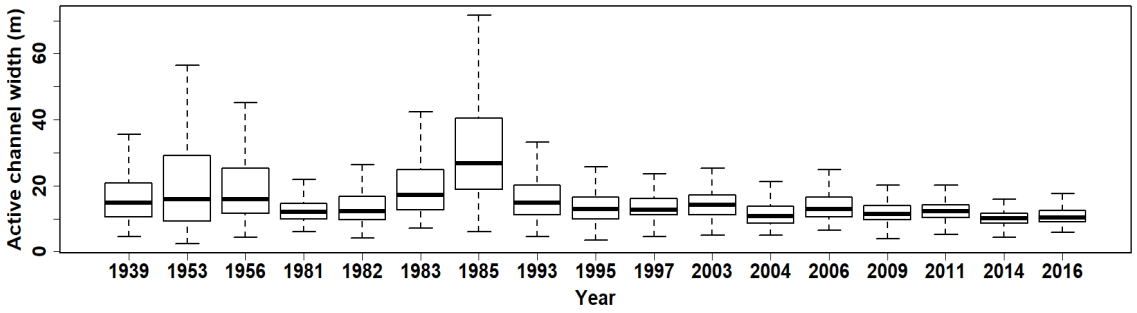

Fig. 4.31. Box plots of active channel width in the Monks Hollow process domain.

The presence of USGS gages in the Monks Hollow process domain allows us to evaluate changes in bed elevation over time. At the Diamond Fork Below Red Hollow gage, there was a period of degradation in the late 1950s that followed the floods of 1952 (Fig. 4.32A). The gage was not active during the floods of the early 1980s, but another period of bed degradation occurred from 1989 to 2001. The periods of degradation may represent the river evacuating the waves of sediment that were delivered during the large floods in 1952 and 1983-1984. At the Diamond Fork Above Red Hollow gage, the streambed elevation was consistent from 2001-2010, then experienced a step increase in elevation during the 2011 spring flood, as the bed aggraded by 0.25 m (Fig. 4.32B). The bed has remained at a stable elevation since 2011, suggesting that the river has not been able to evacuate the sediment that was delivered. Alternatively, this apparent shift in mean bed elevation could have been caused by an unrecorded datum shift.

It is interesting and somewhat perplexing that the bed elevation has not returned to its pre-2011 elevation at the Above Red Hollow USGS gage, because bed material can typically be transported at common floods in the Monks Hollow process domain. Painted rocks at the Monks Hollow sample site were not mobile at 100 cfs, but the majority of tracers were mobile at 150 cfs. Coarser grains did not travel far, 45 mm grains had an average displacement of 2 m and 64 mm traveled 1.5 m on average (Fig. 4.33). The flash flood of July 19th, 2017 delivered large amounts of sand and fine gravel to the Monks Hollow sample site. During the stepped flows, much of this

material was transported downstream, as evidenced by pebble counts from August and October 2017 (Fig. 4.26). The majority of bed material at the site is greater than 45 mm (Fig. 4.34), so the low transport rate of coarse material during the stepped flows suggests that bedload transport initiates at 150 cfs, but is not significant until higher flows.

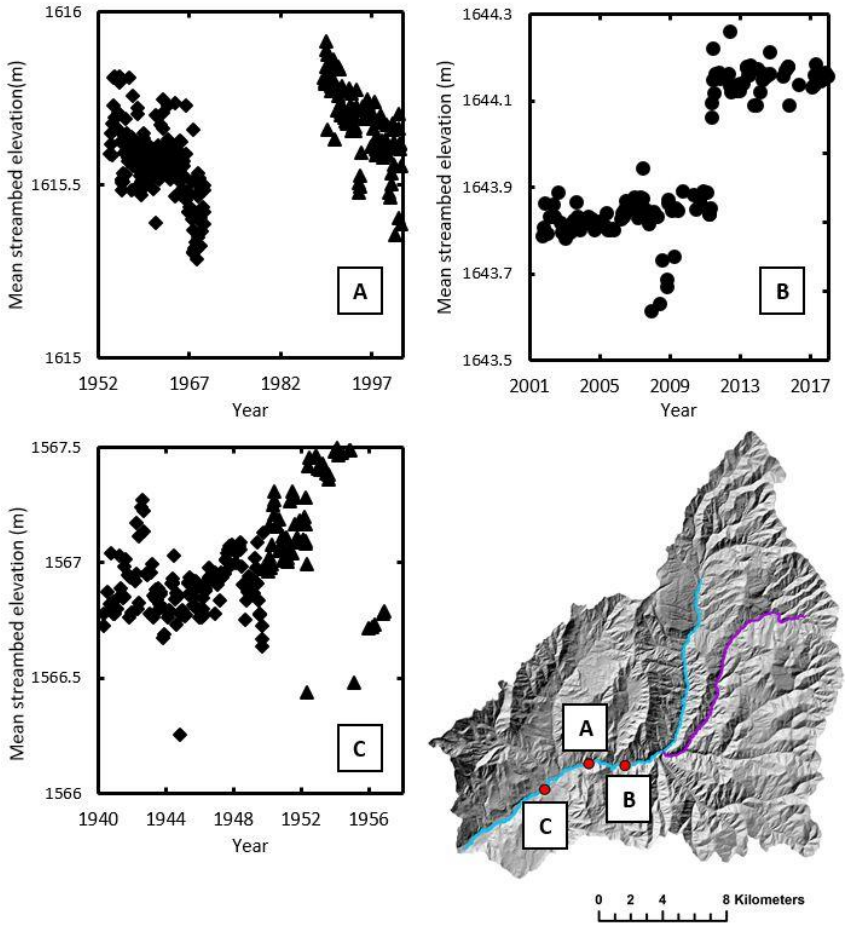

Fig. 4.32. Mean streambed elevation and location map of USGS gages on Diamond Fork. A) Diamond Fork Below Red Hollow, B) Diamond Fork Above Red Hollow, C) Diamond Fork near Thistle, UT.

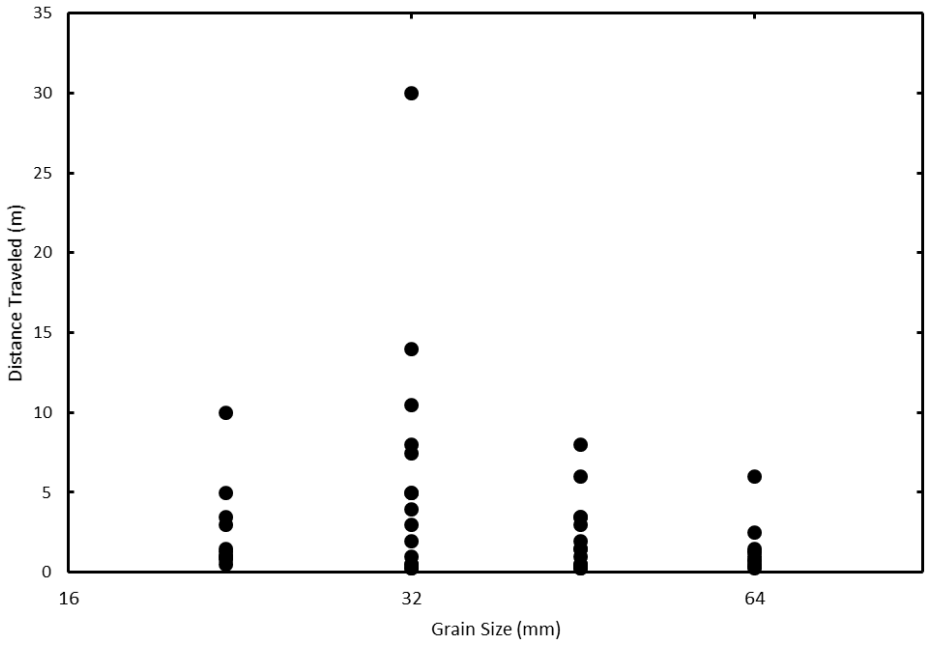

Fig. 4.33. Transport distance of painted gravel tracers at Monks Hollow monitoring site following the 150 cfs flow step.

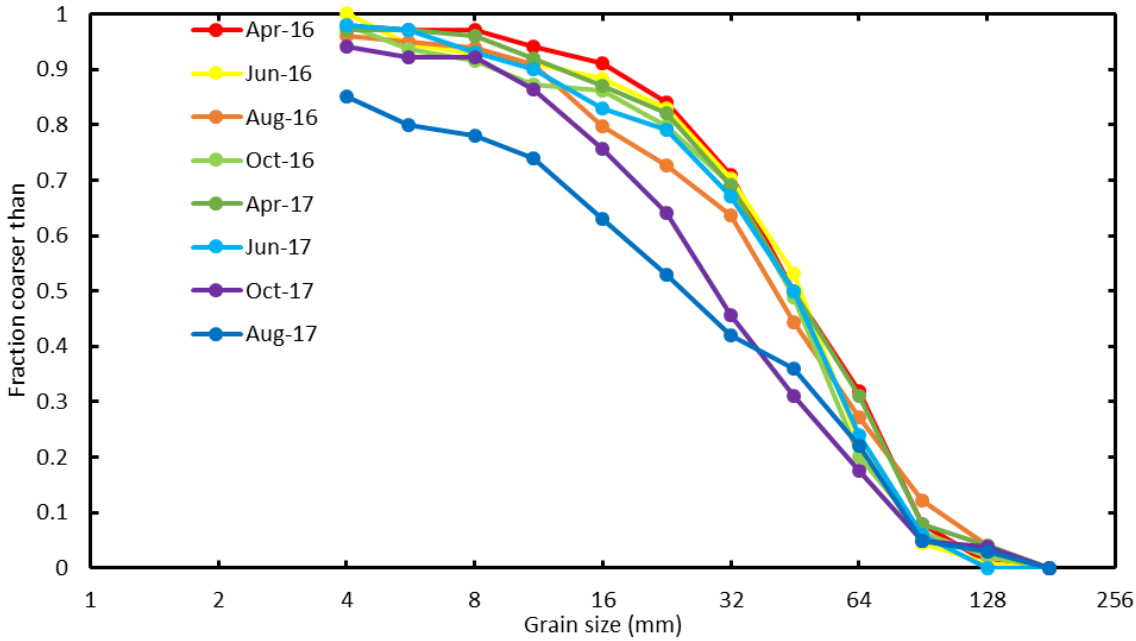

Fig. 4.34. Grain size distributions calculated from pebble counts at the Monks Hollow monitoring site conducted between April 2016 and October 2017.

Structural elements, such as large boulders and in-channel wood, can create significant channel change in the Monks Hollow process domain. During the spring 2017 flood, a large log jam developed downstream of the Monks Hollow sample site, forcing overbank flooding and the development of new channels dissecting the floodplain (Fig. 4.35). A ~1 m knickpoint was created on channel left in sediment that was formerly part of the floodplain. The flash flood on lower Diamond Fork on July 19th, 2017 caused the knickpoint to retreat 10 m upstream and forced the abandonment of the side channels that had developed on the floodplain (Fig. 4.35).

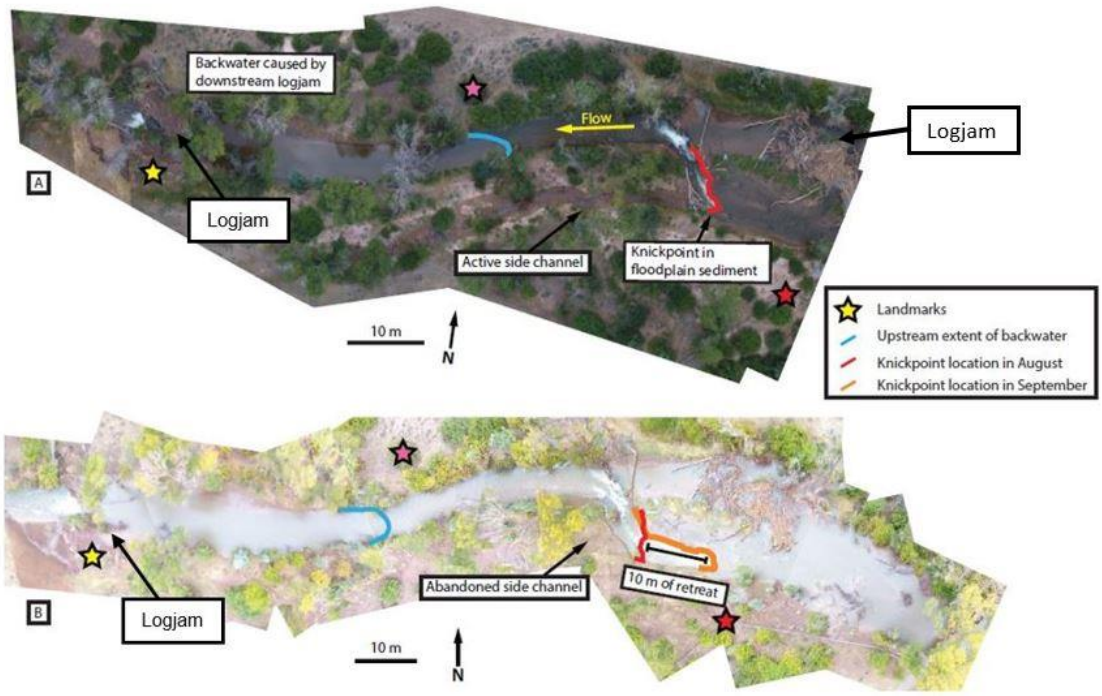

Fig. 4.35. Mosaicked aerial photographs of a logjam downstream of the Monks Hollow sample site captured from a UAV. The logjam developed during the spring runoff in 2017. Images taken A) August 10, 2017 and B) September 22, 2017. B) was taken during the second high flow in the stepped flow experiment.

4.7.3 Diamond Campground

Active channel width and planform character have changed over time in the Diamond Campground process domain. In 1939, unconfined sections of the reach were multi-threaded with active gravel bars (Fig. 4.36). There was also a large island at the downstream end of the reach. By 1953, the river had widened to 30.4 m as several large gravel bars were deposited in the more confined sections of the reach, and the multi-threaded sections remained active. The channel narrowed slightly between 1953 and 1956, to 26.6 m, as vegetation encroached at the edge of the channel, but the channel remained wide and had active bars. By 1981, many of the active bars from the 1950s had become vegetated and the reach narrowed to 16.7 m (Fig. 4.37). There were still active gravel bars present in the channel but they were smaller and more dispersed than in the 1950s. The channel widened in 1983 and 1985, to a maximum of 30.5 m as more large gravel bars were deposited. By 1993, many of the active surfaces were vegetated and the channel narrowed to 19 m. Further encroachment of vegetation occurred in 1997 and 2004, and the channel narrowed to 15 m. Throughout the 1990s and 2000s a small percentage (3-10%) remained multi-threaded. By 2009 the channel had narrowed to 11.9 m (Table 4.9). Spring flows in 2011 deposited fresh gravel, briefly widening the channel to 14 m. Those gravel deposits were vegetated in subsequent years and the average active channel width was 10.7 m in 2016 (Fig. 4.38).

Narrowing of the Diamond Campground reach since 2004 is also recorded in the cross-sections, which have consistently become narrower and deeper over time (Fig. 4.39). Six of the seven cross-sections were narrower in 2017 than in 2005, and six of seven have a greater average depth. The average elevation of cross-sections has remained relatively stable, however the minimum elevations have changed over time. The minimum elevation of 4 of the cross-sections experienced aggradation or degradation of more than 20 cm between measurements, suggesting that the bed has been active frequently since 2005.

Bed material was actively transported during the spring runoff of 2017 (peak 280 cfs) and the stepped flow experiment (peak 150 cfs). During the peak flow, bed sediment in the Diamond Campground process domain was reworked and fresh deposition on bars and erosion of pools occurred (Fig. 4.40). During the stepped flow experiment, the majority of painted tracers were mobile at the higher of the stepped flows (150 cfs). The median transport distance was small, only 2 m, but 20% of grains traveled more than 5 m and one grain traveled ~80 m (Fig. 4.41). The peak flow of 2017 has a return interval of about 2 years, and 150 cfs occurs annually, suggesting that the bed is mobile at common flows.

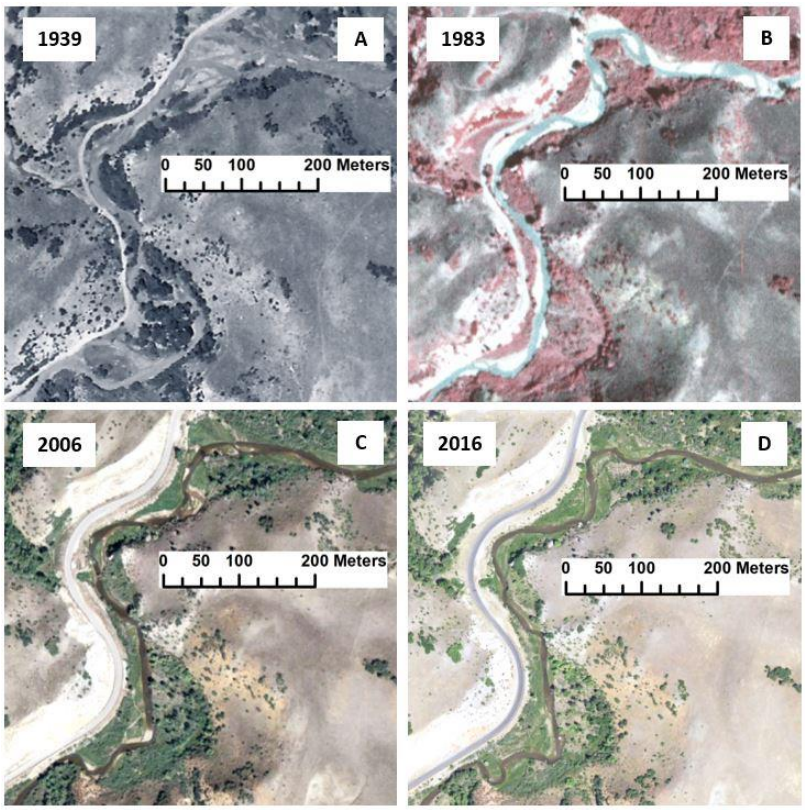

Fig. 4.36. Aerial photographs of a section of Diamond Campground process domain.

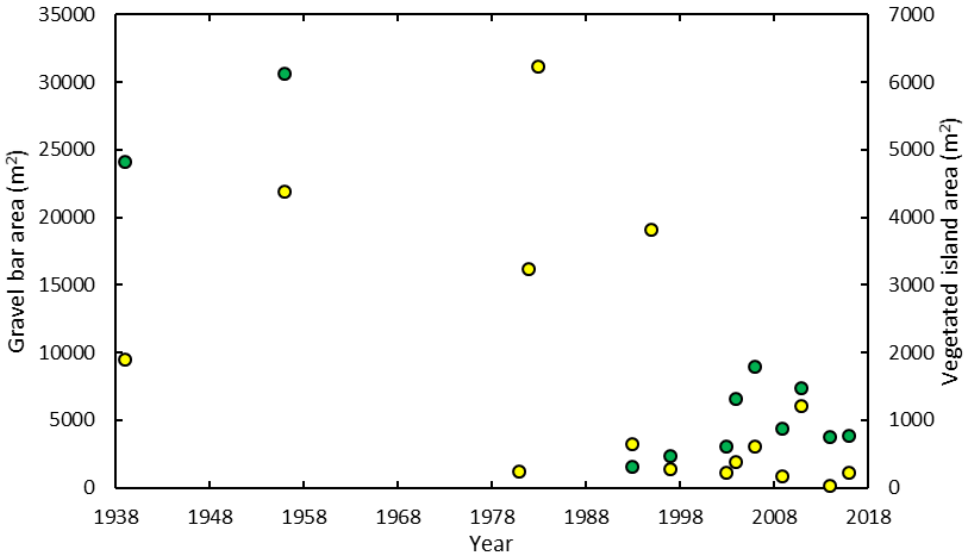

Fig. 4.37. Area of gravel bars (yellow) and vegetated islands (green) in the Diamond Campground process domain.

Table 4.9. Summary of channel attributes of Diamond Campground process domain.

Year	Average width	Sinuosity	Percent multi-threaded
1939	22.1 ± 0.80	1.25	16.7
1953	30.4 ± 0.43	1.20	N/A
1956	26.6 ± 0.41	1.23	18.0
1981	16.7 ± 0.52	1.25	0
1982	17.4 ± 0.54	1.24	7.9
1983	23.2 ± 0.53	1.25	3.6
1985	30.5 ± 0.64	1.27	N/A
1993	18.8 ± 0.38	1.24	1.2
1995	17.7 ± 0.51	1.25	6.1
1997	13.9 ± 0.48	1.26	3.0
2003	16.5 ± 0.31	1.27	3.9
2004	14.8 ± 0.26	1.26	9.3
2006	14.3 ± 0.25	1.27	4.8
2009	11.9 ± 0.26	1.27	4.5
2011	14.5 ± 0.43	1.29	6.3
2014	10.9 ± 0.43	1.29	3.8
2016	10.7 ± 0.43	1.25	6.2

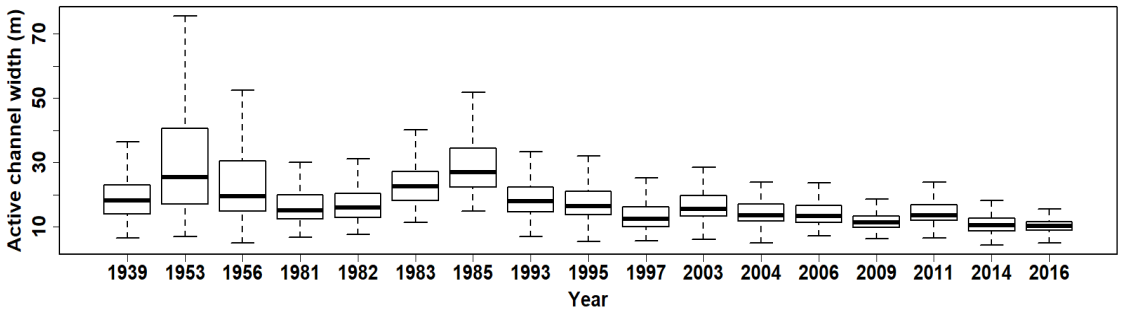

Fig. 4.38. Box plots of active channel width in the Diamond Campground process domain.

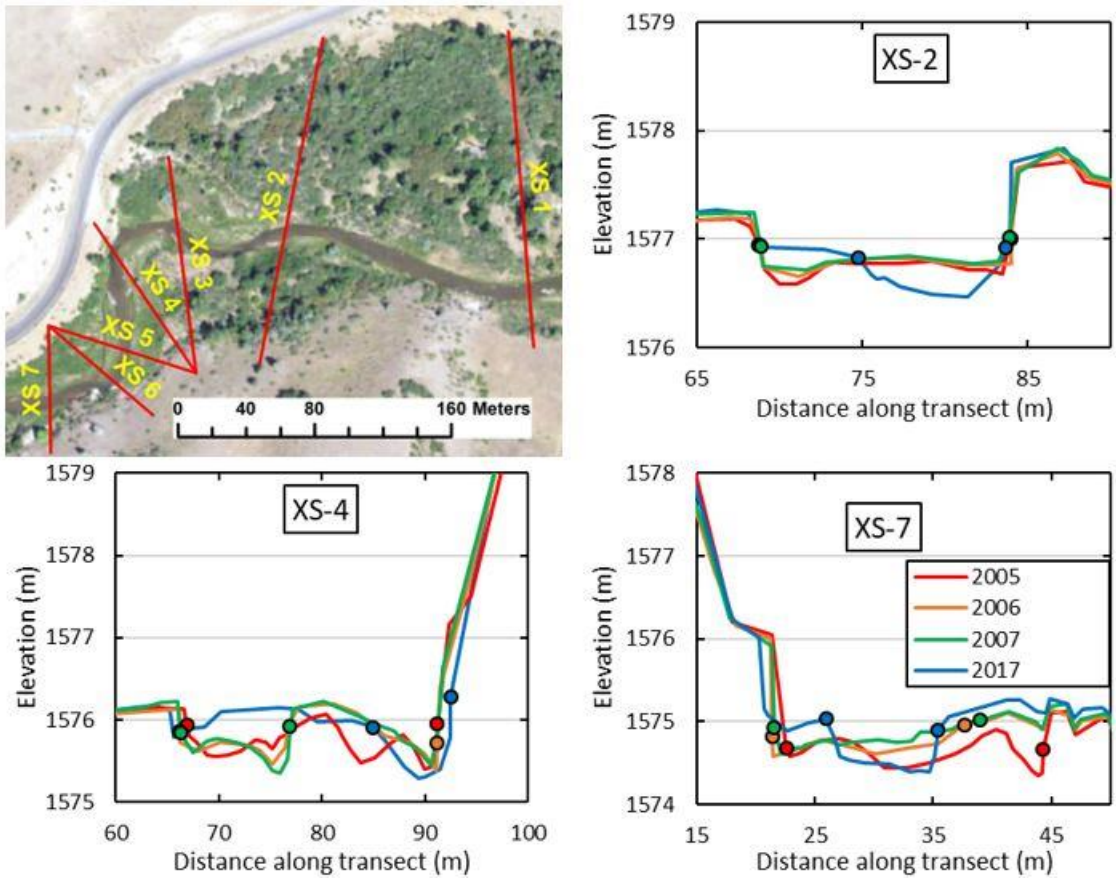

Fig. 4.39. Location of cross-sections at Diamond Campground site and profiles of cross-sections 2, 4, and 7.

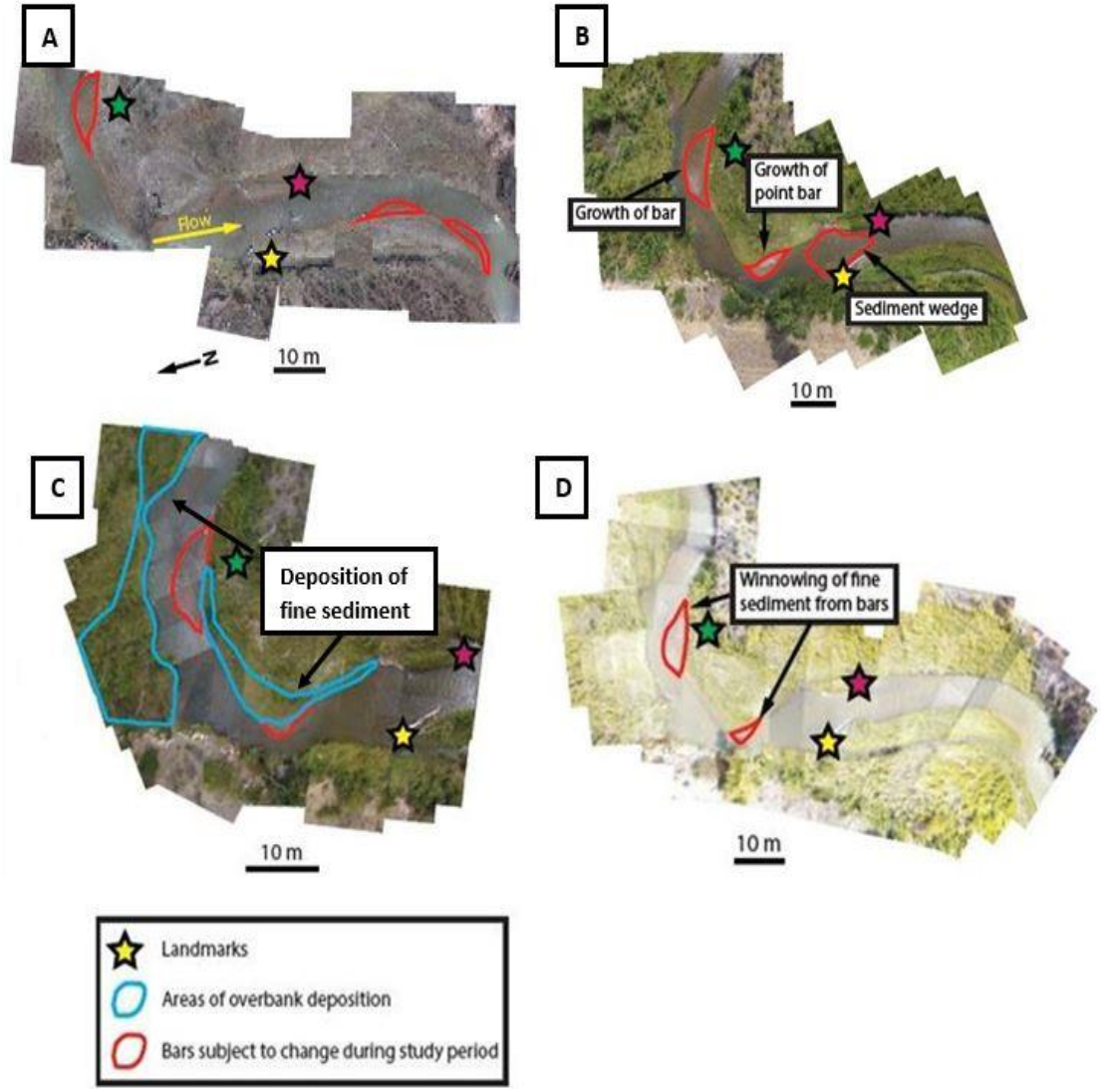

Fig. 4.40. Mosaicked aerial photographs of the Diamond Campground sample site captured from a UAV. Images taken A) April 11, 2016, B) July 11, 2017, C) September 9, 2017, and D) September 22, 2017. B) followed a moderate magnitude spring runoff in 2017, C) was captured during a low flow in the stepped flow experiment, and D) was captured during the second of two high flows in the stepped flow experiment.

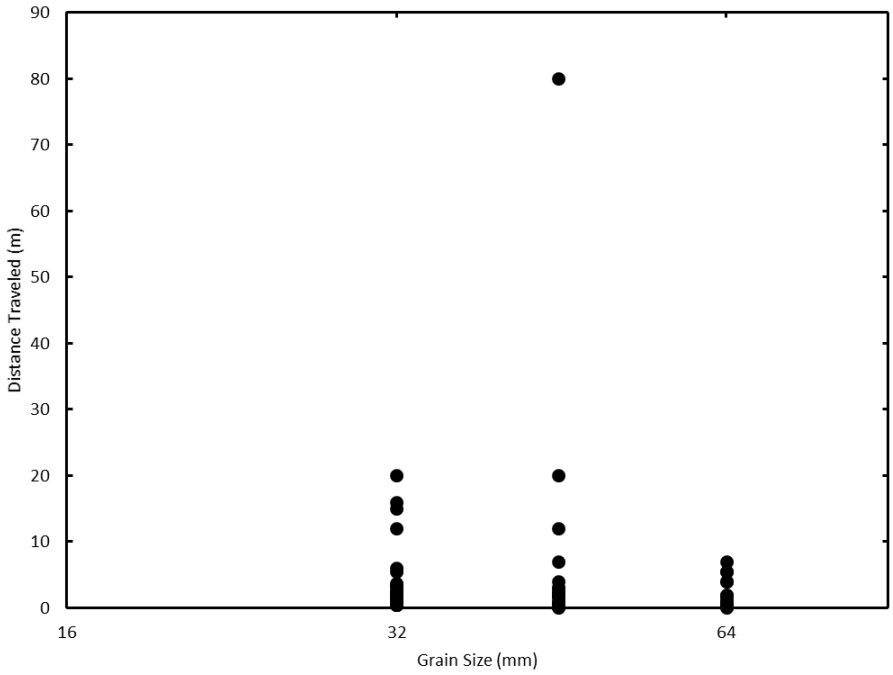

Fig. 4.41. Transport distance of painted gravel tracers at Diamond Campground monitoring site following the 150 cfs flow step.

4.7.4. Diamond Fork Alluvial Valley

Over the period of record, the Alluvial Valley reach has been the most dynamic and has experienced the most dramatic changes. In 1939 there were sections that were single threaded and other sections that were multi-threaded, but multi-thread reaches comprised a small proportion of the process domain. By 1953, a greater proportion of the process domain was multi-threaded and the average, 1st, 2nd, and 3rd quartiles of channel width all greatly increased. Some narrowing occurred between 1953 and 1956, as surfaces that were active at the margin of the valley became vegetated. Despite the narrowing, the channel remained very active with large, dissected gravel bars throughout the process domain and was 25% multi-threaded (Table 4.10). The channel narrowed between 1956 and 1981, from 26.4 to 17.6 m, but the channel remained active, with large unvegetated bars (Fig. 4.42). Channel width reached a peak of 34 m in 1985, following the high flow years of 1983 and 1984. By 1993, the channel had returned to a condition similar to the early 1980s, with wide active, dissected bars and an average width of 20.6 m. By 1995 and 1997,

the channel had begun to narrow as vegetation encroached on formerly active bars (Fig. 4.43). Since 2003, the channel has been less dynamic. By 2003, nearly all of the multi-threaded areas had disappeared from the channel as formerly active bars became vegetated and the widest part of the channel narrowed rapidly (Fig. 4.44). Since 2003, the channel has continued to narrow episodically, as relatively large floods in 2006 and 2011 created fresh gravel deposits that were subsequently vegetated (Fig.4.42, Fig. 4.45).

Table 4.10. Summary of channel attributes of Alluvial Valley process domain.

Year	Average width	Sinuosity	Percent multi-threaded
1939	28.0 ± 0.74	1.37	11.9
1953	41.4 ± 0.44	1.23	N/A
1956	34.5 ± 0.21	1.20	24.3
1981	28.1 ± 0.61	1.20	17.8
1982	27.5 ± 0.56	1.19	16.9
1983	38.1 ± 0.59	1.18	8.1
1985	49.1 ± 0.88	1.16	N/A
1993	33.7 ± 0.38	1.16	17.3
1995	25.6 ± 0.49	1.16	18.5
1997	27.8 ± 0.42	1.19	20.2
2003	20.1 ± 0.3	1.20	9.1
2004	16.7 ± 0.33	1.20	13.4
2006	16.9 ± 0.25	1.22	8.2
2009	13.8 ± 0.25	1.22	7.1
2011	17.2 ± 0.40	1.25	8.6
2014	12.1 ± 0.40	1.25	4.4
2016	11.9 ± 0.40	1.37	3.3

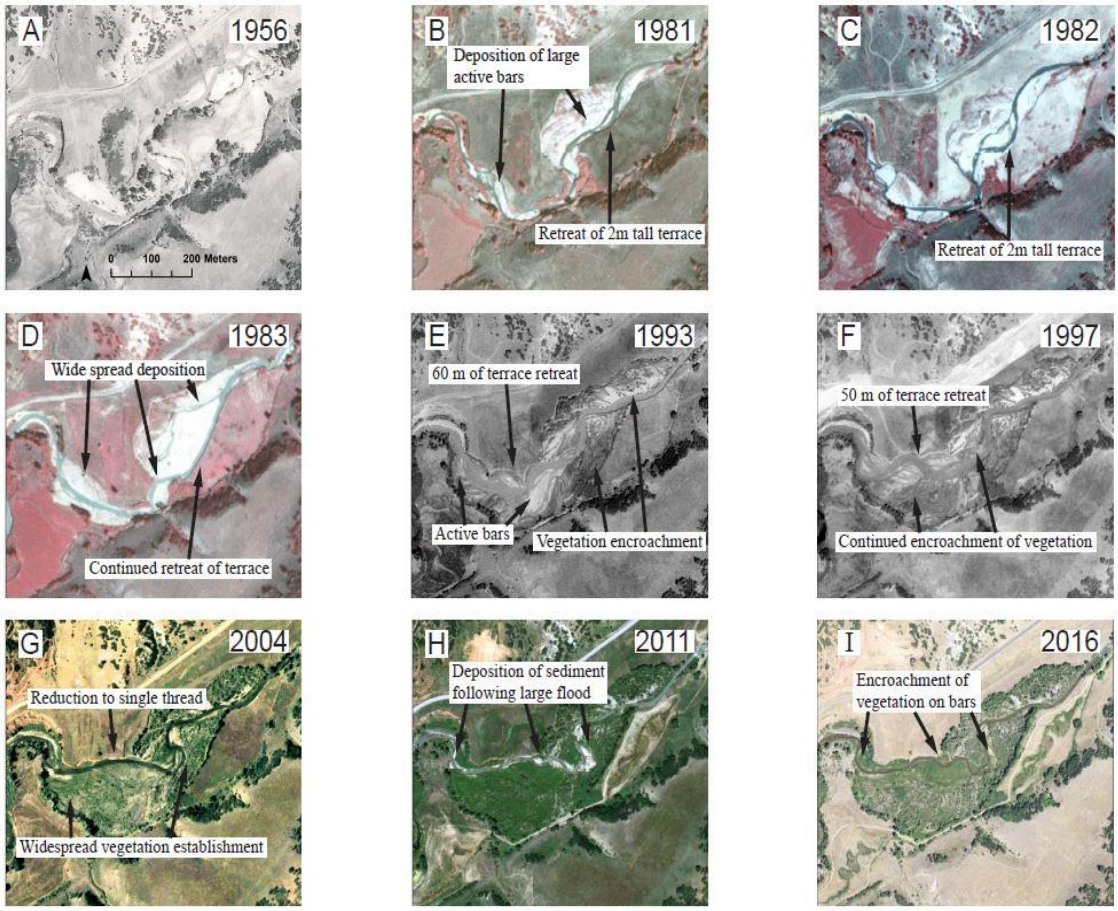

Fig. 4.42. Aerial photographs of the Oxbow site in the Alluvial Valley process domain. The photos show widening of the channel and active bar surfaces from the 1950s - 1990s (A-E), and channel narrowing and vegetation encroachment from 1997 - 2016 (F-I).

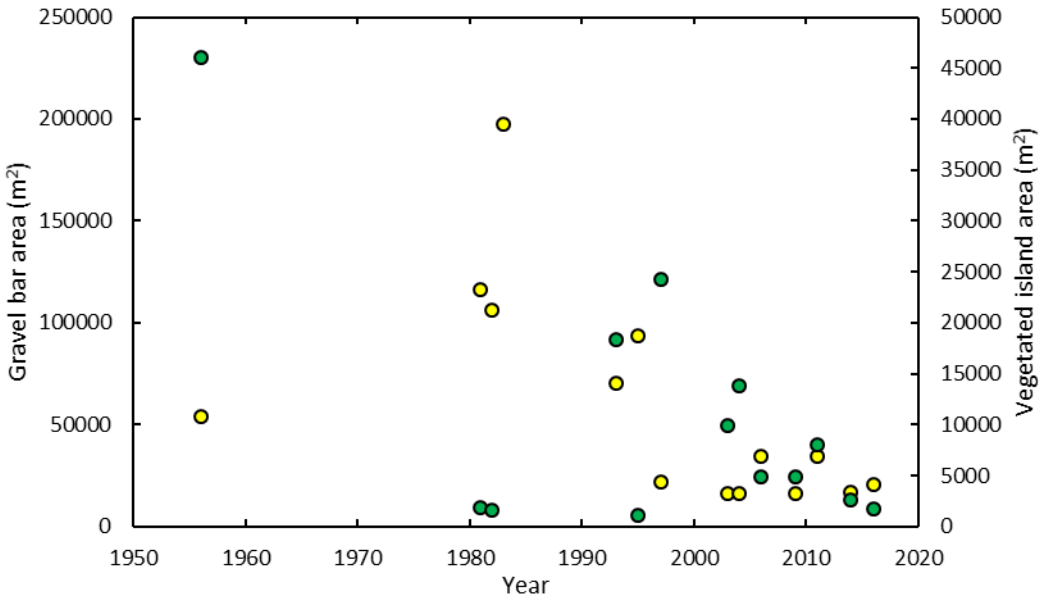

Fig. 4.43. Area of gravel bars and vegetated islands in Alluvial Valley process domain.

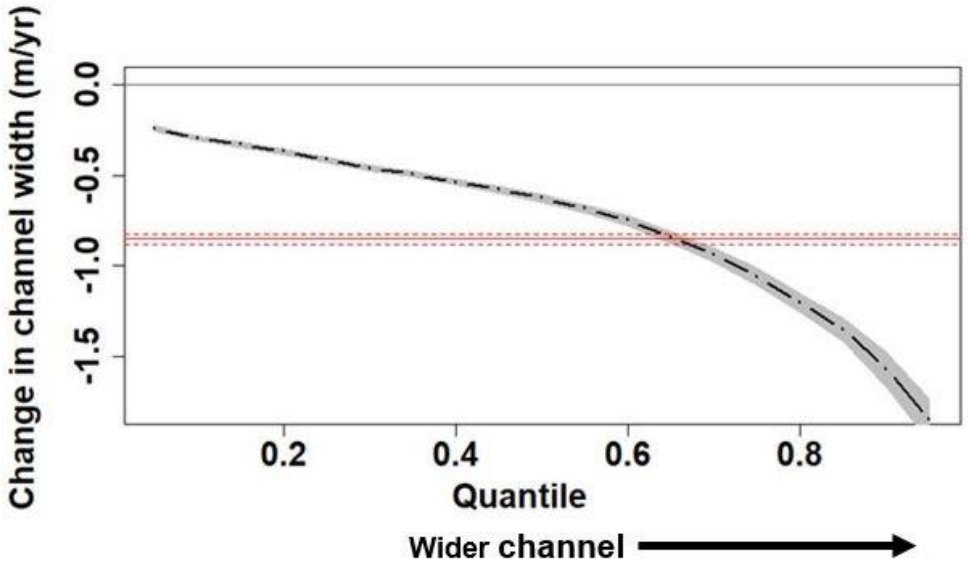

Fig. 4.44. Quantile regression analysis for Alluvial Valley process domain. Larger quantiles represent wider parts of the channel.

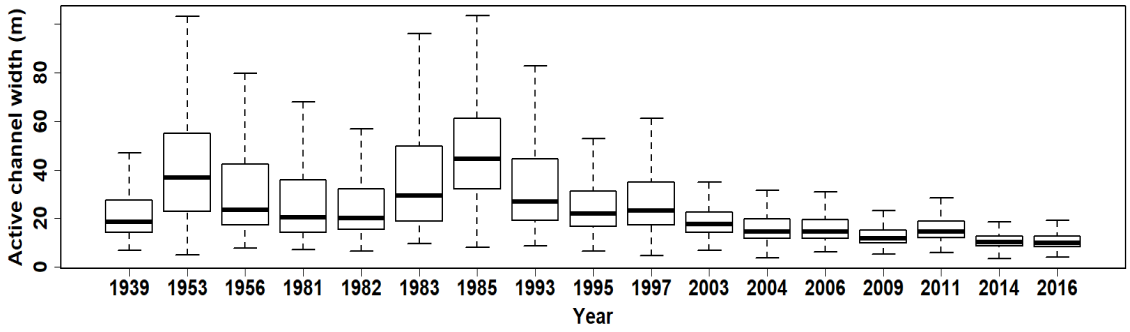

Fig. 4.45. Box plots of active channel width of the Alluvial Valley process domain.

The sinuosity of the reach has changed along with channel width. The reach had high sinuosity in 1939, when much of the reach was still single threaded, but became less sinuous when more of the reach became braided by 1953 (Table 4.10). The sinuosity remained low in the 1980s and reached a minimum in 1993. This low sinuosity corresponded with the braided character of the river between 1953 and 1993. Since 1993, the sinuosity has increased as the channel became single threaded and new meander bends developed. 2016 had a sinuosity equivalent to that of 1939 even though a lower proportion of the channel was multi-threaded in 2016 than in 1939 (Table 4.10).

Historical bed elevations in the Alluvial Valley process domain reflect large flood events that occurred in the 20th Century. The Diamond Fork near Thistle gage was located at the upstream end of the Alluvial Valley process domain. The streambed elevation of the gage has a period of aggradation from the late 1940s until the mid-1950s (Fig. 4.24C). The period of aggradation coincides with the flood of record in 1952 and the second largest recorded flood in 1954.

The Diamond Fork Alluvial Valley reach remains the most dynamic section of the river, due to the lack of lateral confinement, the relatively fine grain size of bed material, and the relatively low slope and transport capacity of the channel. Bed material was mobile at the

Motherlode site during the 150 cfs flow of the stepped flow experiment. During the 100 cfs flow, many grains moved, but the movement probably does not represent true transport, but local adjustment of the artificially placed grains. The median transport distance for all grain sizes was less than 50 cm, and the maximum transport distance was 31.8 m. The 150 cfs flow transported grains greater distances and transported the majority of painted rock tracers (Fig. 4.46). For the RFID tracers, the median transport distance was greater than 7 m for all grain sizes in transport and greater than 25 m for the 22.6, 32, and 64 mm grains. The majority of RFID tracers were deposited on transverse bars, with some deposited in pools or along the channel margin (Fig. 4.46C).

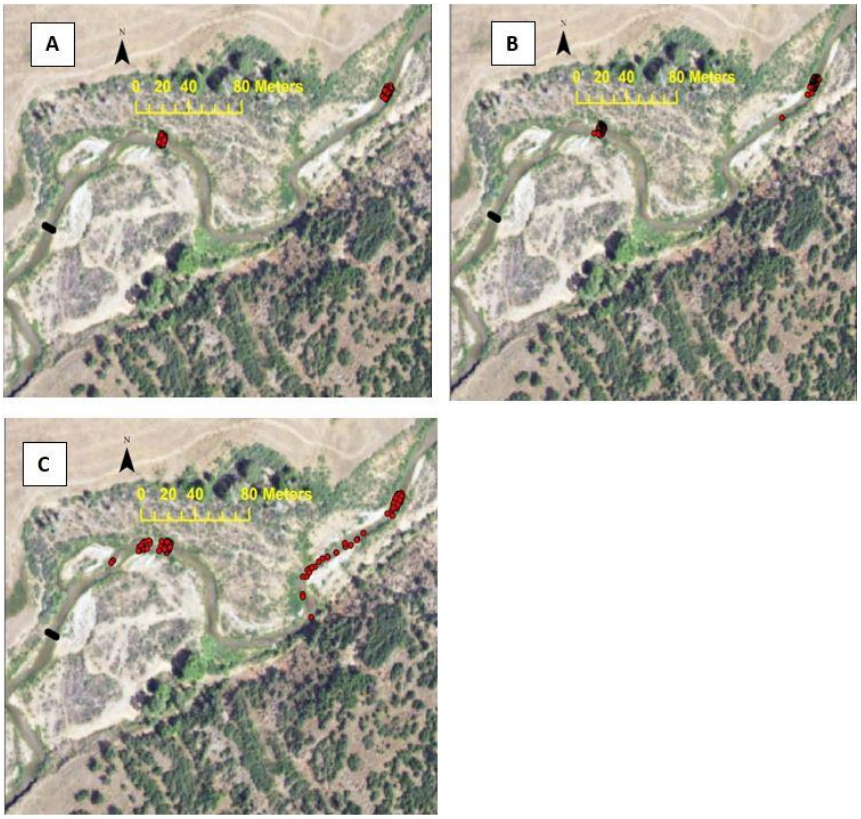

Fig. 4.46. RFID tracer locations A) before the stepped flows, B) following the first stepped flow, and C) following the second stepped flow. Red dot indicates tracer locations. Black bar indicates an automated RFID reader, which was temporarily installed in the channel during the step flow experiments. None of the RFID-tagged gravels reached the automated reader.

Active transport of bed material promotes channel activity, including cross-sectional change. Cross-sections at the Motherlode and the Oxbow site experienced change between 2005 and 2017. At the Motherlode site, cross-sections changed in a consistent way – by narrowing, deepening, and migrating (Fig. 4.47). Of the 6 cross-sections at Motherlode, 4 narrowed while 2 had little change in width. Five of 6 had a greater average depth in 2017 than 2005. Four cross-sections incised and 2 aggraded. All 6 cross-sections migrated between 2005 and 2017.

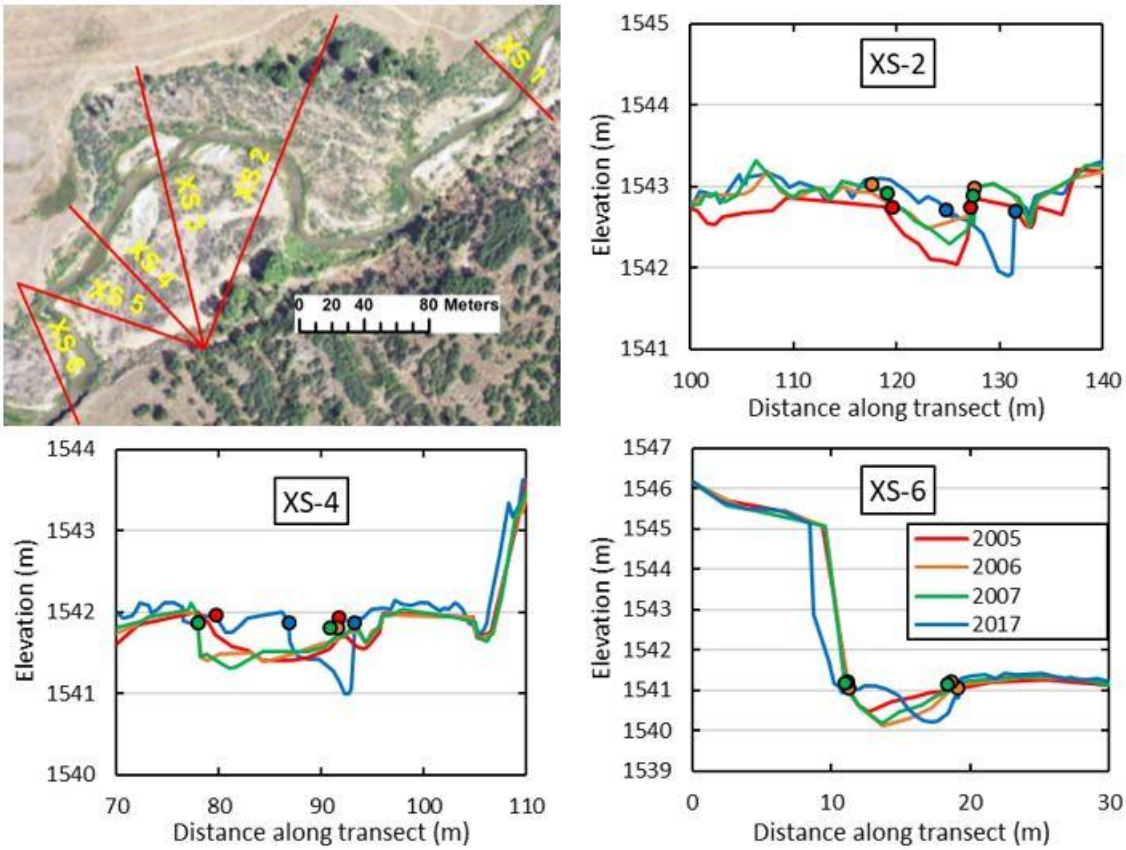

Fig. 4.47. Location of cross-sections at Motherlode monitoring site and profiles of cross-sections 2, 4, and 6.

At the Oxbow site, there was not a consistent trend in width or elevation change for all of the cross-sections (Fig. 4.48). Of the 8 cross-sections, 5 incised and 3 aggraded between 2005 and 2017. Six had a greater average depth in 2017 than in 2005. Four cross-sections were narrower in 2017 than 2005, while 2 had relatively constant width, and 2 were slightly wider. Six of the cross-sections migrated between 2005 and 2017.

The majority of cross-sections surveyed at Diamond Fork monitoring sites narrowed and incised between 2005 and 2017 (Fig. 4.49). 2006 was a relatively large flood year and relatively large magnitude changes were measured between 2005 and 2006. Less change was observed between 2006 and 2007, because the peak flow of 2007 was not large enough to promote extensive channel change. Between 2007 and 2017, the majority of cross-sections experienced narrowing and bed degradation. The few cross-sections that experienced an increase in minimum bed elevation were either located just downstream of a channel constriction, in an area that would promote deposition, or experienced the deposition of a bar and the channel shifted.

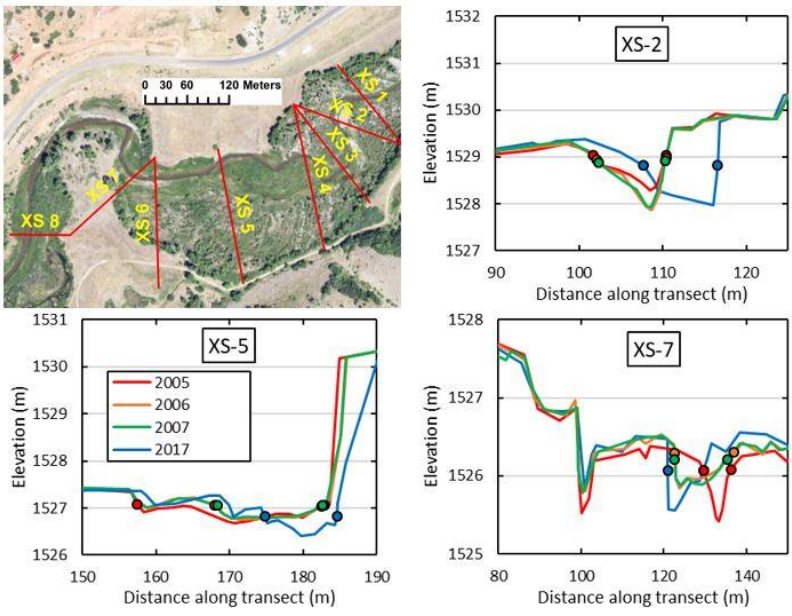

Fig. 4.48. Location of cross-sections at Oxbow monitoring site and profiles of cross-section 2, 5, and 7.

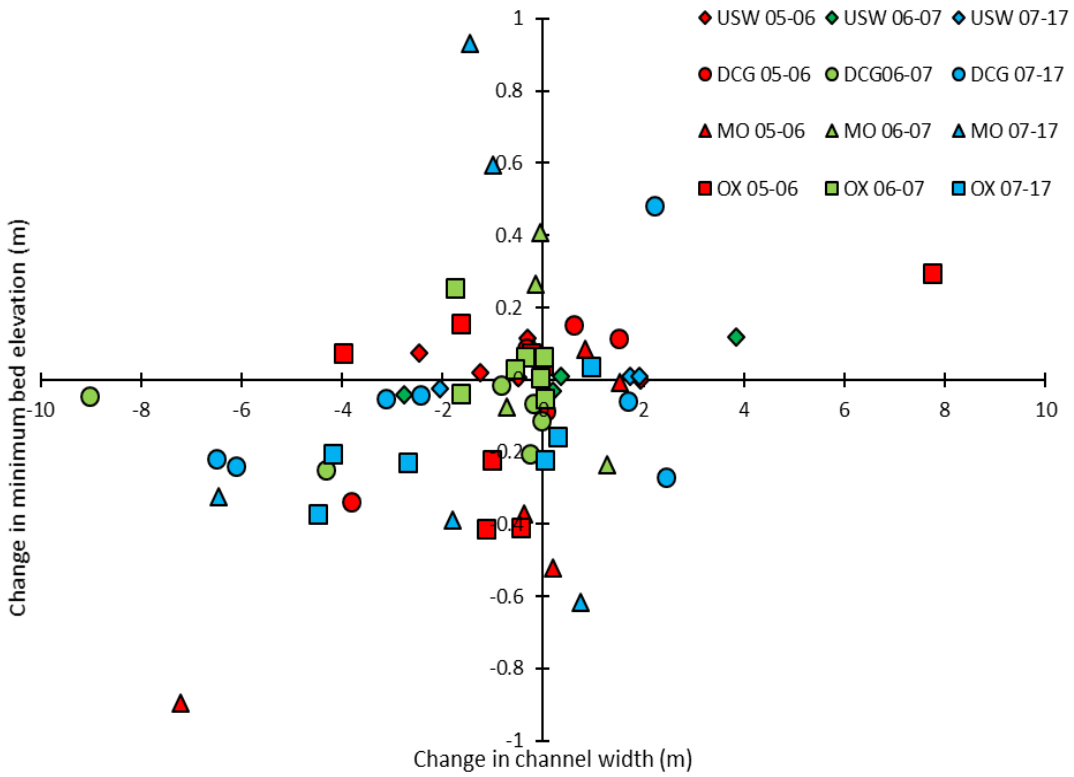

Fig. 4.49. Summary of cross-section changes at Upper Sixth Water (USW), Diamond Campground (DCG), Motherlode (MO), and Oxbow (OX) monitoring sites. Each data point represent a successive survey of a cross-section, with colors representing different years and shapes representing different sites. The X-axis represents channel widening (+) and narrowing (-) and the Y-axis represents aggradation (+) and degradation (-).

4.8. Diamond Fork sediment sources

Ten potential sediment sources were sampled on Diamond Fork, the majority being terraces and alluvial fans between the Diamond Campground and Oxbow sites. Most sediment sources on lower Diamond Fork are coarse grained alluvial deposits, and the grain size distribution of the sampled sources aligns well with bed material on Diamond Fork (Fig. 4.50). Most samples had a larger fraction of fine material than bed samples, but this may be an artifact

of sample method (mass based vs. pebble count). We also sampled the bed of Monks Hollow, a tributary to the lower Diamond Fork. The material in Monks Hollow was finer than the bed material of the Diamond Fork (Fig 4.34, Fig. 4.51), suggesting that floods from tributaries can supply fines to the lower Diamond Fork.

4.9. Diamond Fork fluvial surfaces

Fluvial surfaces are common in the valley of the lower Diamond Fork. The lowest elevation surfaces (<1 m) are especially important because they are inundated frequently and may provide areas for vegetation to colonize, causing further channel narrowing. Their formation, maintenance, and patterns of vegetation hold clues about potential future narrowing of Diamond Fork. Low elevation floodplain surfaces are common in the Alluvial Valley process domain and formed primarily in association with post-1997 channel narrowing (Fig. 4.52). These areas were

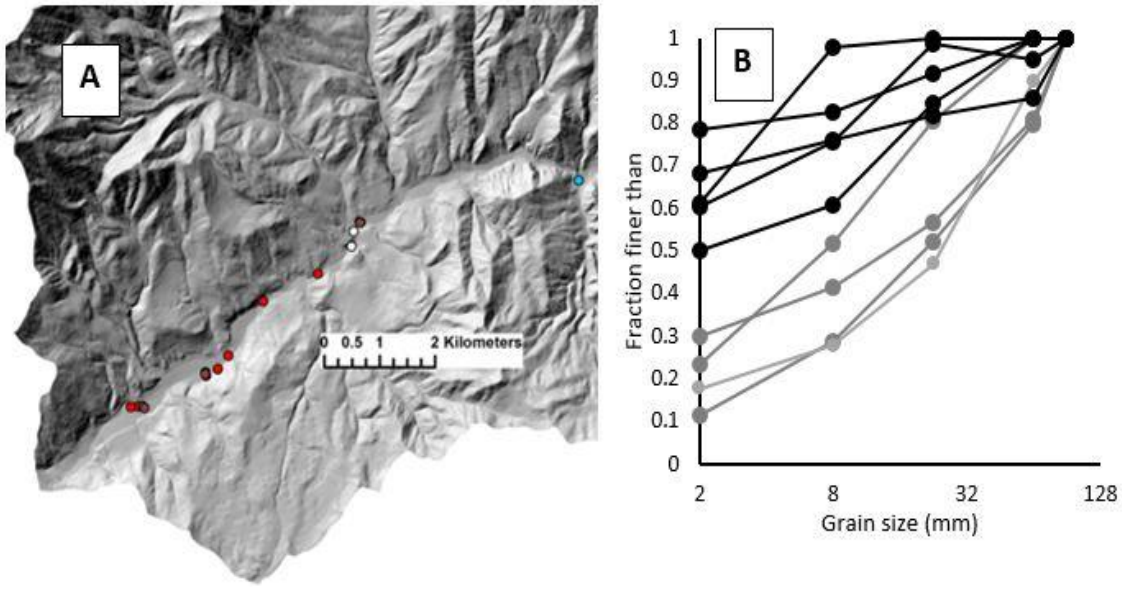

Fig. 4.50. Sediment source samples on lower Diamond Fork. A) Location of sediment source samples including active hillslopes (red), deposits (brown), and a tributary (blue), B) grain size distribution of active hillslope sources.

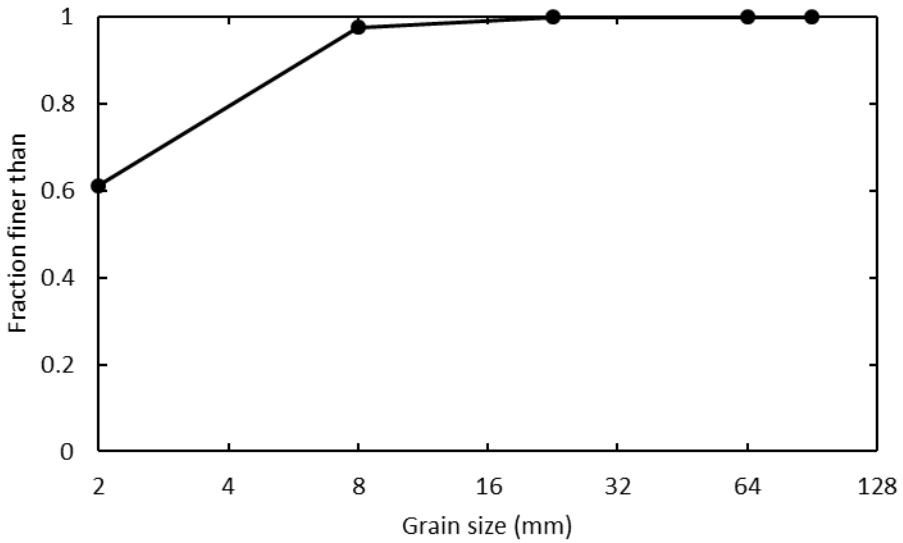

Fig. 4.51. Grain size distribution of Monks Hollow tributary showing a significant fraction of sand sized particles.

active bars during the high flow regime but became vegetated after 1997 and generally have little fine-grained sediment, suggesting there has been minimal vertical aggradation since deposition. The lack of vertical accretion suggests that either portions of the floodplain surfaces are still not inundated by common floods and/or there is insufficient suspended sediment the water column to promote aggradation. During the experimental high flow release (150 cfs), water did not inundate extensive portions of the floodplain, but we observed flow in some relict side channels. These areas also have very gradual transverse and downstream slopes, such that there is not a distinct break in slope at the channel margin. There are fewer low elevation floodplains in the upper, more confined process domains of the lower Diamond Fork (Fig. 4.52), where terraces that are 1 to 2 meters above the present channel are relatively common.

Terraces and floodplains on lower Diamond Fork have been deposited and preserved throughout the period of record. Large areas from 1939 and 1956 are still preserved and can be identified from the lidar data. Preserved surfaces from 1993 comprise the largest area, indicating that bars deposited during the 1983 and 1984 floods have persisted and, in some but not all cases

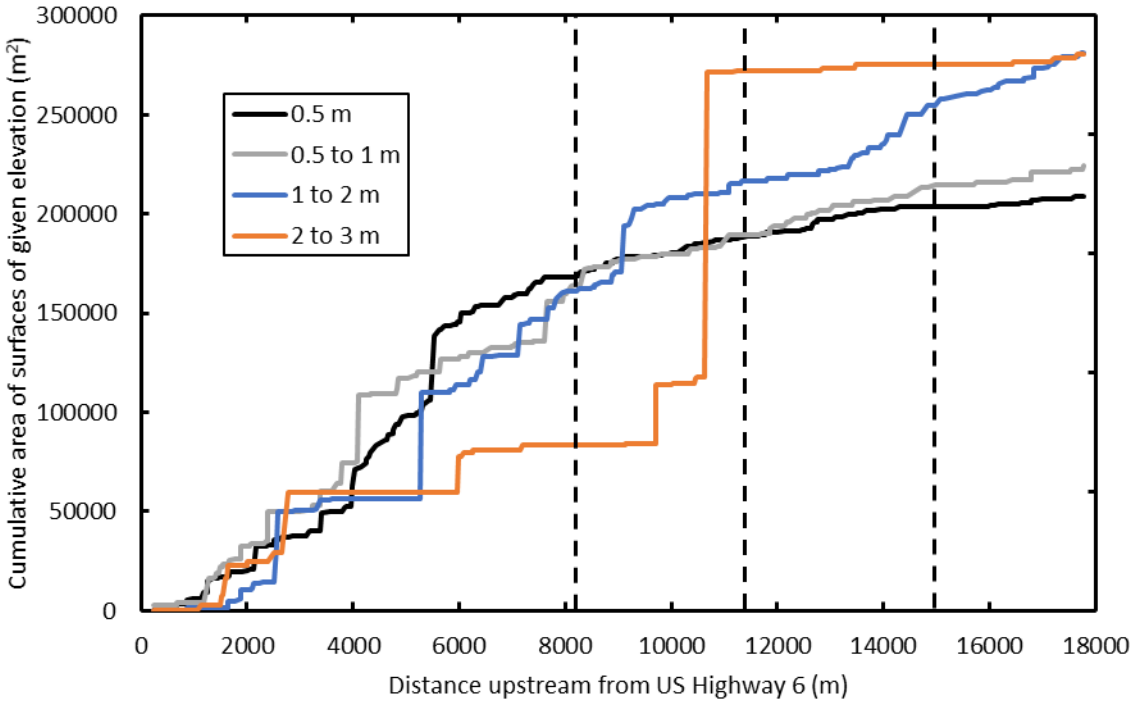

Fig. 4.52. Cumulative area of fluvial surfaces on lower Diamond Fork with distance upstream. Surfaces are separated by their height above the current channel. Vertical dashed lines represent process domain breaks.

became vegetated (Fig. 4.53). A large amount of surfaces were also preserved since 2004, as areas that were active bars in 1997 became vegetated and the channel changed planform, from multi-threaded to single threaded (Fig. 4.42). Deposits from 2006 and 2011 comprise a relatively small area, but are important for the evolution of lower Diamond Fork after the change of flow regime in 2004.

There are several relict channels preserved in floodplains and terraces on lower Diamond Fork that suggest a complex and spatially variable history of aggradation and incision. One relict channel in the Diamond Campground process domain that was formed by the deposition of a bar in 1952 was abandoned by the 1980s and never re-occupied (Fig. 4.54). Based on profiles extracted from the lidar, the abandoned channel is ~1 m above the current channel. Other relict

channels from the Alluvial Valley process domain reveal the complexities of the lower Diamond Fork valley (Fig. 4.55). Figure 4.55 shows that channels that were active in the 1939 and 1981 imagery are less than 0.5 m above the current channel. The reach shown in Figure 4.55 has been very dynamic over the period of record, with large bars regularly being reworked, so it is interesting to see the preservation of channels and to observe their topography. More work is needed to describe and understand the complexity of valley elevation on lower Diamond Fork, but preliminary analysis suggests that incision and aggradation were spatially variable and temporally complex.

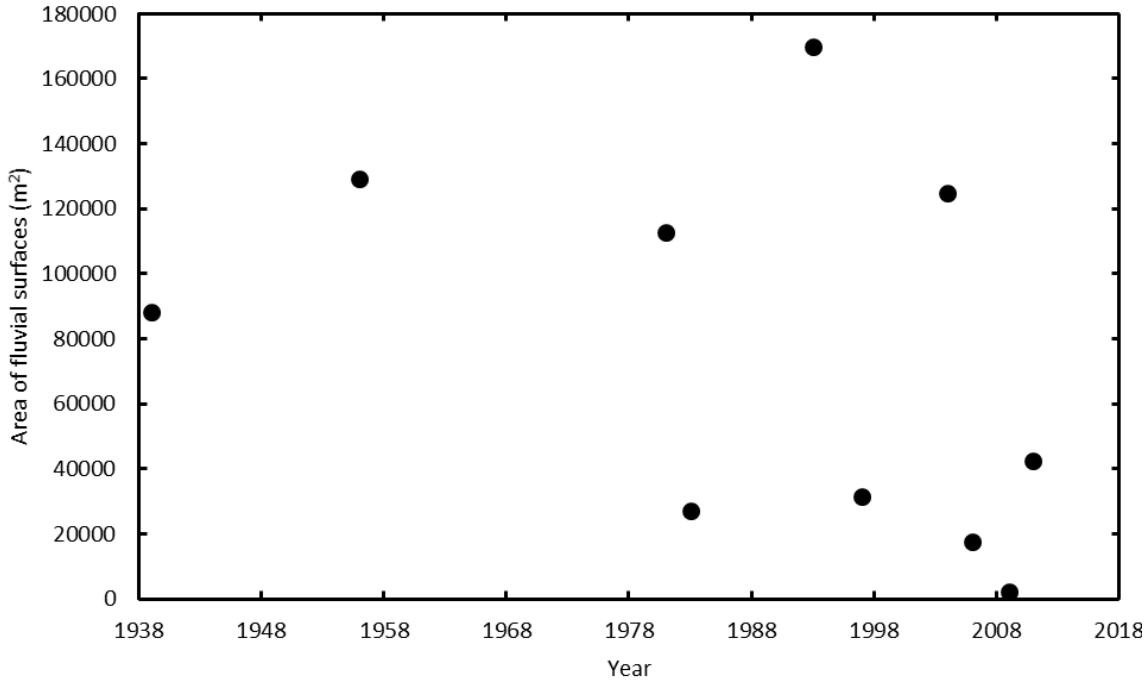

Fig. 4.53. Area of fill terraces on lower Diamond Fork plotted by year of formation.

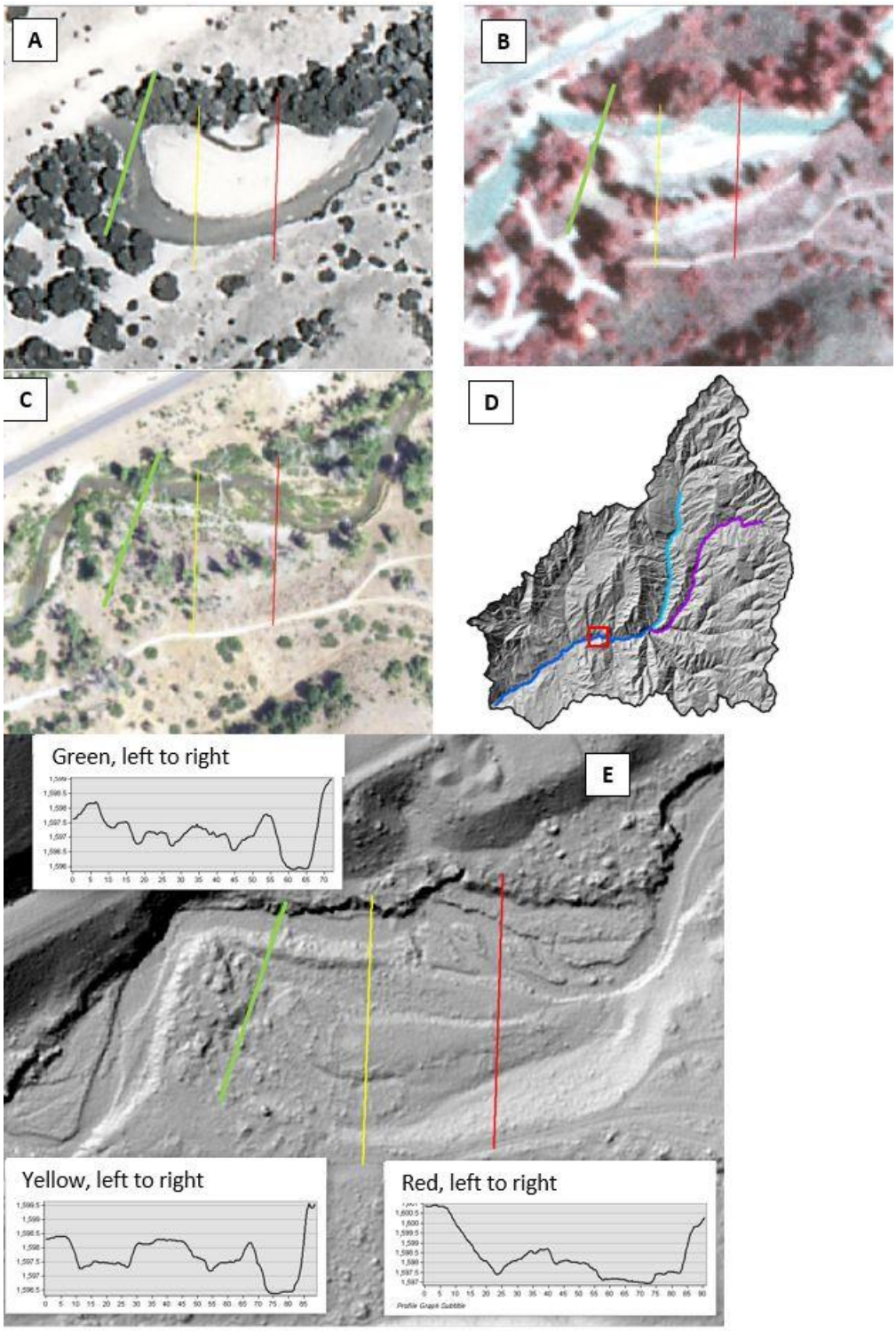

Fig. 4.54. Aerial photographs from A) 1956, B) 1981, and C) 2016 and location (D, red rectangle) of a reach in the Diamond Campground process domain. E) Profiles extracted from lidar showing a relict channel present in the 1956 imagery.

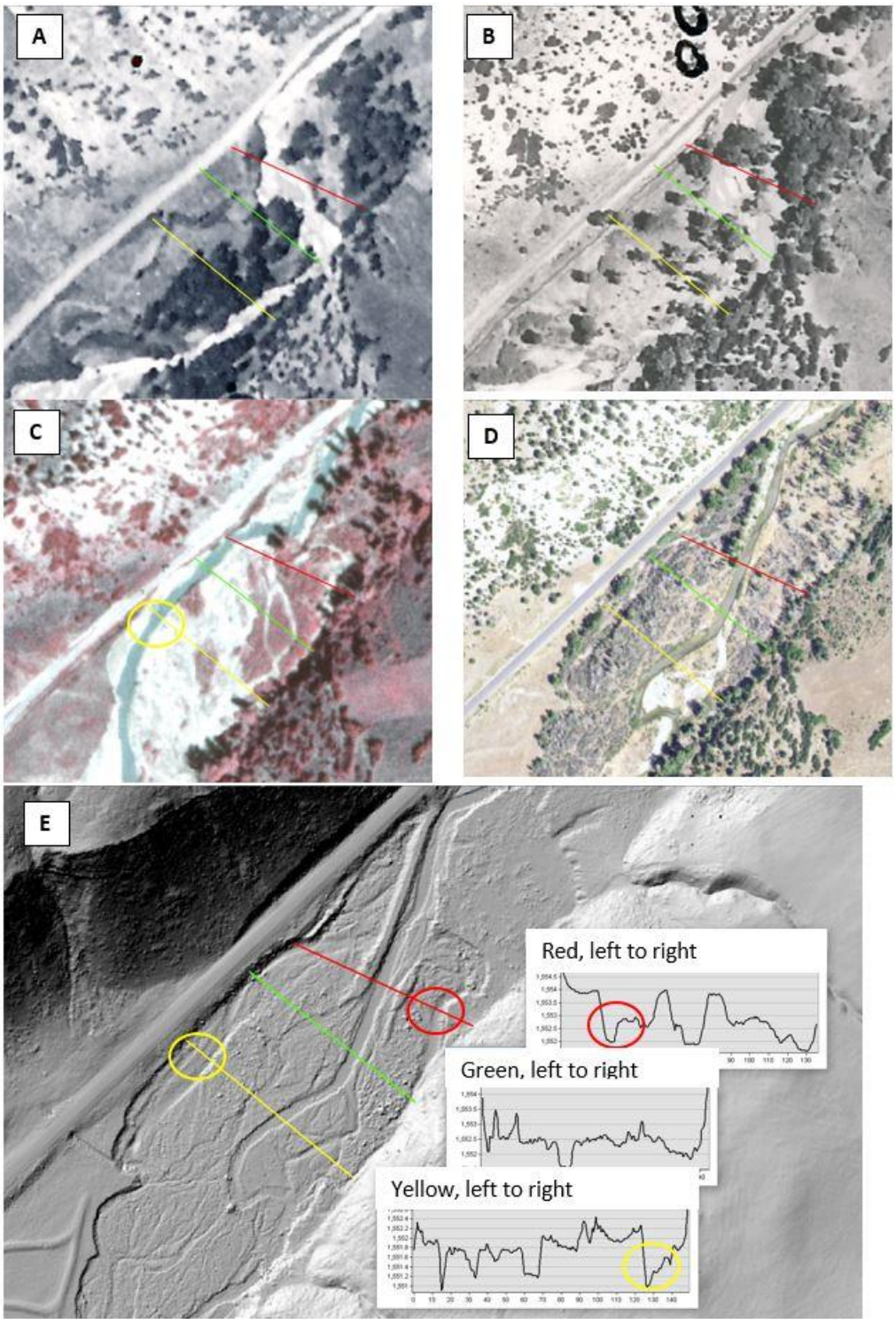

Fig. 4.55. Aerial photographs from A) 1939, B) 1956, C) 1981 and D) 2016 of a reach in the Alluvial Valley process domain. E) Profiles extracted from lidar showing relict channel present in the 1939 (red circle) and 1981 (yellow circle).

4.10. Sediment transport measurements

Bedload samples were collected over a range of discharges at all sites – from 0.1 m^3/s to 3.5 m^3/s on the Upper Diamond Fork, 0.5 to 3.6 m^3/s on Sixth Water, and 0.69 to 9.02 m^3/s on lower Diamond Fork (Fig. 4.56). A total of 95 bedload samples were collected. The number of samples per site ranged from 4 for the site Below the Landslide to 15 at the Childs site. Total mass ranged from fewer than five grams to nearly 10 kg. Transport rates calculated at each site show scatter (Fig. 4.56), but generally less than an order of magnitude, which is common for gravel bed rivers (Hassan and Church, 2001; Erwin et al., 2011). In some cases, this scatter can be attributed to whether a sample was collected on the rising or falling limb of the hydrograph, but this does not explain most of the variation.

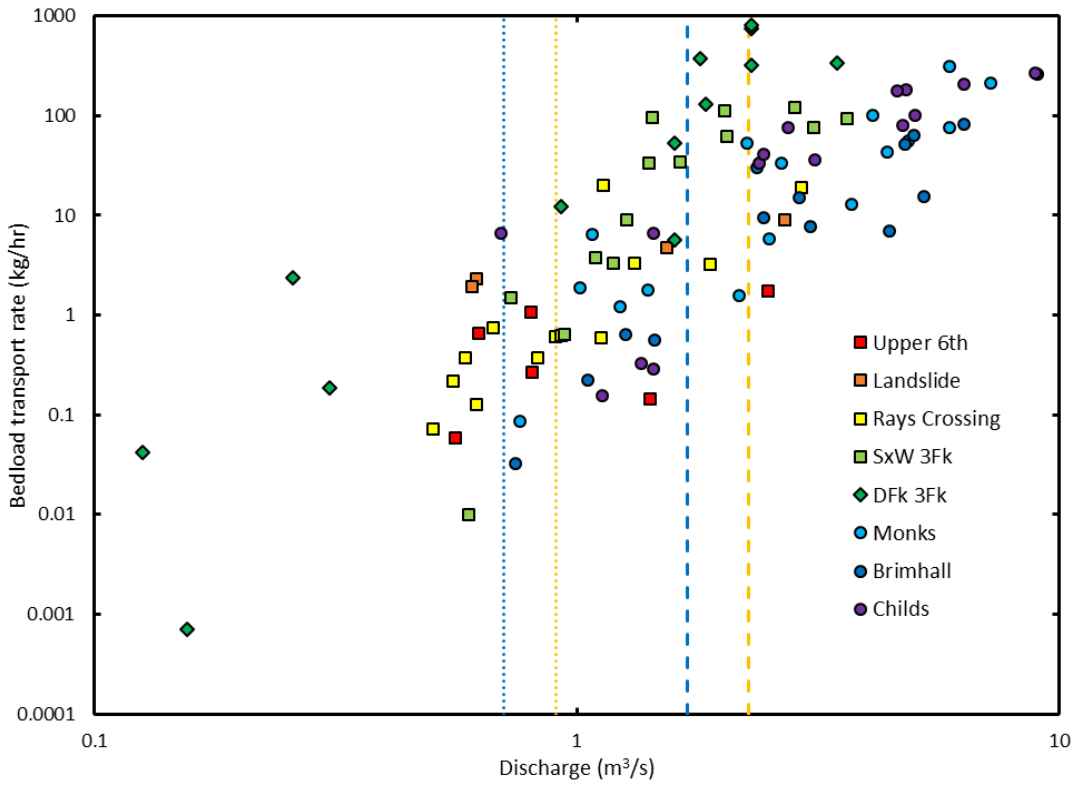

Fig. 4.56. Bedload transport rates for Sixth Water and Diamond Fork sediment transport samples. Vertical dashed lines represent summer (gold) and winter (blue) mandated flows for Sixth Water (lower Q values) and Diamond Fork (higher Q values).

The grain sizes in transport as bedload were generally finer than the bed material (Fig. 4.57). In only two samples was the median size in transport equivalent to the median size of bed material at the nearest monitoring site. Samples collected at discharges equivalent to approximately a two-year recurrence interval flood on Sixth Water and lower Diamond Fork did not include much coarse bed material. This indicates that the bed was largely immobile even at these flows.

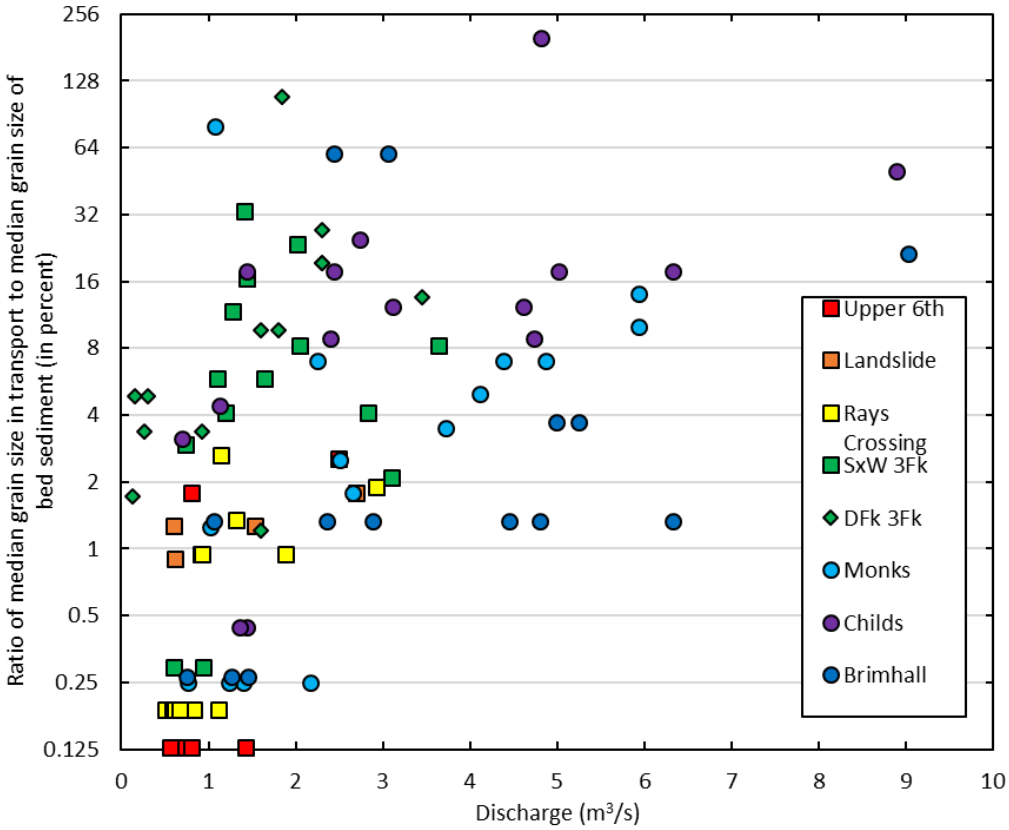

Fig 4.57. Ratio of median grain size in transport to median grain size of bed material at nearest monitoring site. Each data point represents the D_{50} of one bedload sample normalized by the average D_{50} of the nearest monitoring site, as shown in Fig. 4.12.

Suspended sediment was transported at all flows measured on Sixth Water and Diamond Fork. Suspended sediment concentration exceeded 10 mg/L for all but six measurements, with three occurring at the Upper Sixth Water site (Fig. 4.58). Suspended sediment concentration appears to increase as a power function of discharge at all sites except Upper Sixth Water and Below the Landslide, which have the fewest samples. The lower Diamond Fork sites and Sixth Water at 3 Forks have similar trends, with an exponent of the power function ~1.25. Diamond Fork at 3 Forks had relatively high suspended sediment concentrations for all discharges and the Below the Landslide site had the highest concentrations of any site during the high steps of the stepped flows.

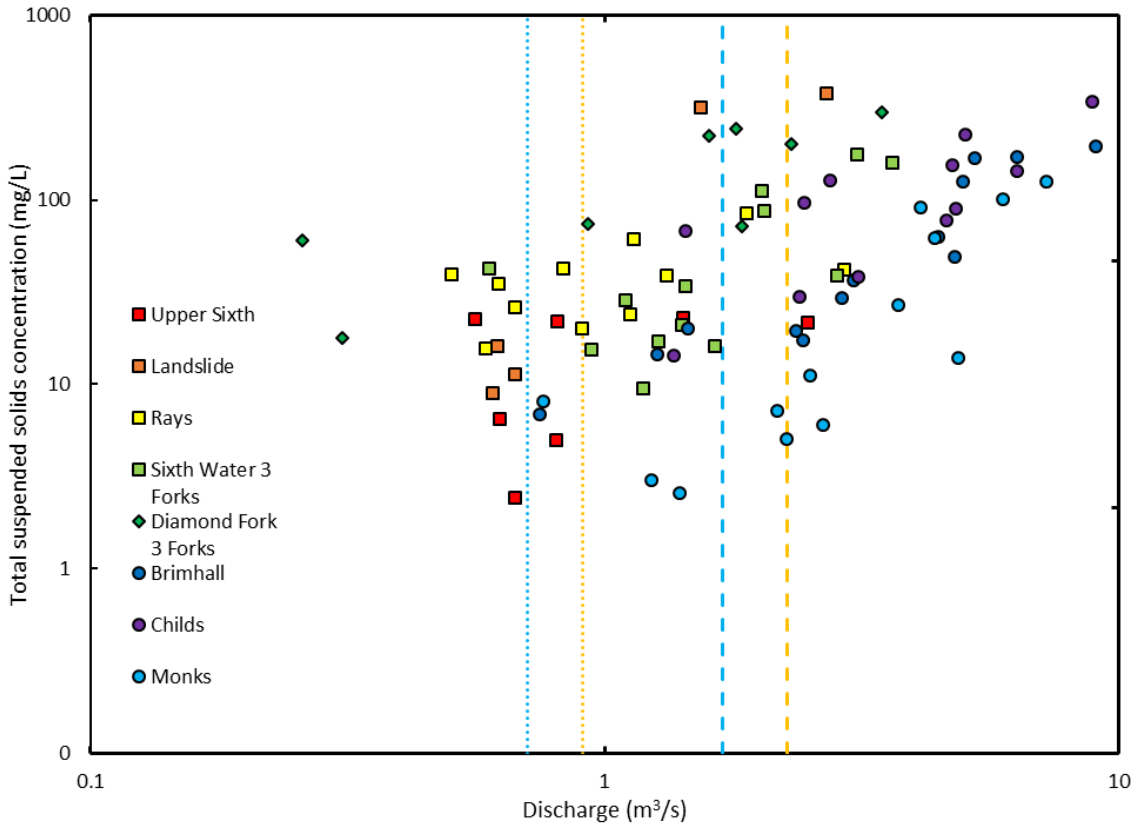

Fig. 4.58. Suspended sediment transport rates for Sixth Water and Diamond Fork sediment transport samples. Vertical dashed lines represent summer (gold) and winter (blue) mandated flows for Sixth Water (lower Q values) and Diamond Fork (higher Q values).

5. DISCUSSION

This study aims to describe the geomorphic history, current behavior, and potential future dynamics of the Sixth Water and Diamond Fork stream channels in the context of changes in water and sediment supply and spatial heterogeneity. Beginning in 1915, enormous changes to hydrology and sediment supply were introduced to Sixth Water and Diamond Fork as the rivers were used to convey trans-basin diversions during the summer far in excess of natural flows. Floods in the 1950s and 1980s also impacted the rivers by conveying large volumes of water and sediment. In 1997, a new outlet for diversion flows was introduced, bypassing large sediment sources and in 2004, the flow regime changed and flows decreased. Spatial variability in valley confinement and channel slope exert a primary control on channel response to the changes in hydrology and sediment supply that occurred at Sixth Water and Diamond Fork. The eight process domains that we identified for the system can be placed into three groups based on the degree of confinement and valley slope: confined (Upper Sixth Water Canyon and Lower Sixth Water Canyon), partially confined (Sixth Water Meadows, Syar, Below Confluence, and Monks Hollow), and unconfined (Diamond Campground and Diamond Fork alluvial valley). The magnitude of hydrologic and sediment supply changes on Sixth Water and Diamond Fork amplifies the differences between reaches with different degrees of confinement.

5.1. Sixth Water channel change

Distinct sections of Sixth Water had different responses to changes in sediment and water supply. The confined Upper Sixth Water Canyon and Lower Sixth Water Canyon process domains were relatively insensitive to changes in discharge so we focus on the more adjustable sections of Sixth Water, the Sixth Water Meadows and Syar process domains.

The Sixth Water Meadows and Syar process domains had a consistent response to changes in hydrology and sediment supply over the period of record. During the period prior to

diversion flows, these reaches were single threaded. Reaches with wide valleys were grazed heavily by cattle, preventing the establishment of a robust riparian corridor (Utah Reclamation and Mitigation Commission, 1999). When the diversion flows began in 1915, large volumes of sediment would have been delivered from upstream, and wide, low slope reaches likely would have accumulated sediment. This occurred by the time the 1952 air photos were captured, either due to diversion flows or due to the flood of 1952 (Fig. 4.7, Fig. 4.13). There was no active gage on Sixth Water during the flood of 1952, so it is difficult to compare the magnitude of the flood and the diversion flows. But given the hydrology of the system, a very large flood would be necessary to match the discharge of the diversion flows.

The bars that were deposited or reworked in 1952 were largely vegetated by the 1981 air photos and were not reworked by the floods of 1983 and 1984. This is in contrast to the lower Diamond Fork, where the floods of the 1980s reworked most of the alluvial corridor. There was no gage record on Sixth Water during the 1950s or the 1980s, so the magnitude of the floods is unknown, but the difference in the effect of the floods is striking. The 1952 flood deposited sediment to the edge of the valley in wide, low slope areas, while the floods of the 1980s had minimal impact, depositing a smaller number of bars (Fig. 4.22). It is likely that the magnitude of the 1983 and 1984 floods were lower than that of the 1952 flood on Sixth Water. It is also possible that the magnitude of floods in 1983/1984 were not as high as the diversion flows. If this were the case, it is unlikely that the floods would have reworked valley sediment, as the channel geometry and bed grain size would be adjusted to accommodate the larger diversion flows.

Alternatively, it may be that the upstream section of Sixth Water had reached a more stable state in terms of hillslope activity, as well as bed and bank stability by the 1980s. In 1952, the channel had been experiencing irrigation flows for 37 years and hillslopes were still very active (Fig. 4.19). By 1983, the channel had been receiving irrigation flows for 68 years and hillslopes were not as active (Fig 4.19), suggesting that sediment supply during the 1980s floods

may have been lower. The decrease in hillslope activity may have been caused by armoring of the channel causing incision to halt. The channel bed would likely have armored after 70 years of diversion flows or the stream could have eroded to resistant bedrock.

Sixth Water Meadows and Syar continued to narrow after the 1980s as vegetation established on the deposits that were formed. As flows dropped in 1997 (Sixth Water Meadows) and 2004 (Syar), the channel narrowed further; the wetted width of the channel decreased and vegetation established on the channel margins (Fig 4.7, Fig. 4.13).

5.2. Lower Diamond Fork channel change

The three upper process domains on lower Diamond Fork – Below the Confluence, Monks Hollow, and Diamond Campground – are partially confined and had similar responses to changes in water and sediment supply. Prior to diversion flows, these process domains were single threaded and meandering (Utah Reclamation and Mitigation Conservation Commission, 1999). When the diversion flows began in 1915, the channel would have been undersized for the flows, and presumably the higher sediment supply, it was receiving and would have adjusted accordingly. By 1939, some of the channel had developed wide bars and in places, multiple threads, but the majority of the valley remained single threaded. Following the flood of 1952, the previously multi-threaded reaches in the Below the Confluence and Monks Hollow process domains primarily reduced to a single thread as large bars formed at the channel margin (Fig. 4.28). Braided areas in the Diamond Campground process domain retained their braided planform following the 1952 flood (Table 4.10). The channel continued to rework sediment at the channel margin in the 1980s and widened in response to the 1983 and 1984 floods, but did not regain the multi-threaded planform (Table 4.8, Table 4.9, 4.10, Fig. 4.28). As the channel recovered from the floods of 1983 and 1984, vegetation established on flood deposits and the channel narrowed. Following the change in sediment and flow regime in 1997 and 2004, vegetation encroachment

continued and the channel became narrower.

The response of the partially confined lower Diamond Fork process domains is similar to that of Sixth Water Meadows and Syar. Each of these process domains is partially confined, with areas where sediment can accumulate and other areas that efficiently transport sediment. During the period of high flows, deposition occurred and bars developed in reaches with locally low slope, where the valley was wide and there was space for sediment to deposit. The flood of 1952, as well as floods in the 1980s deposited large bars at the channel margins, and those deposits were subsequently vegetated as the channel narrowed.

The downstream-most process domain on lower Diamond Fork – Diamond Fork Alluvial Valley – did not respond to changes in flow and sediment supply in the same manner as upstream process domains. In the 1939 air photos, much of lower Diamond Fork was wide and single threaded with riparian areas of large, mature trees despite 24 years of persistently high summer flows. In the imagery from 1956, taken four years after the flood of 1952, the proportion of the reach that was multi-threaded doubled, increasing from 11.9% in 1939 to 24.3% in 1956, and much of the pre-existing vegetation had been removed. The increase in multi-threaded reaches represents a fundamental change in the character of the river. The magnitude of the 1952 flood and the amount of sediment added to the channel, relative to its transport capacity, caused the lower Diamond Fork to cross a geomorphic threshold (Schumm, 1973).

The change in character of the Alluvial Valley process domain may have been caused by progressive accumulation of sediment, with the 1952 flood acting as a tipping point, or the 1952 flood may have provided the majority of the sediment, caused by high transport rates of available sediment from upstream. The streambed elevation analysis does not show any sign of accumulation prior to 1952 and there is a step change in bed elevation following the 1952 flood (Fig 4.32C). There is minimal sub-aerial sediment in the Alluvial Valley process domain in the 1939 air photos, which may suggest that upstream sediment had not reached the lowermost

Diamond Fork by 1939. However, the widening of the channel and erosion of valley margins that occurred between the 1939 and 1953 air photos, probably caused by the flood of 1952, would have produced a large volume of sediment that also would have promoted braiding (Kasprak, 2015). It's likely that a combination of sediment delivered from upstream, as well as sediment sourced from the lower Diamond Fork valley, caused the Alluvial Valley process domain to become braided following the 1952 flood.

In 1956, the Alluvial Valley process domain was still wide and multi-threaded and many of the active bars remained unvegetated. In the 1981 and 1982 air photos, the channel remained multi-threaded but many of the active surfaces from 1956 had been vegetated and the channel was narrower (Fig. 4.42, Fig. 4.45). The floods of 1983 and 1984 widened the channel to its greatest width in the air photos from 1985. By 1993, the channel had narrowed to a width similar to that of 1981 and 1982 and maintained its braided planform (Table 4.10, Fig. 4.45). For both large magnitude floods in the 20th Century, the Alluvial Valley process domain had the same response – widening during the flood, followed by a period of narrowing as flood deposits became vegetated, and then a multi-threaded, steady state condition for the given flow and sediment regime.

When the sediment and flow regime changed, the Alluvial Valley process domain experienced another change in character. During the period from 1997 to 2004, flows were still high downstream of the Syar Tunnel Outlet, but the largest sediment sources in the watershed, the shale bedrock and the large landslide (Fig. 2.1), were no longer accessed by high flows. This likely resulted in a situation where transport capacity exceeded supply throughout lower Sixth Water and lower Diamond Fork. This would cause the channel to evacuate sediment and decrease its slope (Lane, 1955; Clark and Wilcock, 2000). The decrease in slope is evident from the increased sinuosity of the Alluvial Valley process domain, and evacuation of sediment is inferred from the change from a multi-thread to a single thread planform in unconfined reaches (Fig.

4.42). Remnant channels from the braid plain are still present in floodplains formed during this period, suggesting that the braid plain was abandoned due to channel incision.

5.3. Mechanisms of channel narrowing

Many studies have attempted to constrain the mechanisms by which channels narrow, but it is often difficult to precisely describe how channels narrow. This is because channel narrowing may occur over long time periods, requires repeat observation to document, and because the rate of narrowing is often non-linear (Pizzuto, 1994; Dean et al., 2011). Different types of channel narrowing exist; narrowing occurs as a short term response to a perturbation or it may represent a long term change in the character of a river, and thus requiring long term observation. On Sixth Water and Diamond Fork, narrowing has occurred both as a short term response after major perturbations and as a long term response to the change in flow regime beginning in 1997.

Narrowing following a large flood represents a return to steady state conditions after a major perturbation. This type of narrowing occurs after a channel is overwidened by a flood that scours vegetation and deposits sediment on the floodplain. This overbank deposition temporarily widens the active channel, but that width cannot be maintained by more common flows (Wolman and Gerson, 1978; Pizzuto, 1994; Dean and Schmidt, 2013). Flood induced widening and subsequent narrowing occurs within natural climatic variability of a river, and does not necessarily represent altered or disequilibrium condition. It can be beneficial, as periodic scour and reworking of floodplain sediment promotes growth of riparian vegetation and species diversity (Scott et al., 1996; Osterkamp and Hupp, 2009).

Major floods in 1952 and 1983/1984 on Diamond Fork, and possibly only in 1952 on Sixth Water, overwidened the channels. The overwidened channels could not be maintained by subsequent flows. In response, the channels narrowed to an active channel width that could be maintained, as vegetation established on deposits formed during the floods and at the channel

margin. This explains the similarity of channel width and proportion of multi-threaded reaches in the 1981/1982 and 1993/1997. The river had an active channel width that could be maintained by common flows.

While channel narrowing in response to floods is common, narrowing can also represent a fundamental change in the character of a river. Several well documented cases of this type of channel narrowing come from fine-grained rivers in the American West. Flow reductions due to dam construction and upstream water use limited the ability of rivers to mobilize in-channel sediment and to scour sediment stored on floodplains (Pizzuto, 1994; Van Steeter and Pitlick, 1998; Allred and Schmidt, 1999; Cadol et al., 2011; Dean et al., 2011). The introduction of invasive riparian vegetation also increased the trapping efficiency of the floodplain and promoted vertical accretion. The combination of reduced transport capacity and increased trapping of fine sediment led to narrower channels with high banks and reduced in-channel complexity (Van Steeter and Pitlick, 1998; Allred and Schmidt, 1999; Grams and Schmidt, 2002; Cadol et al., 2011; Dean et al., 2011).

The narrowing of Sixth Water and Diamond Fork after 1997 represents a fundamental change in river character, but contrary to other studies in the American West, Sixth Water and Diamond Fork have had minimal storage of fine sediment, and vertical accretion of floodplains did not accompany channel narrowing. Field observations and floodplain samples show that there is only a thin (~10 cm) mantle of fine sediment on most formerly active surfaces. In the current flow regime, fine sediment delivery is low and opportunities for storage of fine sediment are minimal. Fine sediment is transported in Sixth Water and Diamond Fork at the mandated minimum flows, indicating that it is efficiently conveyed in the channel. Although fine sediment transport increases as flow increases, many high flows are contained within the channel and in most areas, a 5-year flood or greater is required to access the floodplain. Due to the limited supply of fine sediment and the rarity of floodplain inundation, minimal deposition and storage of

fine sediment has occurred on Sixth Water and Diamond Fork.

In addition to decreased transport capacity, a decrease in sediment supply relative to transport capacity can cause incision that promotes channel narrowing. Narrowing driven by sediment supply deficit has been documented on several coarse grained Italian Rivers (Rinaldi, 2003; Surian et al., 2009; Ziliani and Surian, 2012; Bollati et al., 2014). For these rivers, reforestation of uplands in the early 20th Century led to decreased sediment supply, but in many cases peak flows were unaltered. The changes in sediment supply promoted incision and vegetation encroachment without significant floodplain accretion. This led to large reductions in channel width and changes from a multi-threaded to a single threaded planform. The changes in sediment supply and channel morphology that occurred on Sixth Water and Diamond Fork between 1997 and 2004 are similar to the Italian case studies. At Sixth Water/Diamond Fork, beginning in 1997, irrigation flows were released from the Syar Tunnel Outlet, bypassing the weak lithology in the upper section of Sixth Water and the large landslide adjacent to Sixth Water (Fig. 2.1). This led to a decrease in sediment supply, while discharge was unchanged for the remainder of the system downstream, leading to an imbalance between sediment supply and transport capacity. The lower Diamond Fork narrowed during this period and multi-threaded reaches changed to a single thread morphology, mirroring the Italian cases.

Incision was well documented in Italy, with streambed elevation changes up to 8 m over a 40 year period, with typical incision of ~2 m. The sediment deficit caused by land use change was further compounded by in-channel gravel mining that promoted further incision (Rinaldi, 2003; Surian et al., 2009; Ziliani and Surian, 2012; Bollati et al., 2014). The Italian Rivers in these studies are much larger than Diamond Fork, so a 2-8 m change in bed elevation would correspond with a smaller, but still measureable, change on Diamond Fork. Comparable incision occurred on Sixth Water (Fig. 4.23, Fig. 4.24, Fig. 4.25), but the record of incision on Diamond Fork is not as clear (Fig. 4.54, Fig. 4.55).

Numerical modeling also suggests that a reduction of sediment supply relative to transport capacity can promote channel narrowing and channel simplification. Kasprak (2015) modeled braided river dynamics using a simplified morphodynamic model and imposed a sediment deficit so that the reach was exporting twice as much sediment as it was receiving. The imposed sediment deficit led to incision and a transition from a multi-threaded to a single-threaded planform, with one dominant anabranch capturing the majority of the flow. This scenario is similar to what occurred on lower Diamond Fork between 1997 and 2004, as sediment supply decreased following the opening of the Syar Tunnel Outlet. During this period, lower Diamond Fork changed from a multi-thread to a single thread planform and the braid plain was abandoned. Relict channels present in the 1997 imagery are still identifiable in the lidar dataset and have experienced minimal vertical accretion, suggesting abandonment by incision of a single dominant channel. However, the model of Kasprak (2015) only considers a decrease in sediment supply, and does not include the influence of vegetation, which also played a role in the narrowing of lower Diamond Fork.

The influence of vegetation is typically an important component of channel narrowing. Even though vegetation at Diamond Fork did not trap large amounts of fine sediment, it may have promoted and reinforced narrowing in other ways. Flume experiments examining the influence of vegetation on river planform have found that the introduction of vegetation can have a pronounced effect (Gran and Paola, 2001; Tal and Paola, 2007; Braudrick et al., 2009; Gurnell, 2014). Tal and Paola (2007) conducted experiments to assess the influence of vegetation on braided streams and found that vegetation could cause a change from a braided to a single-thread planform, even in the absence of cohesive sediment. The vegetation increased hydraulic roughness and provided bank stability that caused weak braid channels to be abandoned and forced flow into preferential pathways (Tal and Paola, 2007; Gurnell, 2014). The results of these flume experiments help to explain the changes on lower Diamond Fork between 1997 and 2004.

Vegetation had begun to establish at channel margins between the 1980s and the 1993 air photos, and was more widespread on channel margins and on vegetated islands in 1997 (Fig. 4.42). The presence of vegetation on channel margins and islands may have helped promote narrowing on lower Diamond Fork, as in the experiments of Tal and Paola. Between 1997 and 2004, large areas of the active channel of lower Diamond Fork became vegetated, and the channel changed from a multi-threaded to a single threaded planform. The concentration of flow into a single channel may have been influenced by the presence of vegetation.

5.4. Potential for future narrowing

One of the central questions for the future of Sixth Water and Diamond Fork is whether or not the channel will continue to narrow, and whether potential reductions in base flows will cause channel change. As lower Diamond Fork narrowed in response to the change sediment supply and flow regime in 1997 and 2004, the variability in channel width that was present in the 20th Century reduced (e.g. Fig. 4.45, Appendix D). The widest, multi-threaded sections of the river narrowed the most, and became single threaded and meandering. Over time, maximum channel width decreased considerably and the average width of different process domains has approached a uniform value, about 11 m on lower Diamond Fork and 8 m on Sixth Water.

Conventional wisdom about alluvial rivers posits that channel width is determined by the magnitude of common floods. Channels adjust their geometry to efficiently convey a flood with a 1.5 to 2 year return interval, and channel width is well correlated with the 1.5 to 2 year flood (Wolman and Miller, 1960; Pizzuto, 1994). For many rivers, variability in channel width is common under a natural flow regime, as longitudinal trends in valley confinement influence channel width (Brierley and Fryirs, 2005). When rivers narrow due to changes in hydrology and sediment supply, wide, unconfined areas of the channel often narrow more rapidly than narrow areas, such that channels approach a more uniform width, regardless of valley setting (Kondolf et

al., 2002; Rinaldi, 2003; Cadol et al., 2011; Dean and Schmidt, 2011). This occurred on Sixth Water and Diamond Fork, as the average width of every process domain on lower Diamond Fork approached 11 m and Sixth Water approached 8 m, and variability in channel width decreased. We propose that it is not the flood regime driving this trend, but that summer base flows for Sixth Water and Diamond Fork exert a control on channel width. The summer base flows, along with sediment deposition during floods, control the area that is available for vegetation to colonize. More generally, for rivers with highly regulated flows, summer base flows may be very important for maintaining channel width.

Since 2004, cross-sectional form and active channel width have been stable on Sixth Water and the Below the Confluence and Monks Hollow process domains, but have changed on lower Diamond Fork. The difference in channel narrowing can be attributed to substrate size and channel form, and the difference in response has implications for future flow scenarios on Sixth Water and Diamond Fork. The results of the painted rock and RFID experiment show that typical bed material on Sixth Water is immobile at 100 cfs. The largest flow released during the stepped flow experiment was 100 cfs, and the magnitude of the spring peak exceeded 100 cfs in four of 18 years in the gage record on Sixth Water. Because Sixth Water experienced extremely high flows from 1915–2004, the bed is currently armored and immobile under natural flows.

The channel is also inset in most places on Sixth Water and in the Below the Confluence and Monks Hollow process domains, where cobble/gravel terraces between 0.5 and 1.5 m above the channel are common features confining the channel. While these terraces are not especially tall, they are composed of coarse sediment, making it difficult for the channel to adjust, even if there is a large flood. Base flows also have little ability to effect the channel margin due to the inset geometry of the channel. Because there are 0.5 to 1.5 m tall banks in these locations, there is very little change in wetted width of the channel with change in discharge, so potentially lower base flows in the future are unlikely to cause narrowing. Additionally, fine sediment delivery is

low in the current flow regime (Fig. 4.58), so there is little potential for fines to deposit at the channel margin and encourage the growth of vegetation.

The Alluvial Valley process domain and sections of Diamond Campground that are wide are more susceptible to continued narrowing than Sixth Water and the Below the Confluence and Monks Hollow process domains because channel substrate is finer grained and the channel margin is more gradual. The finer substrate in the lower portions of Diamond Fork means that sediment transport and reworking of the bed are possible under common magnitude floods. Thus, lower Diamond Fork has the potential to build gravel bars that can be exposed under low flow conditions, such as those that developed in 2011 and 2017 (Fig. 4.40, Fig. 4.42). If summer base flows are decreased, vegetation may be able to colonize these surfaces, causing the channel to narrow. Despite the growth of vegetation since 2004, floodplains have not been built very high and the transition between channel and floodplain has remained gradual. This is especially true in areas that were formerly braided, where the former braid plain was abandoned and the relief between former active bars and the low flow channel is low. The more gradual channel margin can provide space for vegetation to colonize. If summer base flows are decreased, areas of the channel that were previously inundated will likely be sub-aerial, allowing vegetation to establish.

6. CONCLUSION

Sixth Water Creek and Diamond Fork River were subject to extreme hydrologic and sediment supply alteration beginning in 1915 and continuing to the present day, and the channels have been highly altered as a result. During the period where irrigation water was delivered from Strawberry Reservoir through Strawberry Tunnel (1915-1997), water and sediment supply were very high due to erosion at the toes of hillslopes and the landslide on Sixth Water. The effect of the hydrologic alteration was amplified by natural floods in the early 1950s and early 1980s that delivered large quantities of coarse sediment. In response, laterally unconfined areas of Sixth

Water and Diamond Fork widened, and their active channels had large active bars. Confined areas had minimal capacity for adjustment, and the active channel width was less affected during this period.

During the period when irrigation flows were delivered from Syar Tunnel (1997-2004), water supply remained high but sediment supply decreased. The high flows no longer had access to the more easily erodible bedrock and the large landslide, as they are upstream of Syar. During this period, widespread narrowing occurred in unconfined and partially confined areas, as the former braid plain was abandoned due incision, and formerly active bars became vegetated.

Since 2004, in the period of mandated minimum flows, only laterally unconfined areas have continued to narrow, and the narrowing has been periodic. The more confined areas are less sensitive to changes in water supply, and the sediment supply is currently low enough that the channel is not very active. Large floods have the capacity to create change in the lower Diamond Fork, where the channel is unconfined and the sediment size is relatively small. Bed material on Sixth Water is larger and is not mobile at common flood flows, meaning that Sixth Water is less likely to experience geomorphic change.

The record of incision is complicated, but several lines of evidence suggest that Sixth Water and lower Diamond Fork have progressively incised over the period of record. Incision even occurred in the low gradient sections of the lower Diamond Fork. This is in spite of large increases in sediment supply as the Upper Sixth Water valley was excavated and sediment was delivered downstream. Sediment is currently stored in terraces in partially confined and unconfined reaches of Sixth Water and Diamond Fork.

Sixth Water Creek and the Diamond Fork River present a case where hydrologic and sediment supply alterations were extreme, and the periods of hydrology and sediment supply are relatively well constrained. The results of this study inform our understanding of channel response to changes in drivers, and provide context for the management of Sixth Water and

Diamond Fork.

7. REFERENCES

Allred, T.M., Schmidt, J.C., 1999. Channel narrowing by vertical accretion along the Green River near Green River, Utah. GSA Bulletin 111, 1757-1772.

Andrle, R., 1996. Measuring channel planform of meandering rivers. Physical Geography 17, 270-281.

Belmont, P., 2011. Floodplain width adjustments in response to rapid base level fall and knickpoint migration. Geomorphology 128, 92-102.

Belmont, P., Foufoula-Georgiou, E., 2017. Solving water quality problems in agricultural watersheds: New approaches for these nonlinear, multiprocess, multiscale systems. Water Resources Research 53, doi: 10.1002/2017WR020839.

BioWest, 2007. Sixth Water and Diamond Fork Creeks Final 2007 Monitoring Report, 436 p.

Bollati, I.M., Pellegrini, L., Rinaldi, M., Duci, G., Pelfini, 2014. M. Reach-scale morphological adjustments and stages of channel evolution: The case of the Trebbia River (northern Italy). Geomorphology 221, 176-186.

Bradley, C., Smith, D.G., 1984. Meandering channel response to altered flow regime: Milk River, Alberta and Montana. Water Resources Research 20, 1913-1920.

Bradley, D.N., Tucker, G.E., 2012. Measuring gravel transport and dispersion in a mountain river using passive radio tracers, Earth Surface Process and Landforms 37, 1034-1045.

Braudrick, C.A., Dietrich, W.E., Leverich, G.T., Sklar, L.S., 2009. Experimental evidence for the conditions necessary to sustain meandering in coarse-bedded rivers. PNAS 106, 16926-16941.

Brierley, G.J., Fryirs, K.A, 2005. Geomorphology and River Management: Applications of the River Styles Framework. Blackwell Publications, 398 pp.

Buffington, J.M., 2012. Changes in channel morphology over human time scales. In Chuch, M.,

Biron, P.M., Roy, A.R. (Eds.), Gravel-bed Rivers: Processes, Tools, Environments, John Wiley & Sons, West Sussex, UK, pp. 437-462.

Bunte, K., Swingle, K.W., Abt, S.R., 2007. Guidelines for using bedload traps in coarse-bedded mountain streams: construction, installation, operation and sample processing. US Forest Service Rocky Mountain Research Station, General Techinical Report RMRS-GTR-191, 99 pp.

Cade, B.S., Noon, B.R., 2003. A gentle introduction to quantile regression for ecologists. Frontiers in Ecology and the Environment 1, 412-420.

Cadol, D., Rathburn, S.L., Cooper, D.J., 2011. Aerial photographic analysis of channel narrowing and vegetation expansion in Canyon de Chelly National Monument, Arizona, USA, 1935-2004. River Research and Applications 27, 841-856.

Call, B.C., Belmont, P., Schmidt, J.C., Wilcock, P.R., 2017. Changes in floodplain inundation under nonstationary hydrology for an adjustable, alluvial river channel. Water Resources Research 53, doi: 10.1002/2016WR020277.

Clark, J.J., Wilcock, P.R., 2000. Effects of land-use change on channel morphology in northeastern Puerto Rico. GSA Bulletin 112, 1763-1777.

Cluer, B., Thorne, C., 2014. A stream evolution model integrating habitat and ecosystem benefits. River Research Applications 30, 135-154.

Dean, D.J., Schmidt, J.C., 2011. The role of feedback mechanisms in historic channel changes of the lower Rio Grande in the Big Bend region. Geomorphology 126, 333-349.

Dean, D.J., Schmidt, J.C., 2013. The geomorphic effectiveness of a large flood on the Rio Grande in the Big Bend region: Insights on geomorphic controls and post-flood geomorphic response. Geomorphology 201, 183-198.

Dean, D.J., Topping, D.J., Schmidt, J.C., Griffiths, R.E., Sabol, T.A., 2016. Sediment supply versus local hydraulic controls on sediment transport and storage in a river with a large sediment loads. Journal of Geophysical Research: Earth Surface 121, doi: 10.1002/2015JF003436.

Dietrich, W.E., Kirchner, J.W., Ikeda, H, Iseya, F., 1989. Sediment supply and the development of the coarse surface layer in gravel-bedded rivers. Geology 340, 215-217.

Dilts, T.E., 2015. Stream Gradient and Sinuosity Toolbox for ArcGIS 10.1. University of Nevada Reno. Accessed from: http://www.arcgis.com/home/item.html?id=c8eb4ce1384e45258ccba1b33cd4e3cb

Edwards, T.K., Glyson, G.D., 1988. Field methods for measurement of fluvial sediment. USGS Techniques of Water-Resources Investigations, 97 pp.

Erwin, S.O., Schmidt, J.C., Nelson, 2011. Downstream effects of impounding a natural lake: the Snake River downstream from Jackson Lake Dam, Wyoming, USA. Earth Surface Processes and Landforms. 36, 1421-1434.

Friedman, J.M., Osterkamp, W.R., Lewis, Jr., W.M., 1996. The role of vegetation and bed-level fluctuations in the process of channel narrowing. Geomorphology 14, 341-351.

Gaeuman, D., Schmidt, J.C., Wilcock, P.R., 2005. Complex channel responses to changes in stream flow and sediment supply on the lower Duchesne River, Utah. Geomorphology 64, 185-206.

Gartner, J.D., Dade, W.B., Renshaw, C.E., Magilligan, F.J., Buraas, E.M., 2015. Gradients in stream power influence lateral and downstream sediment flux in floods. Geology 43, 983-986.

Gendaszek, A.S., Magiri, C.S., Czuba, C.R., 2012. Geomorphic response to flow regulation and channel and floodplain alteration in the gravel-bedded Cedar River, Washington, USA. Geomorphology 179, 258-268.

Graf, W.L., 1983. Downstream changes in stream power in the Henry Mountains, Utah. Annals of the Association of American Geographers 73, 373-387.

Graf, W.L., 1999. Dam nation: A geographic census of American dams and their large-scale hydrologic impacts. Water Resources Research 35, 1305-1311.

Grams, P.E., Schmidt, J.C., 2002. Streamflow regulation and multi-level floodplain formation: channel narrowing on the aggrading Green River in the eastern Uinta Mountains, Colorado and Utah. Geomorphology 44, 337-360.

Gran, K., Paola, C., 2001. Riparian vegetation controls on braided stream dynamics. Water Resources Research 37, 3275-3283.

Grant, G. E., Schmidt, J.C., Lewis, S.L., 2003. A geological framework for interpreting downstream effects of dams on rivers. In O'Connor, J.E., Grant, G.E. (Eds.), A Peculiar River, American Geophysical Union, Washington D.C., 219 pp.

Gregory, K.J., 2006. The human role in changing river channels. Geomorphology 79, 172-191.

Gurnell, A., 2014. Plants as river system engineers. Earth Surface Processes and Landforms 39, 4-25.

Hassan, M.A., Church, M., 2001. Sensitivity of bed load transport in Harris Creek: Seasonal and spatial variation over a cobble-gravel bar. Water Resources Research 37, 813-825.

Henderson, F.M., 1966. Open Channel Flow. Macmillan Press, London, UK, 522 pp.

Hooke, R.L., 2000. On the history of humans as geomorphic agents. Geology 28, 843-846.

Jacobson, R.B, 1995. Spatial controls on patterns of land-use induced stream disturbance at the drainage-basin scale – an example from gravel-bed streams of the Ozark Plateaus, Missouri. In Costa, J.E., Miller, A.J., Potter, K.W., Wilcock, P.R. (Eds.), AGU Geophysical Monograph 89, The Wolman Volume, pp. 219-239.

James, L.A., 1991. Incision and morphologic evolution of an alluvial channel recovering from hydraulic mining sediment. GSA Bulletin 103, 723-736.

Jones, J. 2018. Sixth Water/Diamond Fork data repository, HydroShare, http://dx.doi.org/10.4211/hs.54062b4895964b778302bcf425594093

Kasprak, A., 2015. Linking form and process in braided rivers using physical and numerical models. PhD Dissertation, Utah State University, Logan, UT, 173 pp.

Kellerhals, R., Church, M., Davies, L.B., 1979. Morphological effects of interbasin river diversions. Canadian Journal of Civil Engineering 6, 18-31.

Kelly, S.A., Takbiri, Z., Belmont, P., Foufoula-Georgiou, E., 2017. Human amplified changes in precipitation-runoff patterns in large river basins of the Midwestern United States. Hydrology and Earth System Sciences 21, 5065-5088.

Kondolf, G.M., Piégay, H., Landon, N., 2002. Channel response to increased and decreased bedload supply from land use change: contrasts between two catchments. Geomorphology 45, 35-51.

Lane, E. W., 1955. The importance of fluvial morphology in hydraulic engineering. Proceedings, American Society of Civil Engineers 81, paper 745, 17 pp.

Langbein, W.B., Leopold, L.B., 1964. Quasi-equilibrium states in channel morphology. American Journal of Science 262, 782-794.

Lauer, J.W., 2006. Channel Planform Statistics Tool. National Center for Earth Surface Dynamics, Minneapolis, MN.

Lauer, J.W., Echterling, C., Lenhart, C., Belmont, P., Rausch, R., 2017. Air-photo based change in channel width in the Minnesota River basin: Modes of adjustment and implications for sediment budget. Geomorphology 297, 170-184.

Lea, D.M., Legleiter, C.J., 2016. Refining measurements of lateral channel movement from image time series by quantifying spatial variations in registration error. Geomorphology 258, 11-20.

Lenhart, C.F., Titov, M.L., Ulrich, J.S., Nieber, J.L., Suppes, B.J., 2013. The role of hydrologic alteration and riparian vegetation dynamics in channel evolution along the lower Minnesota River. Transactions of the American Society of Agricultural and Biological Engineers 56, 549-561.

Leopold, L.B., Maddock, T., 1953. The hydraulic geometry of stream channels and some physiographic implications. USGS Professional Paper 252.

Leopold, L.B., Wolman, M.G., 1957. River channel patterns: braided, meandering, straight. U.S. Geological Survey Professional Paper 282-B, 85 pp.

Li, C., Czapiga, M.J., Eke, E.C., Viparelli, E., Parker, G., 2015. Variable Shields number model for river bankfull geometry: bankfull shear velocity is viscosity-dependent but grain size-independent. Journal of Hydraulic Research 53, 36-48.

Liébault, F., Piégay, H., 2002. Causes of 20th Century channel narrowing in mountain and piedmont rivers of southeastern France. Earth Surface Processes and Landforms 27, 425-444.

Liébault, F., Bellot, H., Capuis, M., Klotz, S., Deschâtres, M., 2012. Bedload tracing in a high-sediment-load mountain stream. Earth Surface Processes and Landforms 37, 385-399.

Lisle, T.E., Iseya, F., Ikeda, H., 1993. Response of a channel with alternate bars to a decrease in supply of mixed-sediment load: a flume experiment. Water Resources Research 29, 3623-3629.

Mount, N., Louis, J., 2005. Estimation and propagation of error in measurements of river channel movement from aerial imagery. Earth Surface Processes and Landforms 30, 635-643.

Olinde, L., Johnson, J.P.L., 2015. Using RFID and accelerometer-embedded tracers to measure probabilities of bed load transport, step lengths, and rest times in a mountain stream. Water Resources Research 51, doi: 10.1002/2014WR016120.

Osterkamp, W.R., Hupp, C.R., 2009. Fluvial processes and vegetation – Glimpses of the past, the present, and perhaps the future. Geomorphology, v. 116, p. 274-285.

Phillips, J.D., 2001. Human impacts on the environment: Unpredictability and the primacy of place. Physical Geography 22, 321-332.

Pizzuto, J.E., 1994. Channel adjustments to changing discharges, Powder River, Montana. GSA Bulletin 106, 1494-1501.

Rhoads, B. L., Lewis, Q.W., Andersen, W., 2016. Historical changes in channel network extent and channel planform in an intensively managed landscape: Natural versus human-induced effects. Geomorphology 252, 17-31.

Rinaldi, M., 2003. Recent channel adjustments in alluvial rivers of Tuscany, Italy. Earth Surface Processes and Landforms 28, 587-608.

Schmidt, J.C., Wilcock, P.R., 2008. Metrics for assessing the downstream effects of dams, Water Resources Research 44, doi:10.1029/2006WR005092.

Schumm, S.A., 1973. Geomorphic thresholds and complex response of drainage systems. In M. Morisawa (Ed.), Fluvial Geomorphology, Binghamton, New York, pp. 299-309.

Schumm, S.A., 1977. The Fluvial System, Wiley & Sons, West Sussex, UK, 338 pp.

Schumm, S.A., 1985. Patterns of alluvial rivers. Annual Reviews in Earth and Planetary Science 13, 5-27.

Schumm, S.A., Khan, H.R., 1972, Experimental study of channel patterns, GSA Bulletin, v. 83, p. 1755-1770.

Schumm, S.A., Harvey, M.D., Watson, C.C., 1984. Incised Channels: Morphology, dynamics, and control. Water Resources Publication, Littleton, Colorado, 200 pp.

Scott, M.L., Friedman, J.M., Auble, G.T., 1996. Fluvial process and the establishment of bottomland trees. Geomorphology 14, 327-339.

Smelser, M.G., Schmidt, J.C., 1998. An assessment methodology for determining historical changes in mountain streams. U.S. Forest Service General Technical Report RMRS-G TR-6, 29 pp.

Snyder, N.P., Kammer, L.L., 2008. Dynamic adjustment in channel width in response to a forced diversion: Gower Gulch, Death Valley National Park, California. Geology 36, 187-190.

Surian, N., Rinaldi, M., Pellegrini, L., Audisio, C., Maraga, F., Teruggi, L., Turitto, O., Zilliani, L., 2009. Channel adjustments in northern and central Italy over the last 200 years. In James, L.A., Rathburn, S.L., Whitecar, G.R. (Eds.), Management and Restoration of Fluvial Systems with Broad Historical Changes and Human Impacts: GSA Special Paper 451, pp. 83-95.

Swanson, B.J., Meyer, G.A., Coonrod, J.E., 2011. Historical channel narrowing along the Rio Grande near Albuquerque, New Mexico in response to peak discharge reductions and engineering: magnitude and uncertainty of change from air photo measurements. Earth Surface Processes and Landforms 36, 885-900.

Tal, M., Paola, C., 2007. Dynamic single-thread channels maintained by the interaction of flow and vegetation. Geology 35, 347-350.

Toone, J., Rice, S.P., Piégay, H., 2014. Spatial discontinuity and temporal evolution of channel morphology along a mixed bedrock-alluvial river, upper Drôme River, southeast France: Contingent responses to external and internal controls. Geomorphology 205, 5-16.

Trihey and Associates, 1997. Conceptual Restoration Plan and Baseline Assessment Lower Diamond Fork, Final Report, 367 pp.

United States Bureau of Reclamation, 1916. Annual Report, 805 pp.

United States Congress, 1992. Public Law 102-575 – Reclamation Projects Authorization and Adjustment Act of 1992, 61 pp.

Utah Reclamation and Mitigation Conservation Commission, 2000. Diamond Fork area assessment, 175 pp.

Van Steeter, M.M., Pitlick, J., 1998. Geomorphology and endangered fish habitats of the upper Colorado River 1. Historic changes in streamflow, sediment load, and channel morphology. Water Resources Research 34, 287-302.

Wheaton, J.M., Brasington, J., Darby, S.E., Sear, D.A., 2010. Accounting for uncertainty in DEMs from repeat topographic surveys: Improved sediment budgets. Earth Surface Processes and Landforms 35, 136-156.

Wilkinson, B.H., McElroy, B.J., 2007. The impact of humans on continental erosion and sedimentation. GSA Bulletin 119, 140-156.

Wolman, M.G., 1954. A method of sampling coarse river-bed material. Transactions of the American Geophysical Union 35, 951-956.

Wolman, M.G., 1967. Effects of construction on fluvial sediment, urban and suburban area of Maryland, Water Resources Research 2, 451-464.

Wolman, M. G., Miller, J. P., 1960, Magnitude and frequency of forces in geomorphic processes, Journal of Geology 68, 54-74.

Wolman, M.G., Gerson, R., 1978. Relative scales of time and effectiveness of climate in watershed geomorphology. Earth Surface Processes and Landforms 3, 189-208.

Yarnell, S.M., Mount, J.F., Larsen, E.W., 2006. The influence of relative sediment supply on riverine habitat heterogeneity. Geomorphology 80, 310-324.

Ziliani, L., Surian, N., 2012. Evolutionary trajectory of channel morphology and controlling factors in a large gravel-bed river. Geomorphology 173-174, 104-117.

APPENDICES

APPENDIX A. TRANSPORT OF PAINTED GRAVEL TRACERS

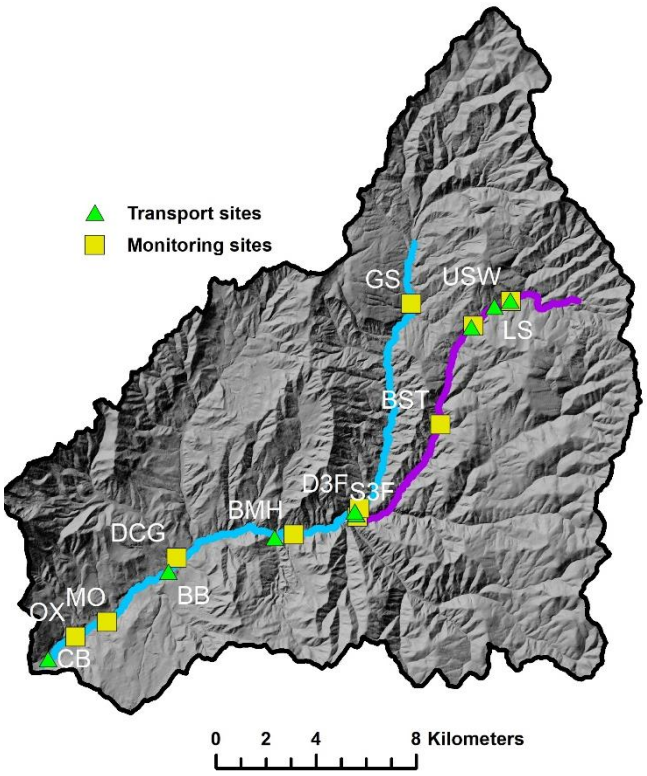

Fig. A.1. Location of monitoring sites in Diamond Fork watershed. Monitoring sites: USW – Upper Sixth Water, LS, Landslide, ARC – Above Rays Crossing, BST – Below Syar Tunnel, S3F – Sixth Water at 3 Forks, GS – Guard Station, D3F – Diamond Fork at 3 Forks, BMH – Below Monks Hollow, DCG – Diamond Campground, and MO – Motherlode.

Table A.1. Summary of painted rock tracer movement during stepped flow experiment on Sixth Water and Diamond Fork.

Site	Discharge (cfs)	Grain size (mm)	Number placed	Number transported	Number recovered[+]	Transport distance (m)*		
						Mean	Median	Maximum
Upper Sixth	50	45	20	0	-	-	-	-
		64	20	0	-	-	-	-
		90	20	0	-	-	-	-
	100	45	20	3	3	0.8	0.3	1.7
		64	20	1	1	0.2	0.2	0.2
		90	20	1	1	0.2	0.2	0.2
Landslide	50	22.6	30	5	5	4.4	4.7	7.8
		32	30	3	3	0.9	1	1.2
		45	30	1	1	5.3	5.3	5.3

Table A.1. (cont.)

	100	22.6	27	24	9	5.2	0.9	30
		32	30	14	7	3.9	1.5	20
		45	30	13	5	7.9	1.5	30
Rays	50	45	30	0	-	-	-	-
Crossing		64	30	0	-	-	-	-
		90	30	0	-	-	-	-
	100	45	29	1	1	0.3	0.3	0.3
		64	30	0	-	-	-	-
		90	30	1	1	0.5	0.5	0.5
Syar Tunnel	50	45	30	2	0	-	-	-
		64	30	0	-	-	-	-
		90	30	0	-	-	-	-
	100	45	28	8	3	0.5	0.4	0.7
		64	30	5	3	0.8	0.8	1.1
		90	30	3	3	0.8	0.4	1.6
Sixth Water	50	32	40	8	5	1.0	0.5	1.8
3 Forks		45	40	6	5	0.4	0.3	0.7
		64	40	5	5	0.5	0.5	0.9
	100	32	37	17	14	3.8	3	15
		45	39	17	16	1.4	1.0	4.0
		64	40	13	10	2.6	2.3	6
Monks	100	22.6	40	13	13	1.4	1.3	3.6
Hollow		32	40	5	5	1.7	1.4	3.6
		45	40	1	1	0.5	0.5	0.5
		64	40	0	-	-	-	-
	150	22.6	37	28	11	2.6	1.3	10
		32	40	27	15	6.1	4.0	30
		45	40	20	15	2.2	1.5	8
		64	40	11	11	1.5	1	6
Diamond	100	32	40	4	4	0.4	0.4	0.8
Campground		45	40	2	2	0.3	0.3	0.3
		64	40	2	2	0.6	0.6	0.8
	150	32	40	29	27	4.1	2	20
		45	40	24	24	6.0	2	80
		64	40	18	15	2.4	1.5	7
Motherlode	100	22.6	40	5	5	0.9	0.6	1.6
		32	40	9	7	0.9	0.6	1.9
		45	40	8	6	0.8	0.6	2.3
	150	22.6	40	21	4	1.4	1.1	3
		32	36	19	7	20	0.8	100
		45	39	20	5	2.0	1	6

Notes: [+]Number that were transported and relocated. *Transport distances are based on rocks that were transported and recovered. The calculations do not include rocks that were not transported and are underestimated if rocks were transported beyond the search region.

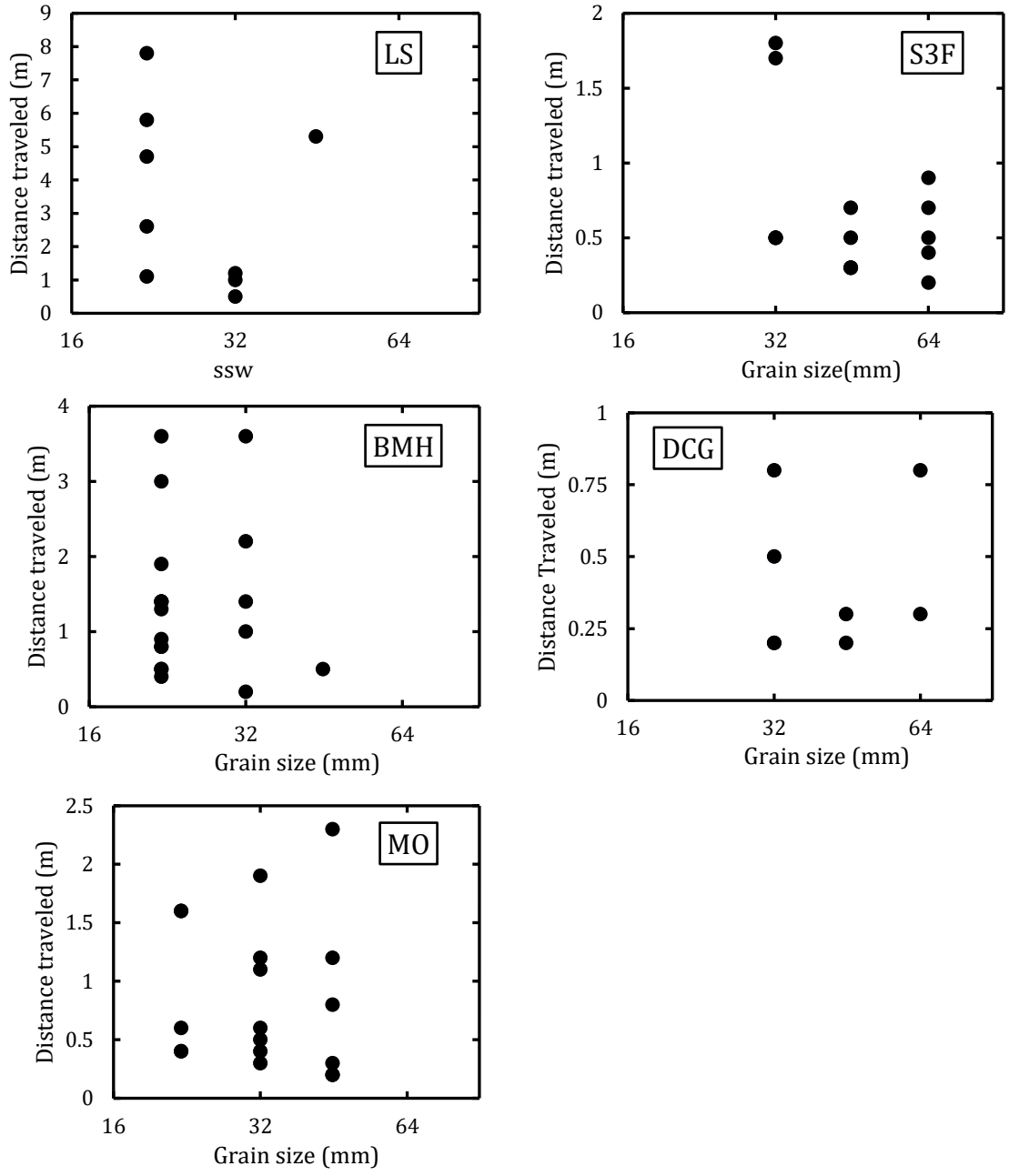

Fig. A.2. Transport distance of painted gravel tracers following the first high flow of the stepped flow experiment. The discharge was ~50 cfs on Sixth Water and ~100 cfs on lower Diamond Fork.

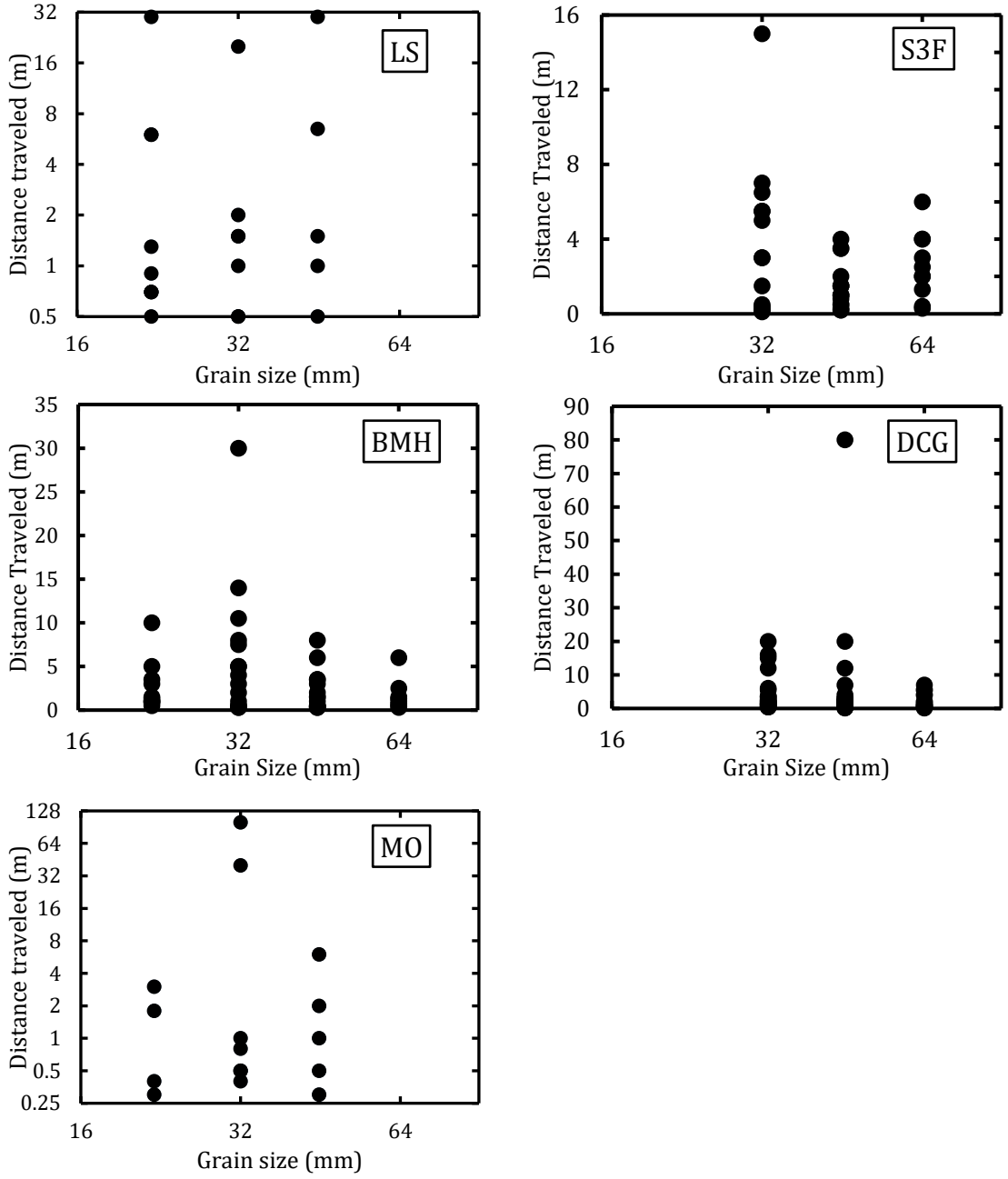

Fig. A.3. Transport distance of painted gravel tracers following the second high flow of the stepped flow experiment. The discharge was ~100 cfs on Sixth Water and ~150 cfs on lower Diamond Fork.

APPENDIX B. TOPOGRAPHIC CROSS-SECTION SURVEYS

Table B.1. Dates of cross-section surveys conducted at Sixth Water and Diamond Fork.

Date	Sites and cross-sections	Discharge at Sixth Water (cfs)	Discharge at Diamond Fork (cfs)
Apr 13, 2005	Oxbow 5, 6, 7, 8	-	76
Apr 14, 2005	Motherlode 3, 4, 5, Oxbow 1,2, 3, 4	-	82
Apr 15, 2005	Diamond Campground 1, 2, 5, 6, 7, Motherlode 1, 2, 6	32.4	84
Apr 18, 2005	Diamond Campground 3, 4	-	112
Apr 20, 2005	Upper Sixth Water 1, 2, 3	46	-
Apr 21, 2005	Upper Sixth Water 4, 5, 6	43	-
Aug 8, 2006	Upper Sixth Water 2, 3, 4, 5, 6	37	-
Aug 9, 2006	Upper Sixth Water 1	37	-
Sep 13, 2006	Rays Crossing 1, 2, 3, 4, 5, 6	38	-
Nov 8, 2006	Diamond Campground 1, 2, 3, 4, 5, 6, 7	-	68
Nov 9, 2006	Motherlode 1, 2, 3, 4, 5, 6, Oxbow 8	-	68
Nov 10, 2006	Oxbow 1, 2, 3, 4, 5, 6, 7	-	65
Oct 10, 2007	Upper Sixth Water 1, 2, 3, 4, 5, 6	33	-
Oct 24, 2007	Diamond Campground 1, 2, 3, 4, 5, 6, 7	-	71
Oct 25, 2007	Oxbow 1, 2, 3, 4, 5, 6, 7, 8	-	70
Oct 26, 2007	Motherlode 1, 2, 3, 4, 5, 6	-	70
June 20, 2017	Oxbow 1, 2, 3, 7, 8	-	83
June 22, 2017	Diamond Campground 1, 2, 3, 4, 5, 6, 7, Oxbow 4, 5, 6	-	82
June 23, 2017	Rays Crossing 1, 2, 3, 4	37	-
July 17, 2017	Upper Sixth Water 1, 2, 3, 4, 5, 6	32	-
July 19, 2017	Motherlode 4, 5, 6, Rays Crossing 5, 6	32	82
Aug 11, 2017	Motherlode 1, 2, 3	-	83

B.1. Upper Sixth Water

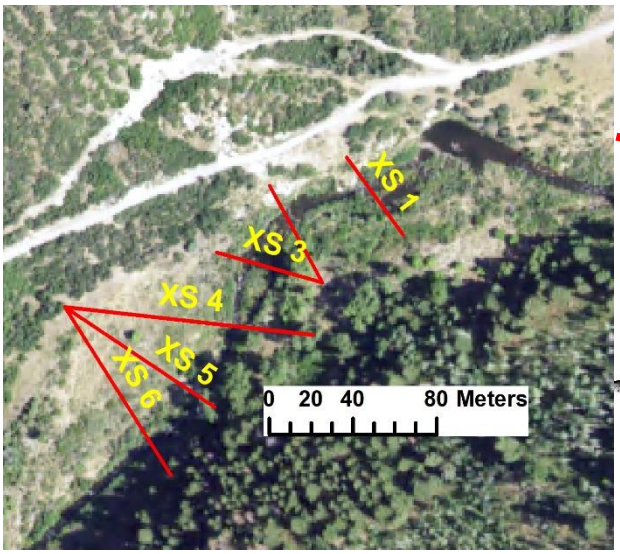

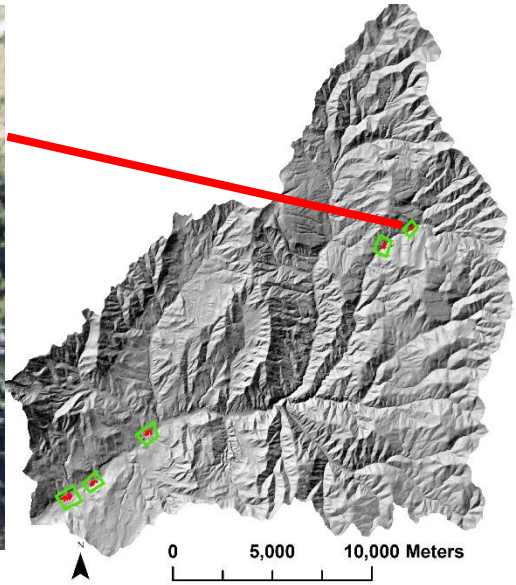

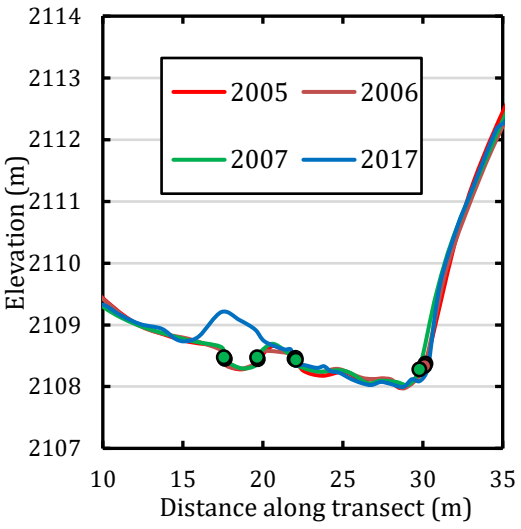

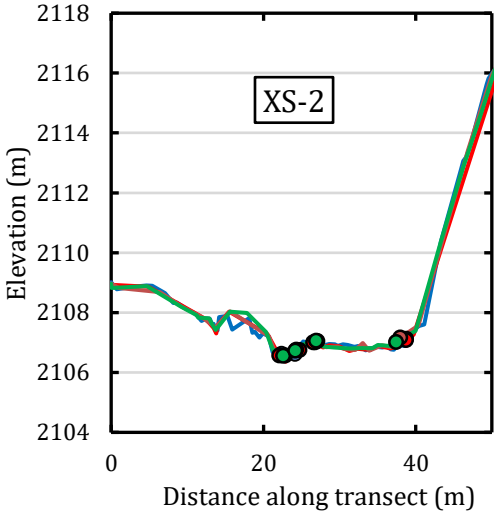

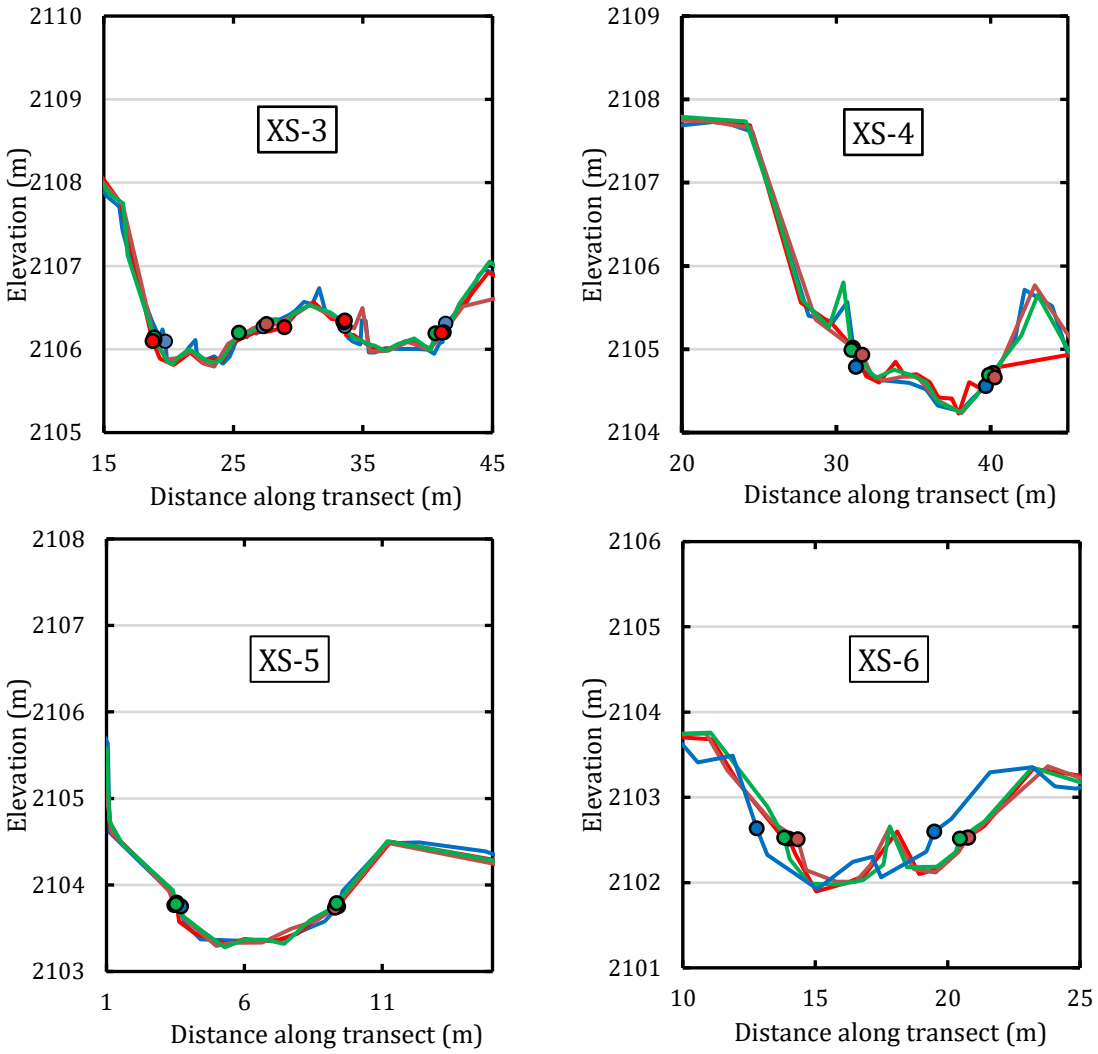
XS-3
Elevation (m)
2110
2109
2108
2107
2106
2105
15
25
35
45
Distance along transect (m)
XS-4
Elevation (m)
2109
2108
2107
2106
2105
2104
20
30
40
Distance along transect (m)
XS-5
Elevation (m)
2108
2107
2106
2105
2104
2103
1
6
11
Distance along transect (m)
XS-6
Elevation (m)
2106
2105
2104
2103
2102
2101
10
15
20
25
Distance along transect (m)

B.2. Diamond Campground

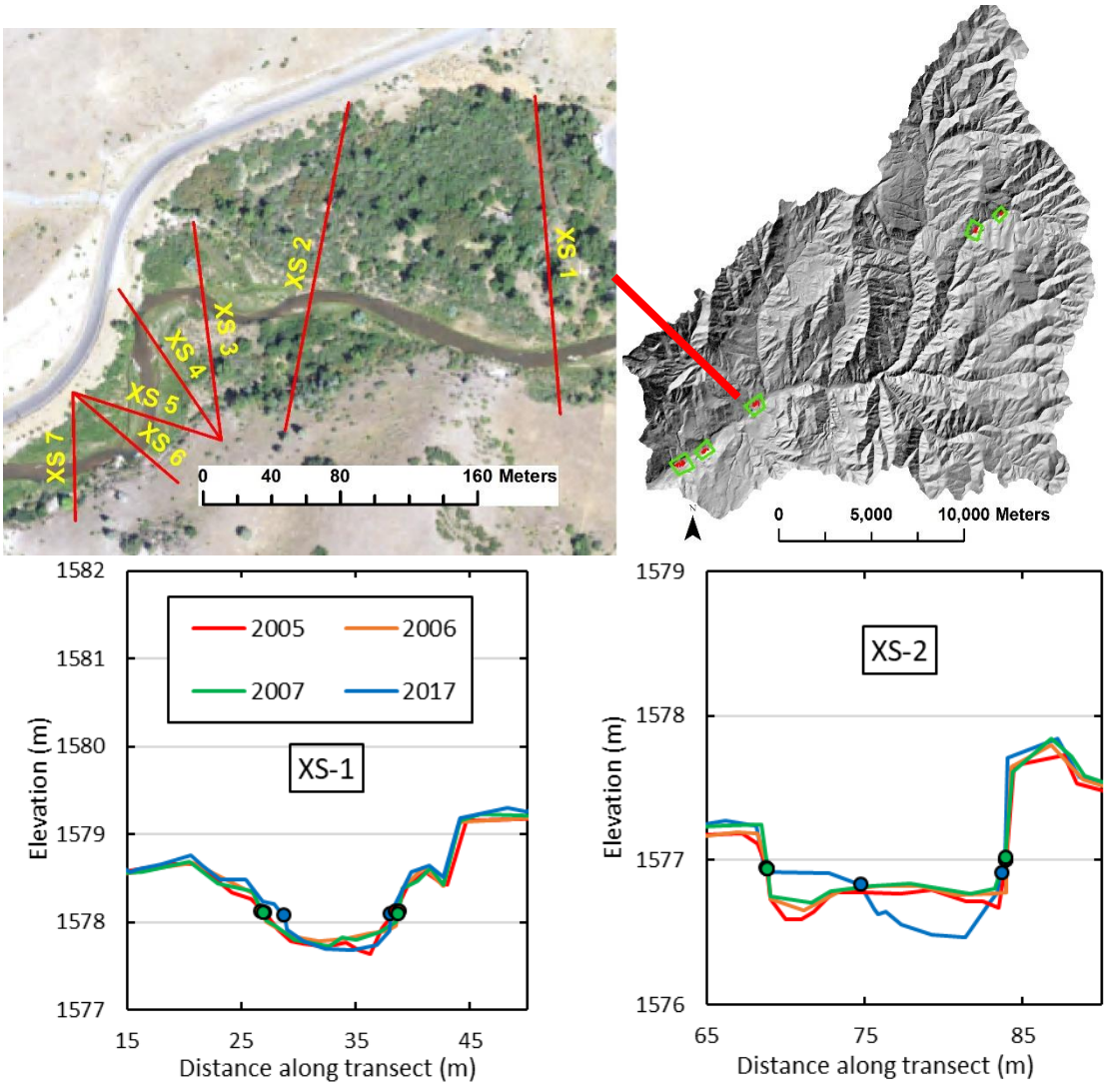

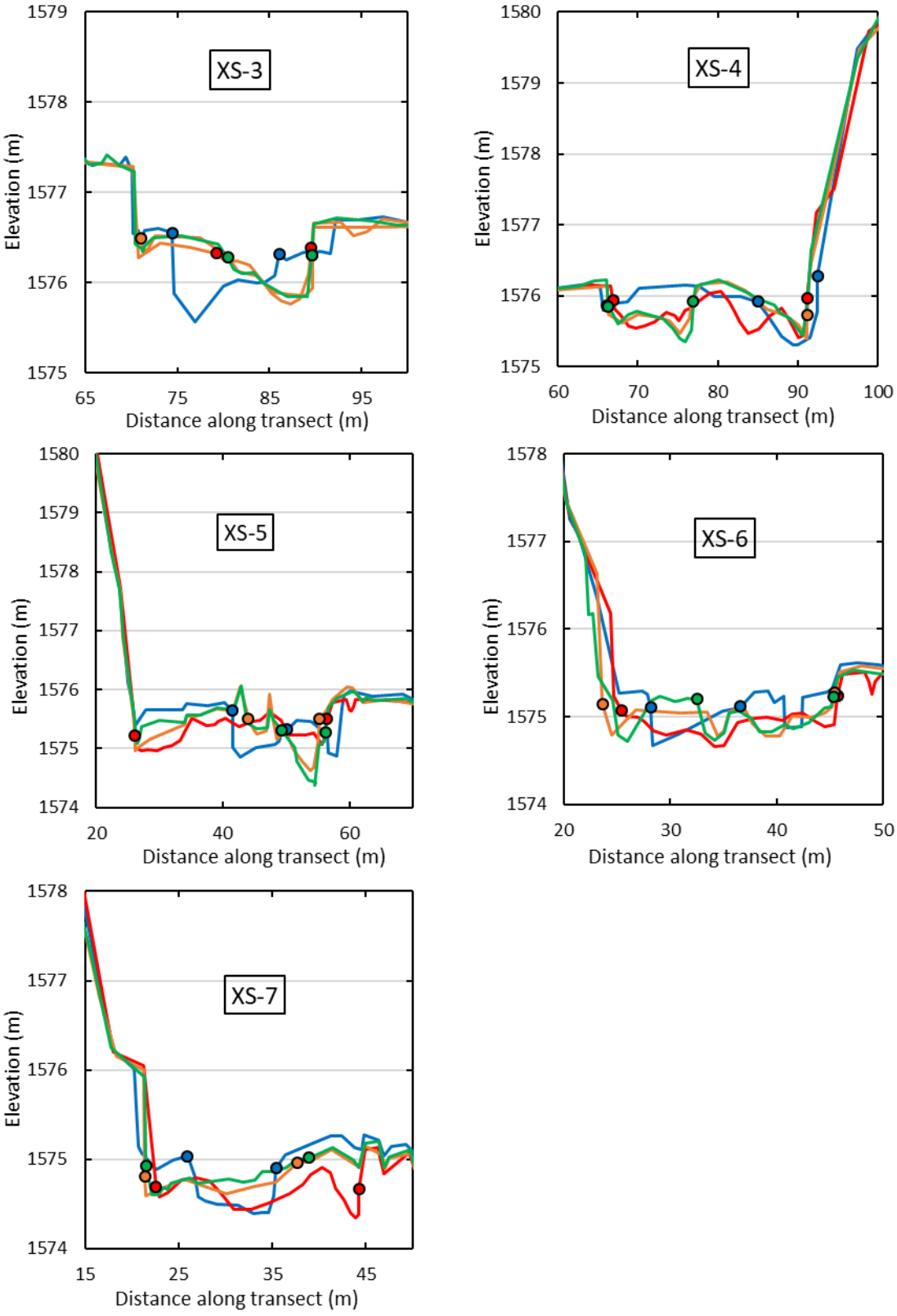
XS-3
Elevation (m)
1579
1578
1577
1576
1575
65
75
85
95
Distance along transect (m)
XS-4
Elevation (m)
1580
1579
1578
1577
1576
1575
60
70
80
90
100
Distance along transect (m)
XS-5
Elevation (m)
1580
1579
1578
1577
1576
1575
1574
20
40
60
Distance along transect (m)
XS-6
Elevation (m)
1578
1577
1576
1575
1574
20
30
40
50
Distance along transect (m)
XS-7
Elevation (m)
1578
1577
1576
1575
1574
15
25
35
45
Distance along transect (m)

B.3. Motherlode

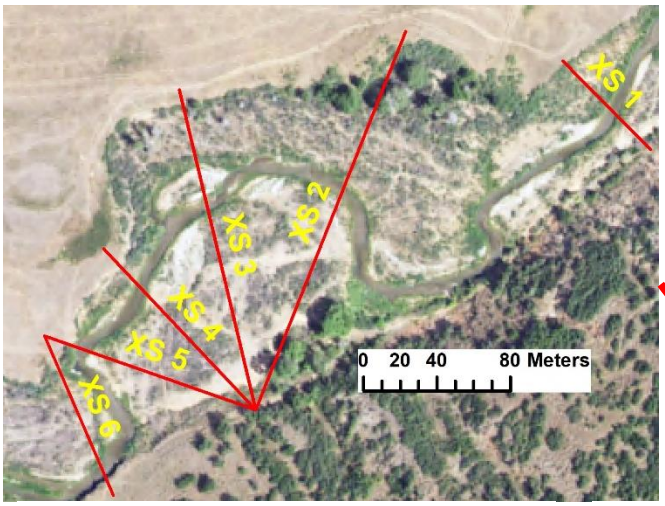

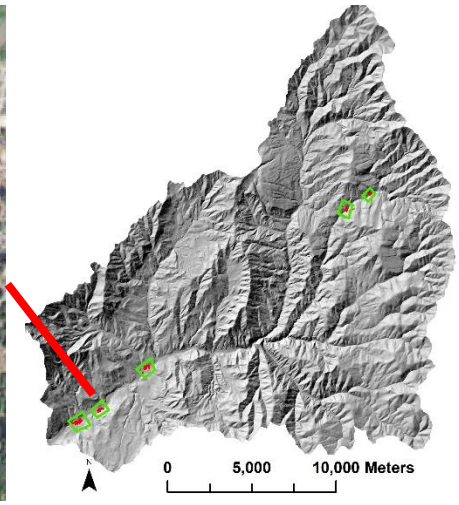

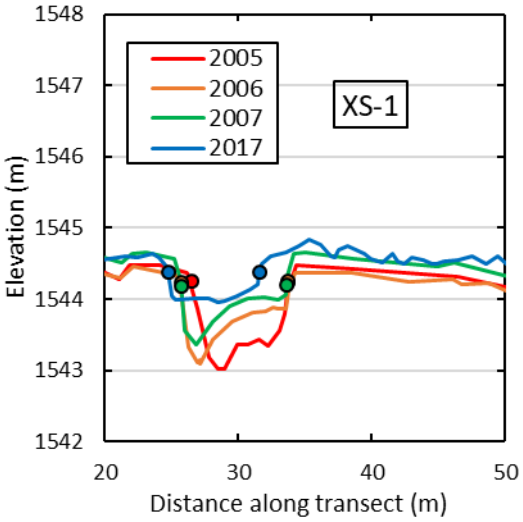

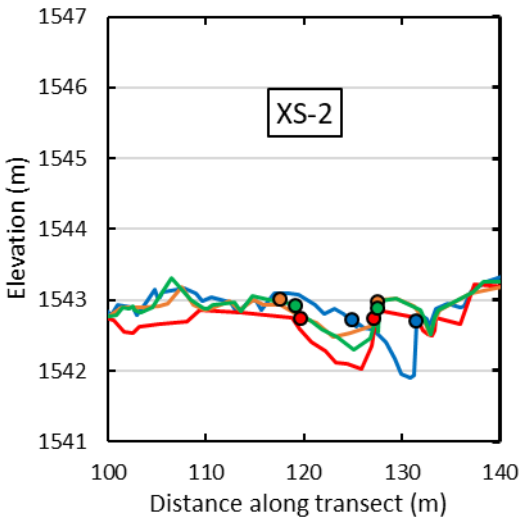

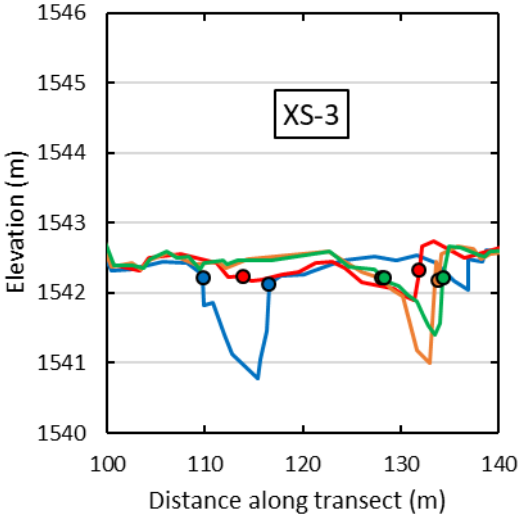

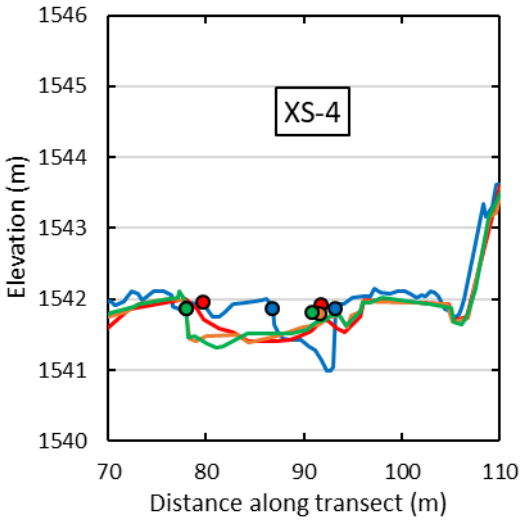

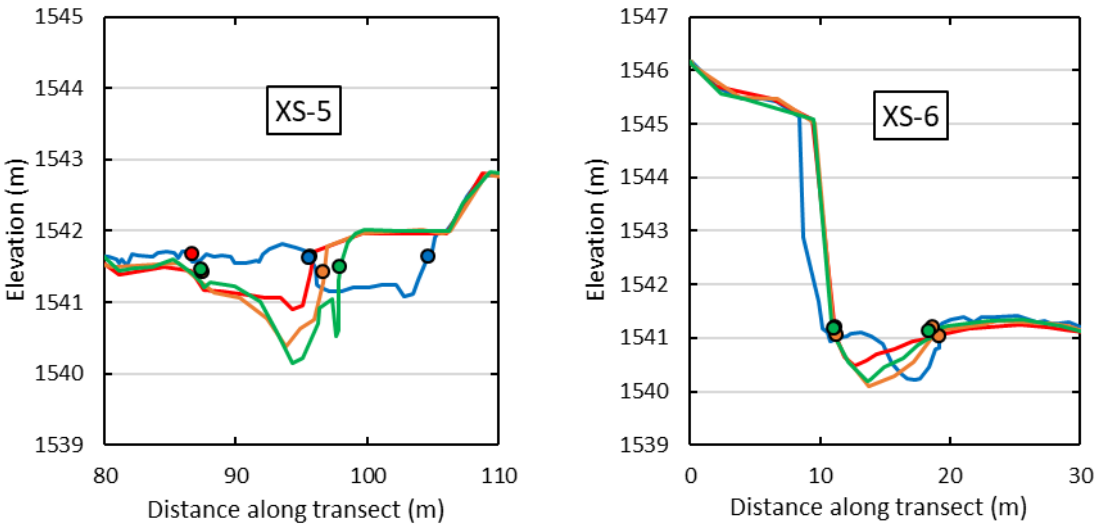
XS-5
Elevation (m)
1545
1544
1543
1542
1541
1540
1539
80
90
100
110
Distance along transect (m)
XS-6
Elevation (m)
1547
1546
1545
1544
1543
1542
1541
1540
1539
0
10
20
30
Distance along transect (m)

B.3. Oxbow

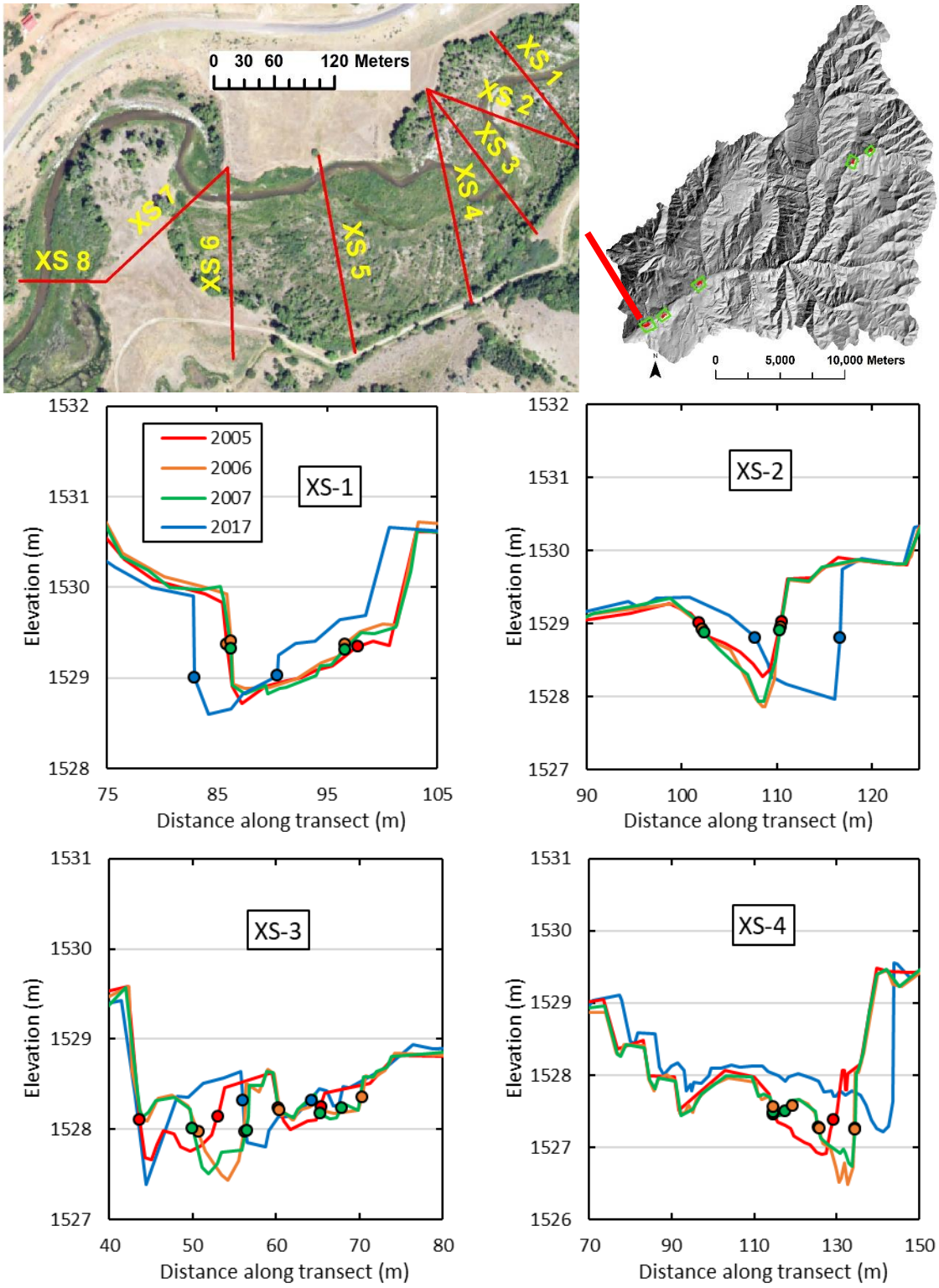
0 30 60 120 Meters
XS 1
XS 2
XS 3
XS 4
XS 5
XS 6
XS 7
XS 8
0 5,000 10,000 Meters
2005
2006
2007
2017
XS-1
XS-2
XS-3
XS-4
Elevation (m)
Distance along transect (m)

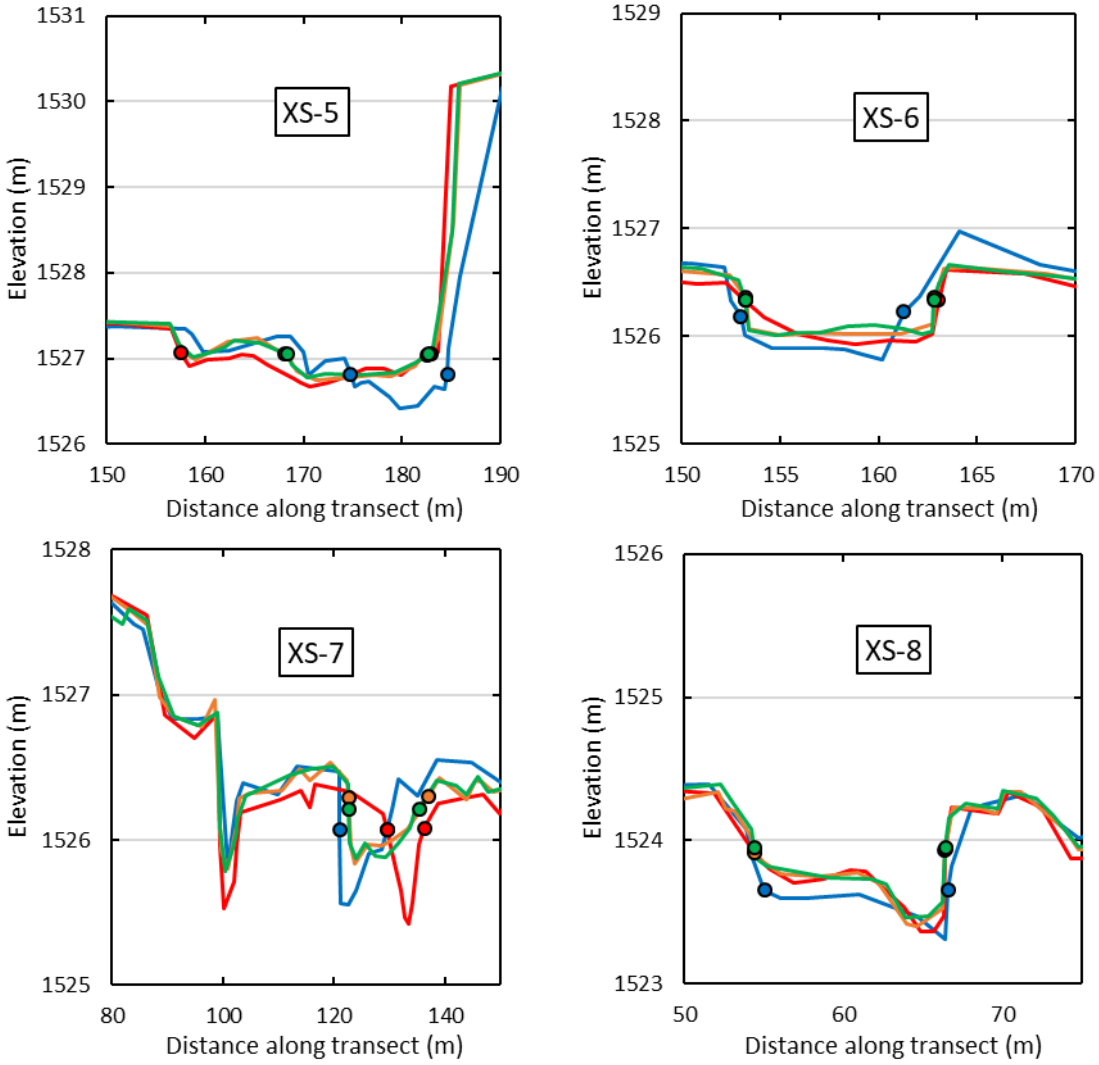
XS-5
Elevation (m)
1531
1530
1529
1528
1527
1526
150
160
170
180
190
Distance along transect (m)
XS-6
Elevation (m)
1529
1528
1527
1526
1525
150
155
160
165
170
Distance along transect (m)
XS-7
Elevation (m)
1528
1527
1526
1525
80
100
120
140
Distance along transect (m)
XS-8
Elevation (m)
1526
1525
1524
1523
50
60
70
Distance along transect (m)

APPENDIX C. GRAIN SIZE DISTRIBUTION OF BED MATERIAL AT MONITORING SITES

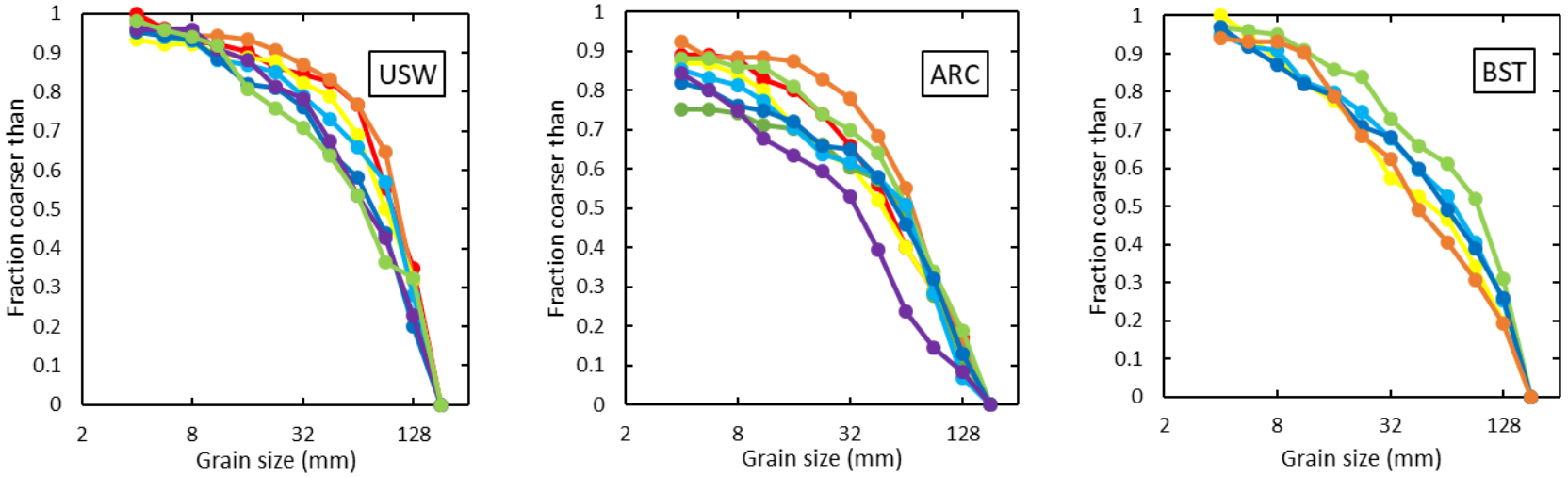

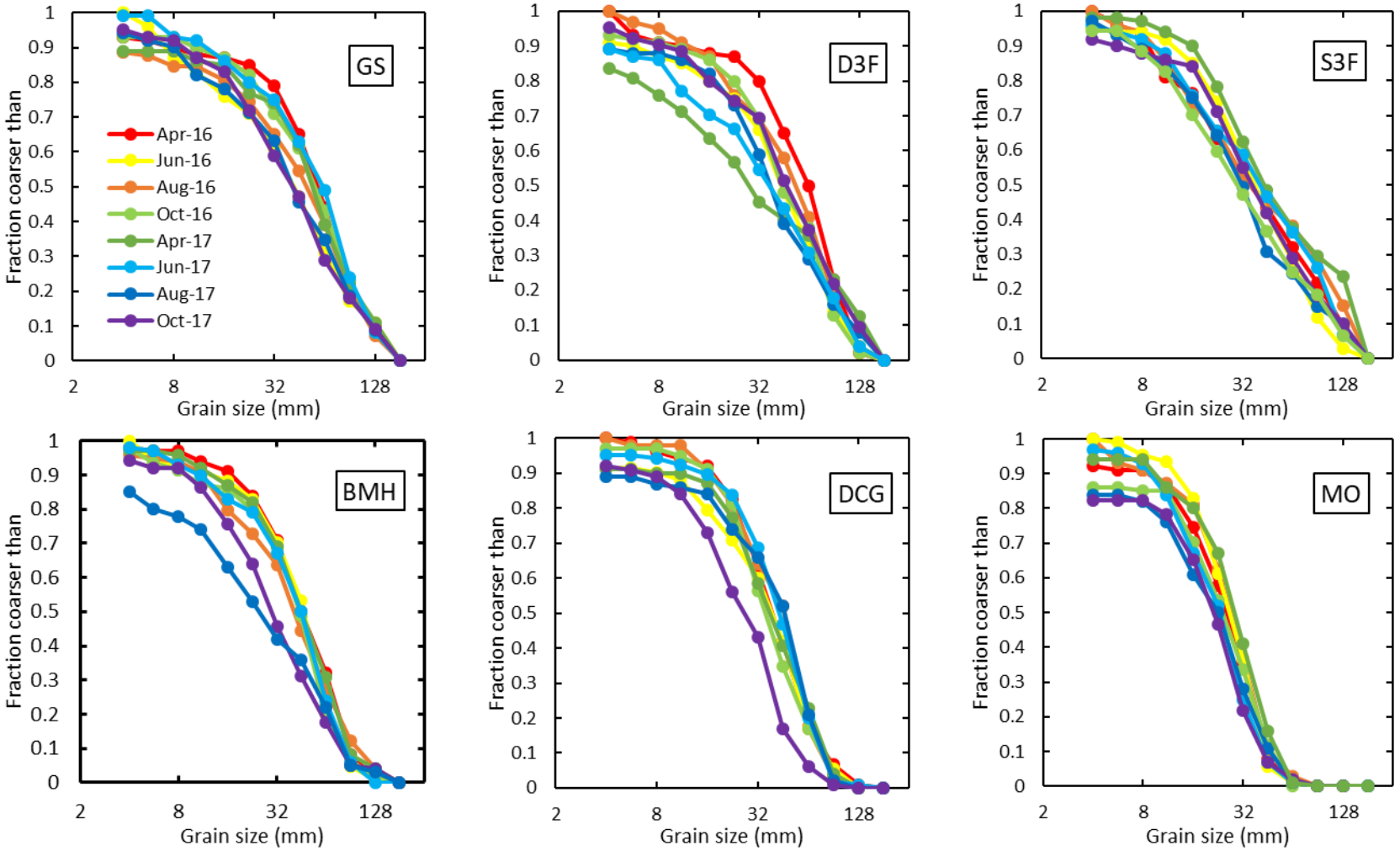

Fig. C.1. Grain size distribution determined from pebble counts at monitoring sites. Color legend is the same for all plots.

APPENDIX D. QUANTILE REGRESSION RESULTS FOR ALL PROCESS DOMAINS

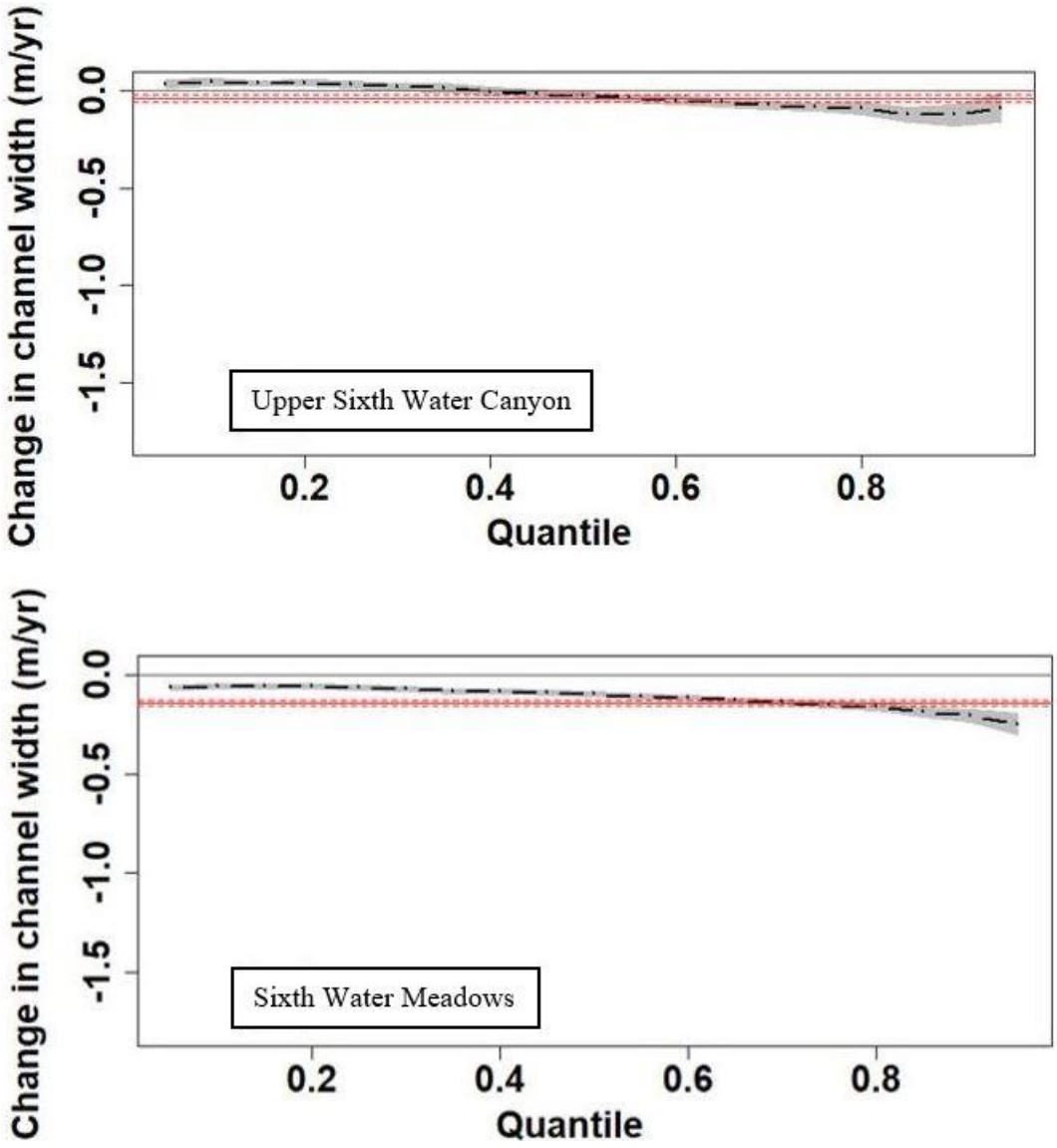

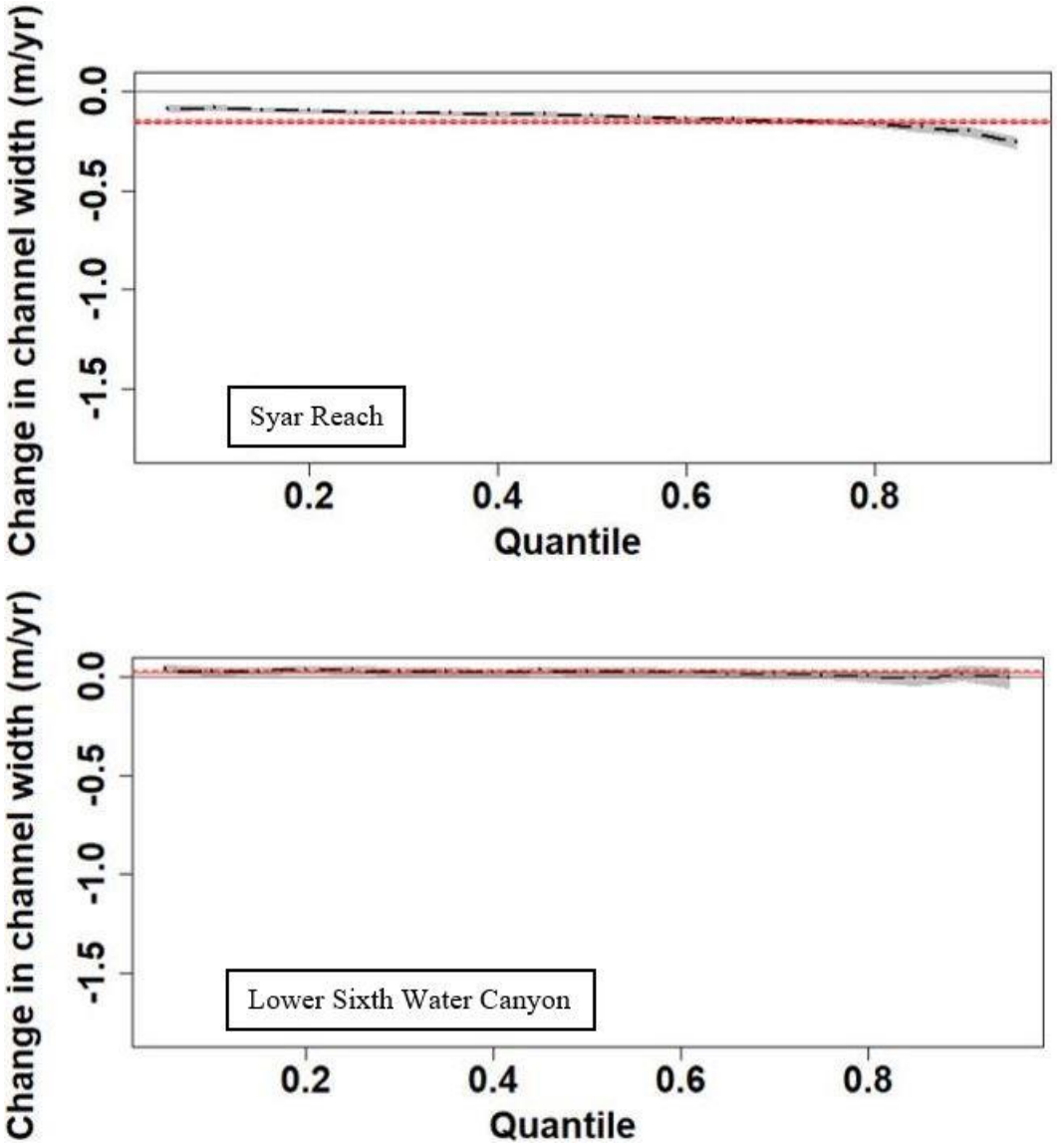
Change in channel width (m/yr)
0.0
-0.5
-1.0
-1.5
Syar Reach
0.2
0.4
0.6
0.8
Quantile
Change in channel width (m/yr)
0.0
-0.5
-1.0
-1.5
Lower Sixth Water Canyon
0.2
0.4
0.6
0.8
Quantile

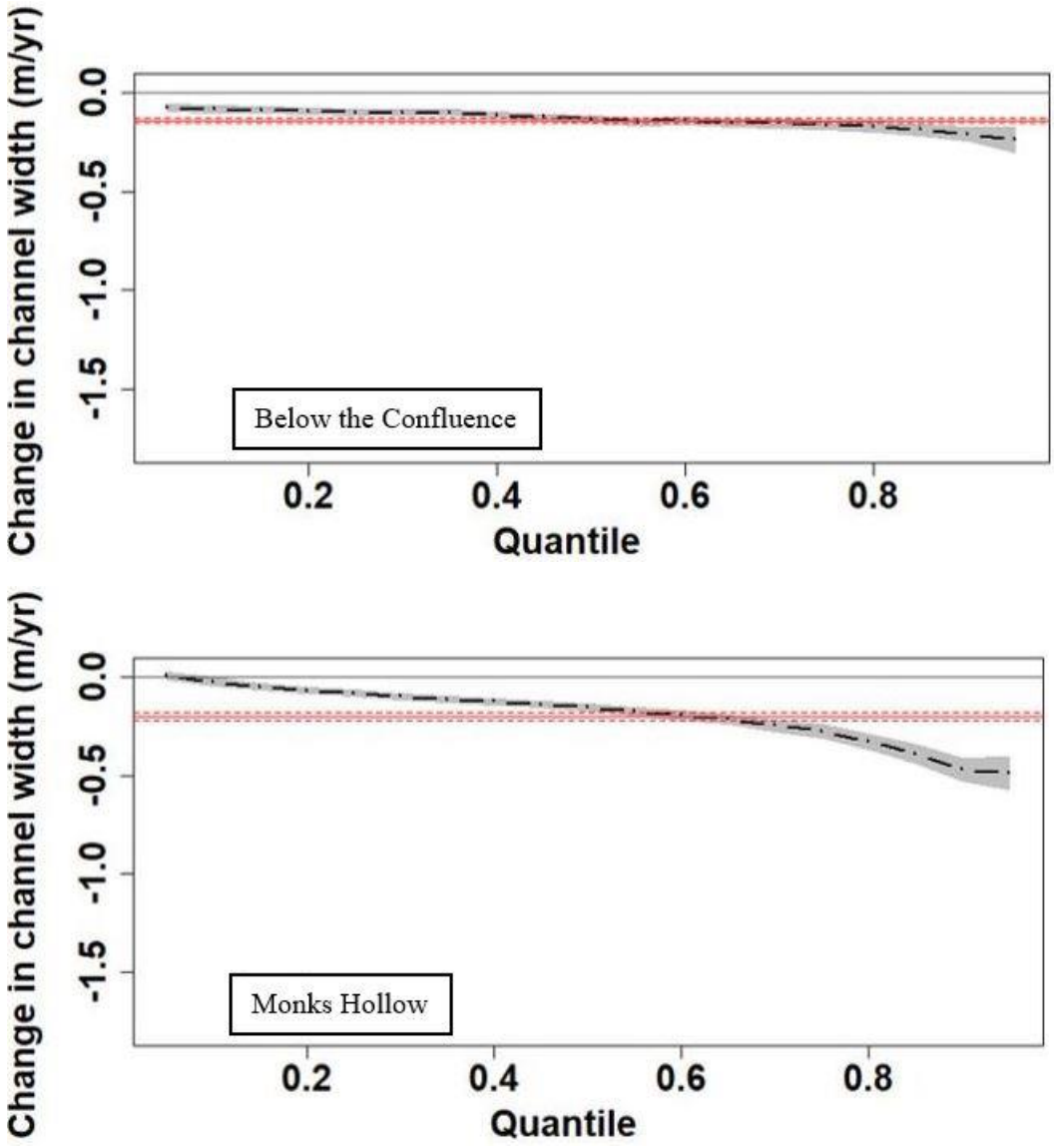
Change in channel width (m/yr)
0.0
-0.5
-1.0
-1.5
Below the Confluence
0.2
0.4
0.6
0.8
Quantile
Change in channel width (m/yr)
0.0
-0.5
-1.0
-1.5
Monks Hollow
0.2
0.4
0.6
0.8
Quantile

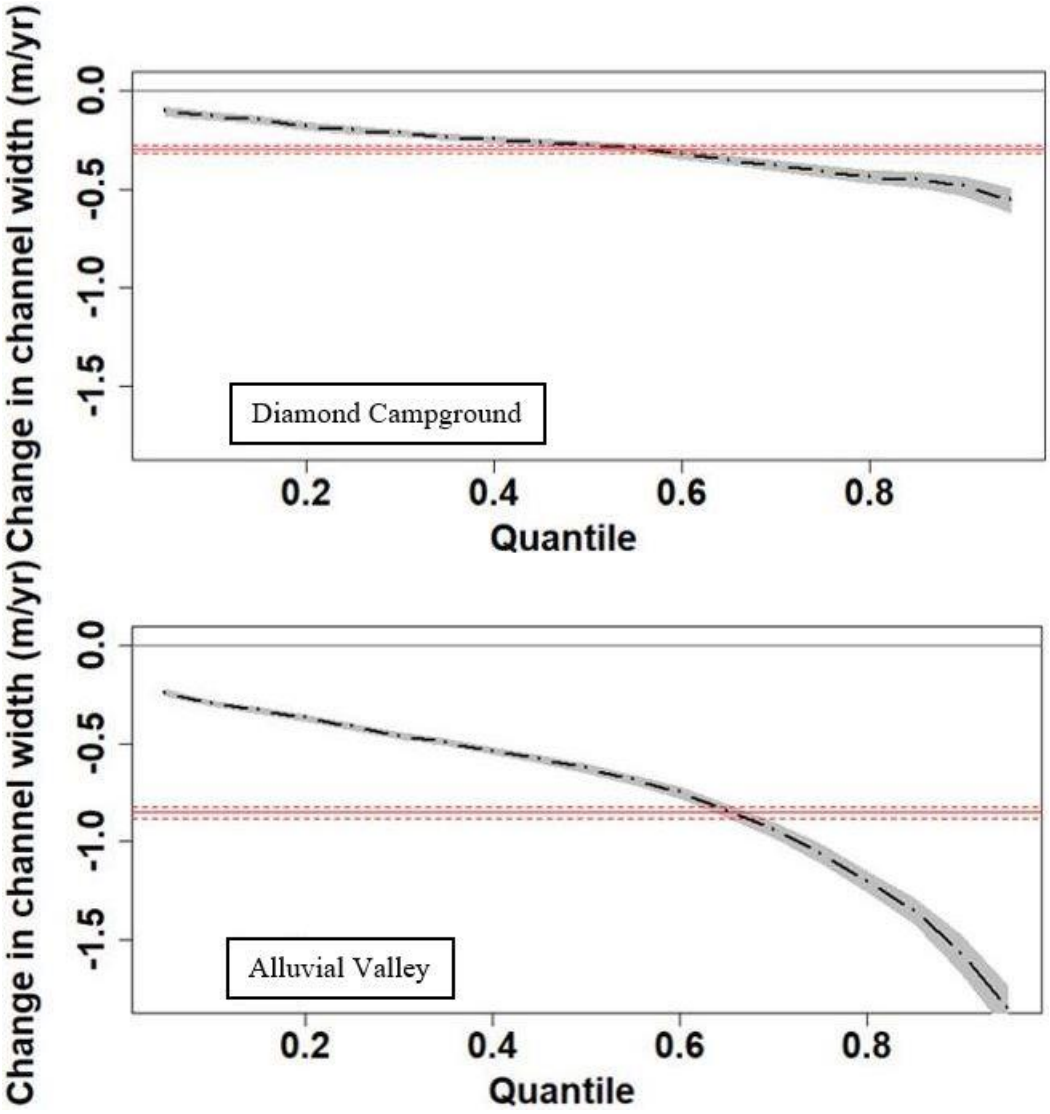

Fig. D.1. Results of quantile regression for all process domains on Sixth Water and Diamond Fork. We conducted quantile regression for width data from 1993 to 2016. Larger quantiles represent wider parts of the channel.